AD_____

AWARD NUMBER: DAMD17-03-1-0243

TITLE: Role of the Conserved Oligomeric Golgi Complex in the Abnormalities of Glycoprotein Processing in Breast Cancer Cells

PRINCIPAL INVESTIGATOR: Sergey N. Zolov, Ph.D.

CONTRACTING ORGANIZATION: University of Arkansas
Little Rock, Arkansas 72205

REPORT DATE: May 2006

TYPE OF REPORT: Annual Summary

PREPARED FOR: U.S. Army Medical Research and Materiel Command
Fort Detrick, Maryland 21702-5012

# REPORT DOCUMENTATION PAGE

*Form Approved*
*OMB No. 0704-0188*



| **1. REPORT DATE** *(DD-MM-YYYY)* | **2. REPORT TYPE** | **3. DATES COVERED** *(From - To)* |
|---|---|---|
| 01-05-2006 | Annual Summary | 1 May 2003 – 30 Apr 2006 |

**4. TITLE AND SUBTITLE**

Role of the Conserved Oligomeric Golgi Complex in the Abnormalities of Glycoprotein Processing in Breast Cancer Cells

**5a. CONTRACT NUMBER**

**5b. GRANT NUMBER**
DAMD17-03-1-0243

**5c. PROGRAM ELEMENT NUMBER**

**6. AUTHOR(S)**

Sergey N. Zolov, Ph.D.

E-Mail:

**5d. PROJECT NUMBER**

**5e. TASK NUMBER**

**5f. WORK UNIT NUMBER**

**7. PERFORMING ORGANIZATION NAME(S) AND ADDRESS(ES)**

University of Arkansas
Little Rock, Arkansas 72205

**8. PERFORMING ORGANIZATION REPORT NUMBER**

**9. SPONSORING / MONITORING AGENCY NAME(S) AND ADDRESS(ES)**
U.S. Army Medical Research and Materiel Command
Fort Detrick, Maryland 21702-5012

**10. SPONSOR/MONITOR'S ACRONYM(S)**

**11. SPONSOR/MONITOR'S REPORT NUMBER(S)**

**12. DISTRIBUTION / AVAILABILITY STATEMENT**
Approved for Public Release; Distribution Unlimited

**13. SUPPLEMENTARY NOTES**

**14. ABSTRACT**

The conserved oligomeric Golgi (COG) complex consists of eight subunits that are thought to be involved in vesicle tethering. Available mutants with the mutations in COG complex subunits exhibit defects in basic Golgi functions: protein glycosylation and its sorting. For analysis of COG complex function we utilized RNA interference assay to knockdown COG3p subunit of COG complex in normal and breast cancer cells and other tumor cell lines. Acute knockdown of the COG3 was accompanied by reduction in Cog1, 2 and 4 protein levels, rapid Golgi fragmentation and accumulation of COG complex dependent (CCD) vesicles. Constantly cycling medial-Golgi enzymes are transported from distal compartments in CCD vesicles. Dysfunction of COG complex leads to separation of glycosyltransferases from anterograde cargo molecules passing along secretory pathway, thus affecting normal protein glycosylation. Altered level of COG3p (or COG complex) expression could be a common feature of cancer cells defective in protein trafficking and Golgi modifications. The importance of the COG complex for both function and architecture of the Golgi apparatus does not depend on cell type. Partial malfunction of the COG complex may play a role in establishing of cancer phenotype.

**15. SUBJECT TERMS**
CELL BIOLOGY, INTRACELLULAR VESICULAR TRAFFICKING, GOLGI STRUCTURE AND FUNCTION, PROCESSING OF GLYCOPROTEINS, EXOCYTOSIS, PROTEIN DELIVERY SYSTEMS, GENE EXPRESSION, WESTERN AND NOTHERN BLOT ANALYSIS, IMMUNOFLUORESCENCE GRADIENT CENTRIFUGATION

| **16. SECURITY CLASSIFICATION OF:** | | | **17. LIMITATION OF ABSTRACT** | **18. NUMBER OF PAGES** | **19a. NAME OF RESPONSIBLE PERSON** |
|---|---|---|---|---|---|
| **a. REPORT** | **b. ABSTRACT** | **c. THIS PAGE** | | | **19b. TELEPHONE NUMBER** *(include area code)* |
| U | U | U | UU | 52 | USAMRMC |

**Standard Form 298 (Rev. 8-98)**
**Prescribed by ANSI Std. Z39.18**

## Table of Contents

## Introduction

In breast, colon and skin cancers, the unusual production and secretion of aberrantly glycosylated proteins and lipids on the surface are associated with disease progression, metastasis and poor clinical outcome (1). Glycosylation abnormalities concern both N-linked and O-linked carbohydrate chains on glycoproteins and glycolipids (2). They likely impair many basic cellular functions, since terminal oligosaccharide units serve as highly specific biological recognition molecules implicated in major regulatory processes of the cell. These phenotypic changes in malignant cells highly correlate with marked structural and functional disorganization of the Golgi apparatus (2).

The **C**onserved **O**ligomeric **G**olgi (**COG**) complex is a peripheral membrane protein complex localized on cis/medial Golgi cistern. This evolutionary conserved complex is composed of eight subunits that are thought to be located in two lobes, the first lobe A containing the COGs 1-4 and the second lobe B the COGs 5-8 (3). Mutations in the COG complex subunits result in defects in basic Golgi functions: glycosylation of secretory proteins, protein sorting and retention of Golgi resident proteins. Cog1 and Cog2 deficient CHO cells are viable, but exhibit defects in multiple Golgi glycosylation pathways establishing a role for the COG complex in mammalian Golgi function (3, 4). Recently, two siblings were described with a fatal form of congenital disorders of glycosylation (CDG) caused by a mutation in the gene encoding COG7. The mutation impairs integrity of the of the COG complex and alters Golgi trafficking, resulting in disruption of multiple glycosylation pathways (5).

All these data indicate that COG complex may participate in Golgi protein trafficking, but the role of the COG complex in the abnormal glycosylation and secretion of tumor markers in breast cancer cells remains elusive.

## Body

During my traineeship the focus of my research was directed towards the study of the functioning of COG complex in normal and tumor cells. In this work siRNA strategy was used to achieve an efficient knockdown (KD) of Cog3p in normal and breast cancer cells and other tumor cells (HeLa cells). I have established a novel vesicle docking system *in vitro* for COG complex-dependent docking of isolated vesicles to support their role as functional trafficking intermediates. For this study HeLa cells and MCF7 cells lines were obtained from ATCC (American Type Culture Collection, Rockville, MD); human breast cancer (HBC) cells SUM 52PE, 159PT, 229PE and 1315MO2 (6) were kindly provided from Dr. Steve Ethier's laboratory (University of Michigan, http://www.cancer.med.umich.edu/breast_cell/Production) and normal breast cells (HB2) line was kindly provided from Dr. Kurten (University of Arkansas for Medical Sciences, Arkansas).

**1. COG3 protein is localized on Golgi in normal conditions. In breast cancer cells it is also localized on peripheral structures.**

COG complex localization in cancer cells probably reflects mislocalization of its membrane receptor(s) (Figure 1).

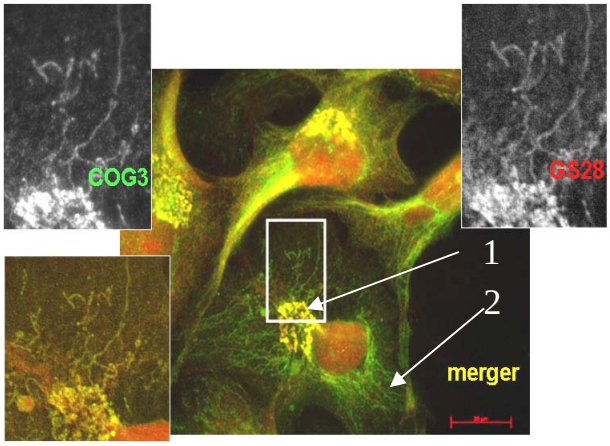


**Figure 1. Localization of COG3p in HBC SUM1315MO2.** Immunofluorescence was revealed that COG complex localized both on Golgi structure (1) and on peripheral structures (2). I discovered that GS28 is colocalized with COG3 on peripheral structures in breast cancer SUM1315MO2 cells.

**2. COG complex malfunction causes Golgi fragmentation into mini-stacks and vesicle accumulation.**

I utilized RNA interference assay to knockdown COG3 protein. Three different siRNAs have been used. Only one of them was active in HeLa cells. The left panel (Figure 2) shows control cells transfected only with reagent. On the right panel are cells after 72 h of siRNA transfection. The quantity of COG3p was dramatically reduced in siRNA transfected cells.

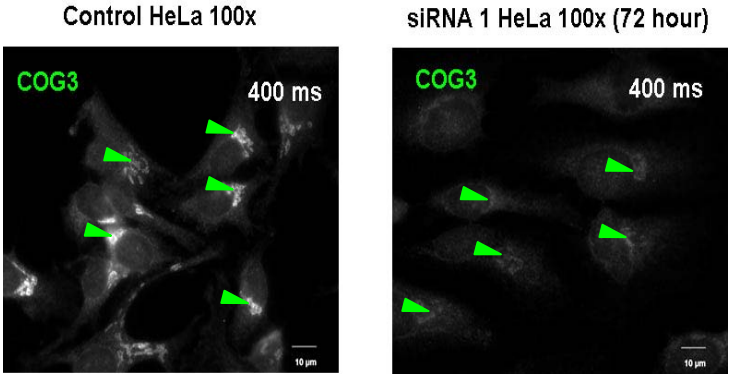


**Figure 2. siRNA COG3 transfection induces degradation of COG3p.** Immunofluorescence localization of COG3p in HeLa cells after transfected by siRNA COG3.

COG3 siRNA-depended Cog3p depletion is accompanied by reduction in Cog1, 2 and 4 protein levels and by accumulation of **C**OG **c**omplex **d**ependent (**CCD**) vesicles. Blockage in CCD vesicles tethering is accompanied by extensive fragmentation of the Golgi ribbon. Fragmented Golgi

membranes maintained their juxtanuclear localization, cisternal organization and are competent for the anterograde trafficking of vesicular stomatitis virus G protein to the plasma membrane. In a contrast, Cog3p KD resulted in inhibition of retrograde trafficking of the Shiga toxin (7).

*These data clearly demonstrate the importance of the COG complex for both function and architecture of the Golgi apparatus. The COG complex operates as a vesicle tether that resides on the cis/medial Golgi compartment and determines accurate docking and fusion of retrograde COG complex dependent intra-Golgi vesicles.*

**3. Prolonged knockdown of COG3p affects glycosylation in secretory pathway.** Cog3p acute depletion caused accumulation of non-tethered vesicles and Golgi fragmentation but, at least initially, did not affect glycosylation of three different glycoproteins: GPP130 (Golgi phosphoprotein of 130 kDa), a 130-kDa phosphorylated and glycosylated integral membrane protein localized to the cis/medial Golgi (7, 8), CD44 (endogenous heavily glycosylated plasma membrane glycoprotein (9)) and Lamp2 (Lysosome-associated transmembrane glycoprotein (10)). This result was not expected, since severe Golgi glycosylation defects were previously observed in both ΔCOG1 (ldlB) and ΔCOG2 (ldlC) Chinese hamster ovary (CHO) mutants (11), and similar glycosylation abnormalities were detected in yeast cog3-ts (sec34-2) mutant (12). To resolve the discrepancy in mutant phenotypes we tested whether the extended deficiency in Cog3p function affects Golgi glycosylation machinery (Figure 3) (13).

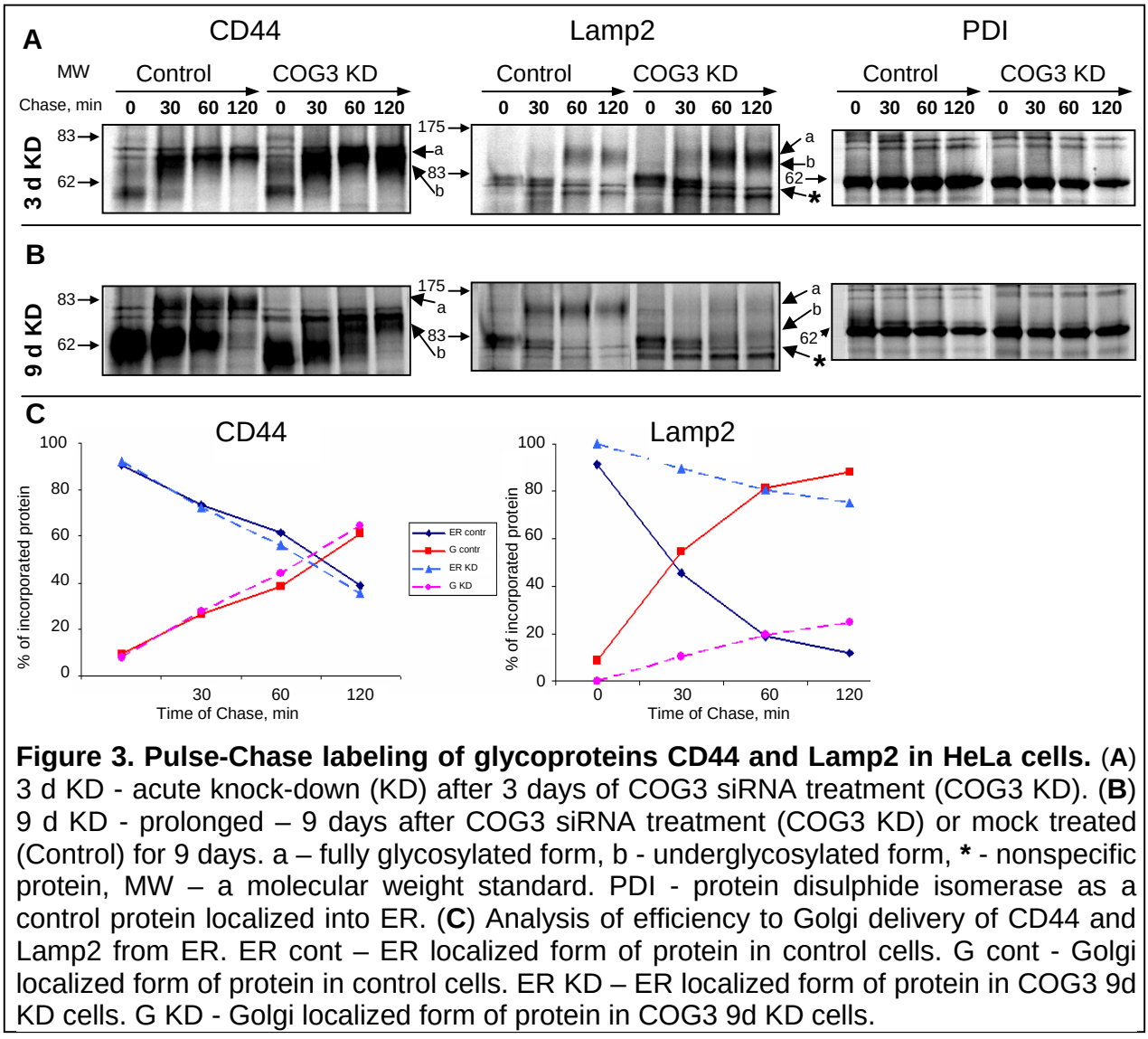


**Figure 3. Pulse-Chase labeling of glycoproteins CD44 and Lamp2 in HeLa cells.** (**A**) 3 d KD - acute knock-down (KD) after 3 days of COG3 siRNA treatment (COG3 KD). (**B**) 9 d KD - prolonged – 9 days after COG3 siRNA treatment (COG3 KD) or mock treated (Control) for 9 days. a – fully glycosylated form, b - underglycosylated form, ***** - nonspecific protein, MW – a molecular weight standard. PDI - protein disulphide isomerase as a control protein localized into ER. (**C**) Analysis of efficiency to Golgi delivery of CD44 and Lamp2 from ER. ER cont – ER localized form of protein in control cells. G cont - Golgi localized form of protein in control cells. ER KD – ER localized form of protein in COG3 9d KD cells. G KD - Golgi localized form of protein in COG3 9d KD cells.

Wild type HeLa cells were treated with COG3 siRNA for different time. Acute KD is referred as 3 days after siRNA treatment, prolonged – 9 days after siRNA treatment or mock-treated for 9 days. To study the glycosylation process in COG complex depleted cells series of Pulse-Chase experiments have been performed. HeLa cells after 3 days of COG3 KD were pulsed for 10 minutes with $^{35}$S-Methionine and then chased in unlabeled methionine rich medium for 0, 30, 60 and 120 minutes (Figure 3 A, B). Cells were lysed in defined time points and consequently immunoprecipitated with anti-CD44, Lamp2 and PDI, samples were loaded on SDS-PAGE and visualized by autoradiography. There was no difference in speed of delivery to Golgi and efficiency of glycosylation detected. Within 120 minutes majority of CD44 and Lamp2 became fully glycosylated in both control and 3 days COG3 KD HeLa cells (Figure 3 A). In contrasts to 3 days of COG3 KD, a pronounced defect in glycosylation of CD44 and Lamp2 has been shown after 9 days of COG3 KD (Figure 3 B). Even after 2 hours of chase in 9 days after COG3 KD, CD44 as well as Lamp2 never reached the level of control ones, saying that defects in glycosylation are developing in accordance with duration of COG complex KD and thus are developed due to some secondary effects which accumulated in COG3 depleted cells, leading to underglycosyaltion disorder. However, only for Lamp2 we detected significant decrease of Golgi glycosylation (Figure 3 C). The glycosylation defect was even more pronounced 9 days after COG3 KD. Interestingly, even four days of COG3 KD was enough for changes in gel mobility of both CD44 and Lamp-2, indicating production of under-glycosylated protein species (Figure 4).

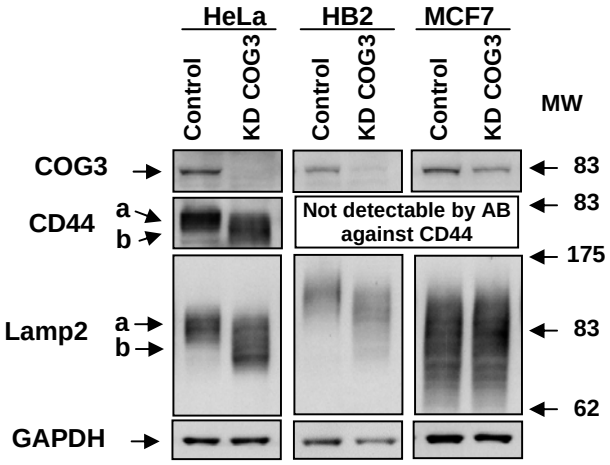


**Figure 4. 96 h Cog3p knockdown affects glycosylation of membrane glycoproteins of secretory pathway.** HeLa, HB2 and MCF7 cells were subjected to 4 days of COG3 knock down. Total cell lysates were analyzed by WB with indicated antibodies.

*These findings suggested that after COG3 KD: 1) either glycoproteins are not targeted properly and thus can not encounter Golgi glycosylation machinery or 2) Golgi glycosylation machinery itself is mislocalized, thus not allowing Golgi enzymes to process proteins.*

**4. COG complex component expression and localization in normal and cancer cells.** It was previously detected that the COG3p protein level in a MCF7 cell is elevated in comparison to HB2 cells. We have proposed that altered level of expression of COG3p (or COG complex) could be a common feature of cancer cells defective in protein trafficking and Golgi modifications. To test this prediction the protein expression of COG complex subunits and its intracellular localization in normal and cancer cells were determined. Protein samples prepared from the normal cells (HB2 and CHO), mutants of CHO cells (ΔCOG1 (ldlB) and ΔCOG2 (ldlC)) and cancer cells (MCF7 and HeLa) were separated on SDS-PAGE (9%) and analyzed by Western blot (WB) with anti-COG3p and anti-COG4p (LobA of COG complex), anti-COG6 and anti-COG7p (LobB of COG complex) Abs and control anti-GAPDH Abs (Figure 5).

We have found that not only level of COG3p but also other subunits of COG complex in breast cancer cells MCF7 had been elevated 2-4 times in comparison to HB2 cells (Figure 5 A). The expression of

Cog4p subunit of lobe A COG in normal breast cells HB2 was also reduced 96 h after COG3 KD, whereas protein level of the lobe B Cog6 and 7 subunits remained unchanged as was shown for HeLa cells (7) (Figure 5 B). Efficiency of KD for MCF7 cells was lower as compared to HeLa cells (about 50%) but COG4p was reduced. Detailed analysis of COG3 KD cells by immunofluorescence (IF) revealed that Cog3p depletion induces Golgi fragmentation in both normal and breast cancer cell lines (Figure 6.), as was shown for HeLa cells (7). This result points out that the importance of the COG complex for both function and architecture of the Golgi apparatus does not depend on type of cells.

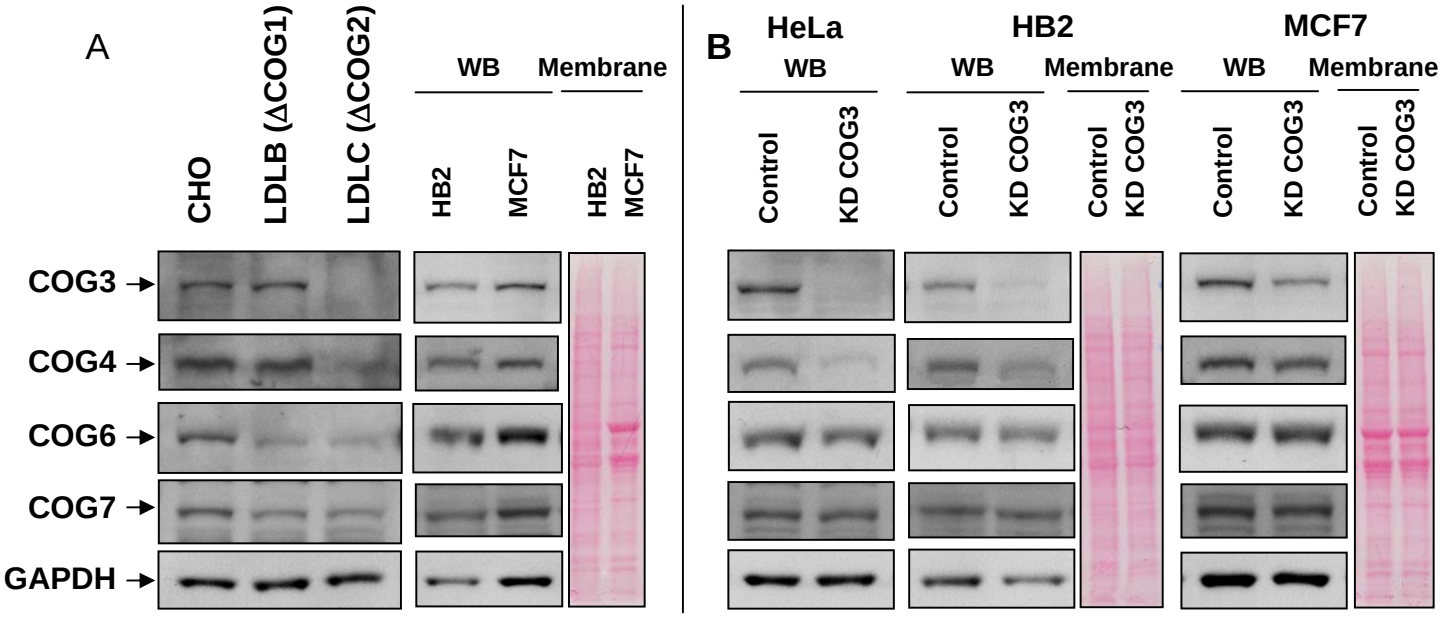


**Figure 5. The expression level of the COG complex subunits in normal and cancerous cell lines. SiRNA-induced COG3 KD is destabilizing Lobe A COG complex subunits.** (A) Expression of COG subunits in normal (HB2) and breast cancer cells (MCF7). (B) WB of cell lysates from control and 96 h COG3 KD cells. Average levels of the COG subunits after 96 h of COG3 KD were determined by quantitative WB. To normalize the sample loading for WB analysis, protein content was measured using the BCA reagent (Pierce Chemical Co.). Membrane before WB analysis was stained with Ponceau solution.

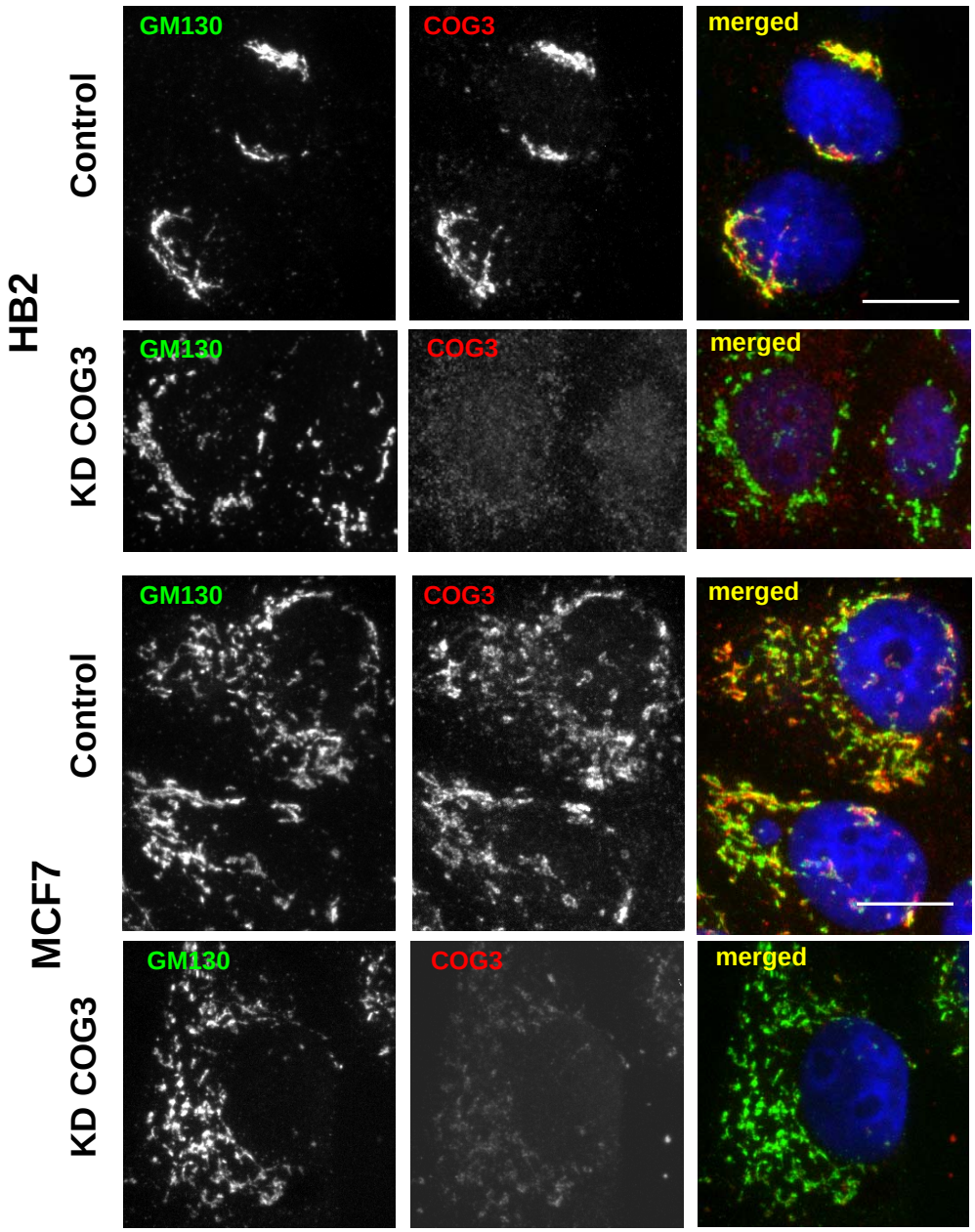


**Figure 6. Cog3p depletion induces Golgi fragmentation.** HB2 and MCF7 cells were transfected with COG3 siRNA (KD COG3) or mock transfected (Control). 72 h after transfection, cells were incubated in OPTI-MEM for 24 h after that fixed and processed for IF with anti-Cog3p (COG3 red), and anti-GM130 (GM130 green) antibodies. The right row represents merged three-color images. Bars, 10 mm.

**5. Analysis of CathD secretion and glycosylation levels of mucin1 after inhibition of the COG function by COG3 siRNA.** Mucins are a family of highly glycosylated, secreted proteins with a basic structure consisting of a variable number of tandem repeats (VNTRs) encoded by 60 base pairs (Mucin 1) (14). Mucin 1 proteins vary from 160 kDa to 230 kDa and Mucin 1 is aberrantly expressed in epithelial tumors including breast carcinomas. Cathepsin D (CathD), an aspartic lysosomal protease expressed in all tissues is secreted from carcinomas. A large number of independent clinical studies associated high Cath-D concentrations in primary breast cancers with increased risk of subsequent metastasis (15). Analysis of glycosylation of Mucin1 and trafficking of the lysosomal

enzyme Cath-D in COG3 KD breast cells line revealed that disturbance of COG complex function in HB2 cells lead to abnormalities of glycoprotein processing for Mucin1 and its secretion into the medium (Figure 7). Furthermore COG3 KD in HB2 causes increase of mislocalization and secretion of preCathD into the medium imitating cancer phenotype.

*These findings allowed suggestion that partial malfunction of the COG complex may play a role in establishing of cancer phenotype.*

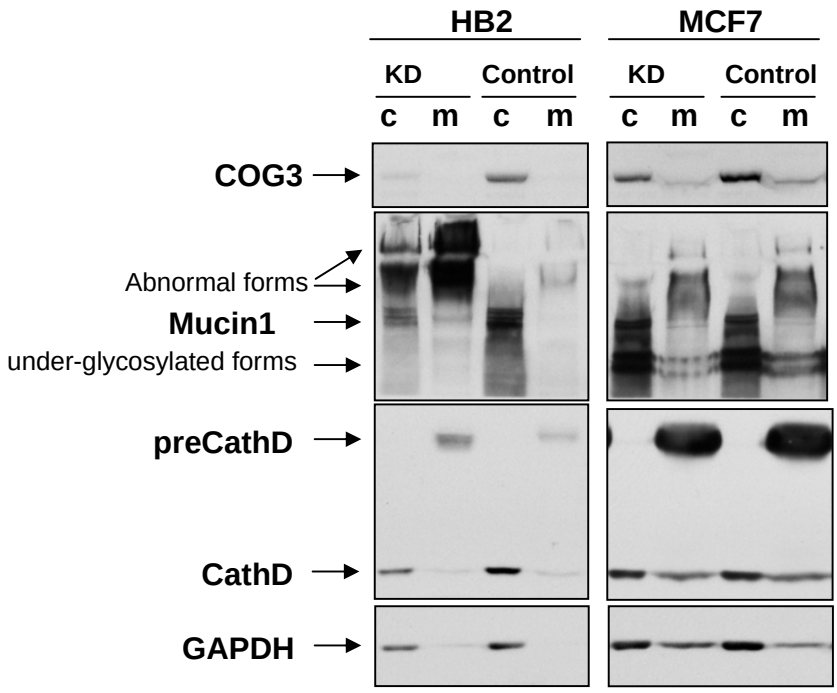


**Figure** 7**. Alterations in protein glycosylation of Mucin1 and trafficking of the lysosomal enzyme Cath-D in COG3 KD breast cells line.** After 72 h KD COG3 HB2 and MCF7 were started for analysis of CathD and Mucin1 secretion and glycosylation by incubation on OPTI-MEM for 24 h. Then medium was collected, cells and debris were precipitated by low and high centrifugation and concentrated by TCA precipitation (16) for overnight in a cold room. Cells were lysed by 1%SDS at 95ºC for 15 min and loaded 2% of cell lysate volume and 50% of medium after concentration on a gel for analyzed by WB. c – cells, m – medium.

**6. Initial characterization of CCD vesicles.** COG3 KD HeLa cells accumulate ~50 nm vesicles that could be detected by IF or electro microscopy (EM) (Figure 8A) (7) techniques. These vesicles have been enriched and partially purified from other cellular membranes by differential centrifugation, **g**lycerol **v**elocity **g**radient (**GVG**), gel-filtration, and immunoprecipitation. Glycerol velocity gradient centrifugation allows separation of CCD vesicles from other cellular organelles based on size. These data indicate that COG3 KD cells specifically accumulate vesicles positive for GPP130, GlcNAcT1, Mann II, and GS15 as a single peak (fractions 3-5) upon separation on glycerol velocity gradient (Figure 8B and data not shown) (13). Control cells do not accumulate these markers in vesicular fractions (Figure 8C).

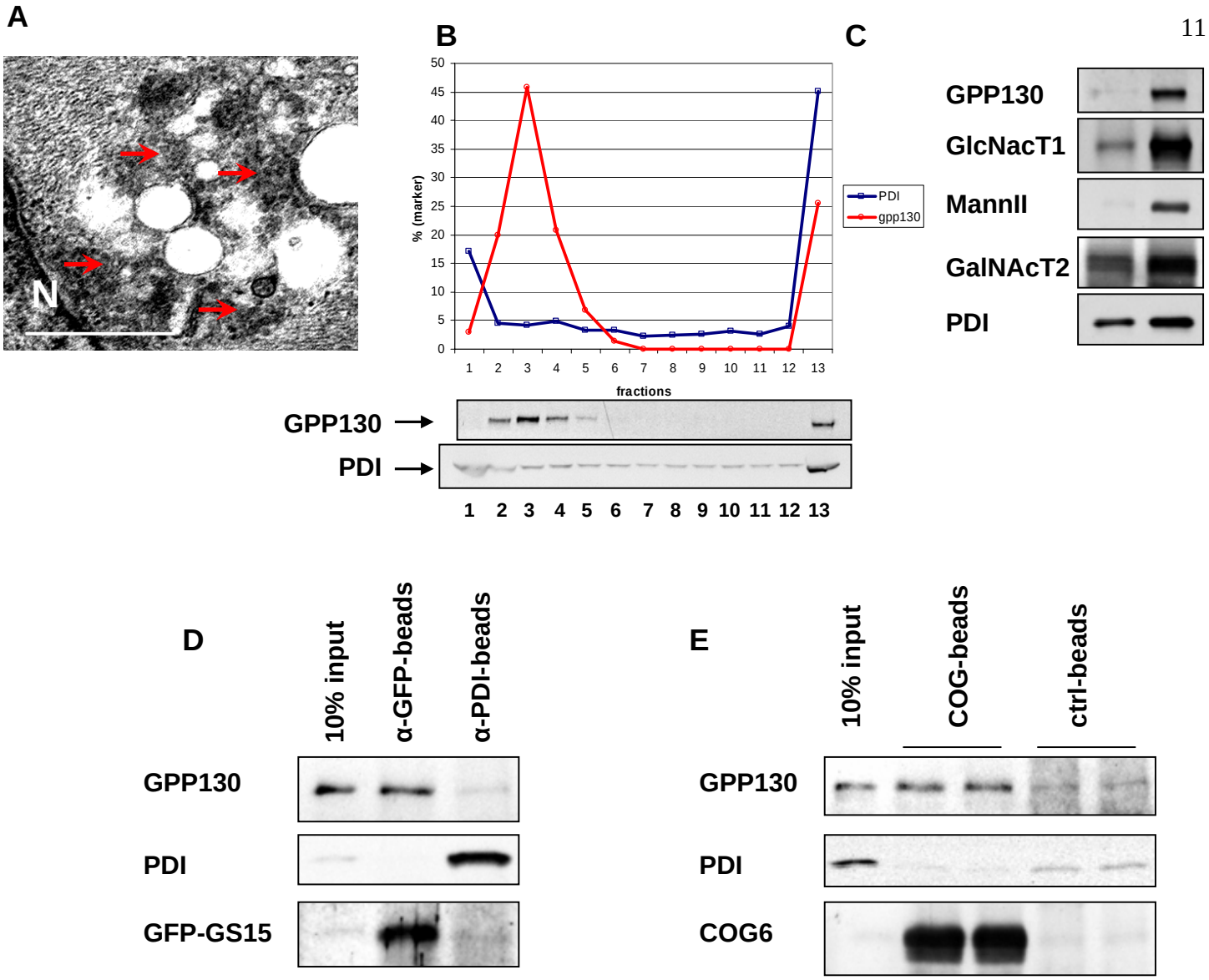


**Figures 8. Partial purification and initial characterization of CCD vesicles.** (**A**) Ultrastructural analysis of COG3 KD HeLa cells indicated accumulation of 50 nm vesicles (arrows). (**B**) **G**lycerol **v**elocity **g**radient (**GVG**) separation. GPP130 –containing CCD vesicles (fr. 3-4) are separated from large membranes (fr. 13) and cytosol (fr.1). (**C**) Vesicle fractions 3-4 from glycerol gradient are enriched in GPP130 and medial-Golgi enzymes. (**D**) GPP130-containing CCD vesicles are affinity precipitated with α-GFP-beads. Input was a GVG vesicle pool obtained from COG3 KD HeLa cells that stably express GFP-GS15. (**E**) CCD vesicles are specifically recovered on beads preloaded with COG complex. Input was a GVG vesicle pool (fr. 3-4) obtained from COG3 KD HeLa cells.

For the next experiment were used semi-pure CCD vesicles obtained from HeLa cells stably expressing GFP-GS15 (obtained in this work) (Figure 8D). In this experiment more than 50% of GFP-GS15-containing vesicles were precipitated under native conditions on beads loaded with anti-GFP antibodies. These beads also precipitate ~15% of GPP130. Control anti-PDI beads did not precipitate GFP-GS15 or GPP130, indicating that vesicle binding is specific. This result indicates that CCD vesicles can be quantitatively precipitated and that these vesicles also contain GPP130. These

experiments will be expanded to determine if other putative CCD cargo is enriched in GFP-GS15 vesicles.

As it has been shown that CCD vesicles obtained from a 20,000xg supernatant (S20) of COG3 KD cells can be specifically recovered on beads preloaded with COG complex (7). The major caveat of this approach was low (~4%) binding efficiency of CCD vesicles to COG beads. Now vesicle yield has improved by modifying our procedure for preparing COG beads and by using vesicles purified on glycerol velocity gradient. COG complex was isolated on anti-GFP beads from lysates of HeLa cells that stably express YFP-COG3 (obtained in this work). Protein levels of YFP-COG3 and endogenous Cog3p in these cells were similar (data not shown). As a result, beads contained almost equal amounts of different COG subunits (10µl of beads contained ~1µg of YFP-COG3 and 0.24 µg of COG6). Beads were incubated for 2 h at 4$^{o}$C with semi-purified vesicles, washed, and analyzed by WB. More than 10% GPP130-containing CCD vesicles were recovered on beads loaded with the COG complex and less than 2% was recovered on control beads (Figure 8E).

**7. Docking of isolated CCD vesicles to Golgi membranes is reconstituted *in vitro*.** Results were shown above indicated that both medial-Golgi glycosyltransferases and intra-Golgi SNAREs are transiently accumulated in CCD vesicles in COG3 KD cells. To test if these vesicles represent a functional intra-Golgi transport intermediate, I designed an in vitro system that measured vesicle docking/fusion with isolated rat liver Golgi. The system design was based on the sedimentation properties of rat liver Golgi (RLG, pelleted at 10,000xg) and CCD vesicles (not pelleted at 20,000xg). Both GlcNAcT1-myc and GPP130 were used as vesicle markers (Figures 9, 10).

**Figure 9. *In vitro* system scheme of vesicles docking/fusion with rat liver Golgi**

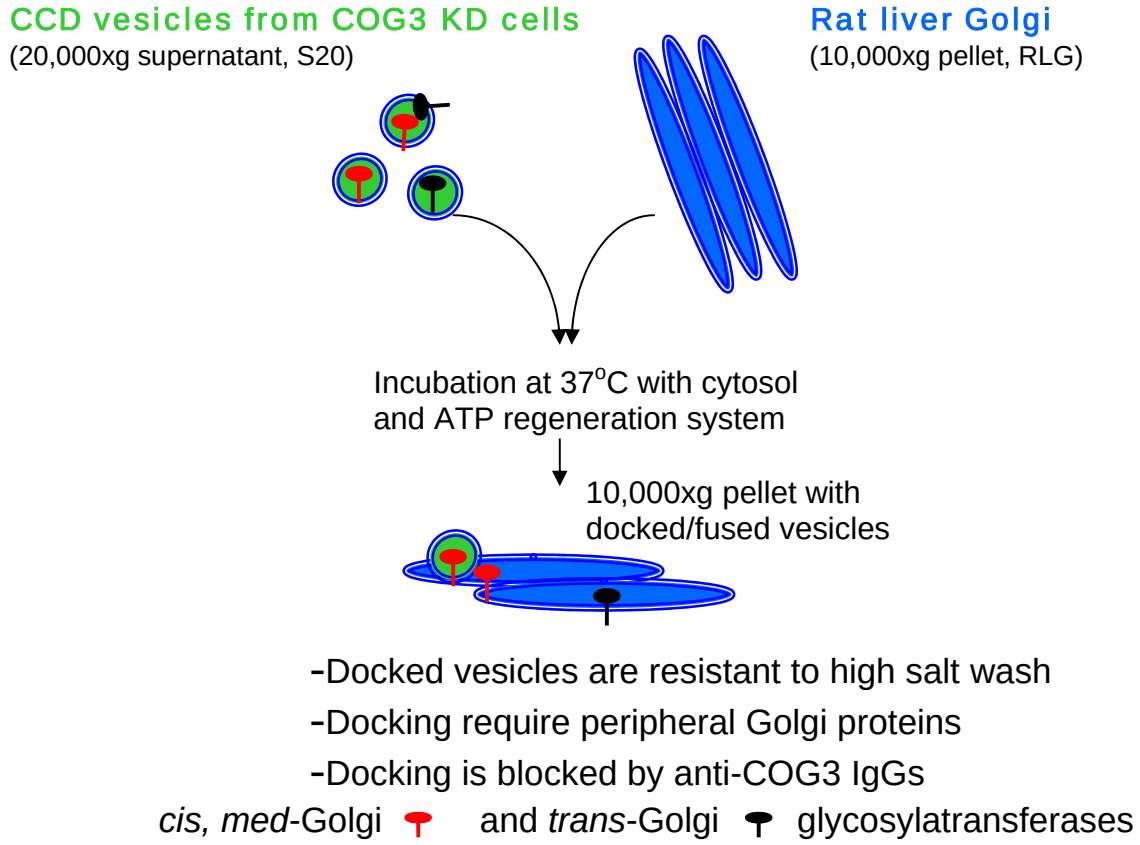

**Figure 10. Antibodies recognized specific antigens in rat liver Golgi (RLG) and COG3 KD HeLa S20 fractions.**

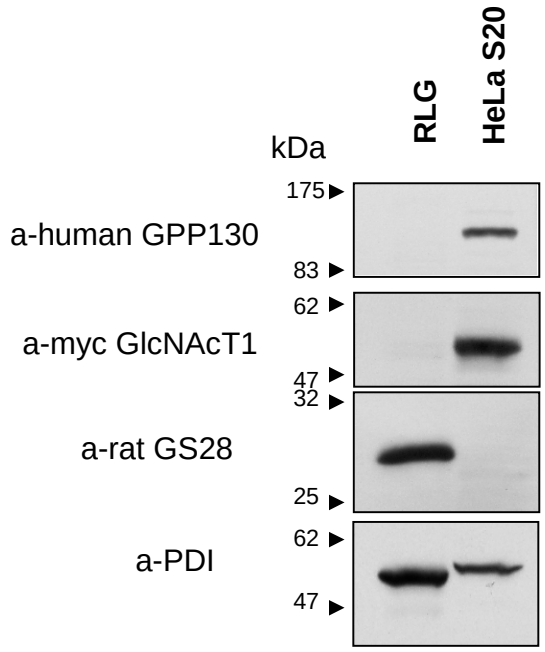


Aliquots of RLG and COG3 KD HeLa S20 (~ 10 µg each) were separated on 10% SDSPAGE and immunoblotted with antibodies as indicated.

In the first experiment, 20,000xg supernatant (S20) from COG3 KD cell lysates was mixed with different amounts of purified RLG and incubated for 30 min at 37ºC. At the end of incubation, RLG with bound vesicles were pelleted and washed with low salt buffer or with buffer with 250 mM KCl. I have found that CCD vesicles were able to dock to isolated Golgi (Figure 11A). The amount of sedimentable vesicle marker (up to 30% from total input) was proportional to the amount of added Golgi membranes and vesicle-Golgi association was resistant to 250mM salt wash, which normally strips vesicles from Golgi membranes (17), indicating tight association and/or complete fusion.

**A**

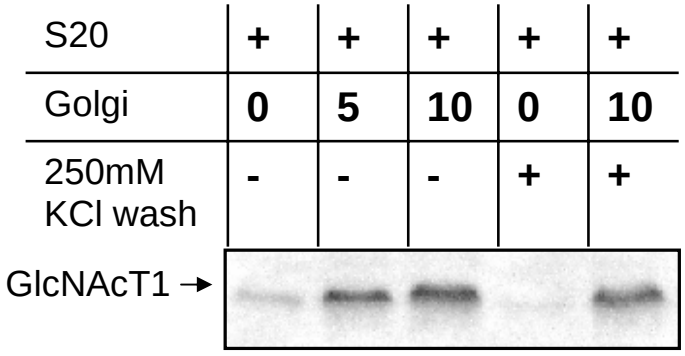


**Figure 11. Reconstitution of CCD vesicles docking to Golgi *in vitro*.** (**A**) GlcNacT1-containing vesicles are specifically cosedimented with rat liver Golgi (RLG). S20 (vesicle fraction) from COG3 KD HeLa cells was incubated with indicated amounts of RLG for 30 min at 37ºC and then Golgi were pelleted at 10,000xg. Vesicle binding was estimated by WB.

Second experiment (Figure 11B) performed under the same conditions was designed to test if vesicle docking is COG dependent. Docking to acceptor Golgi membranes was sensitive to proteinase K pretreatment, indicating involvement of peripheral and/or transmembrane proteins. Indeed, both Golgi SNARE GS28 and Cog3p were completely destroyed by Proteinase K treatment (Figure 11B lane rat GS28 and data not shown). Most importantly, docking of CCD vesicles was sensitive (~70% inhibition) to addition of anti-COG3 IgGs.

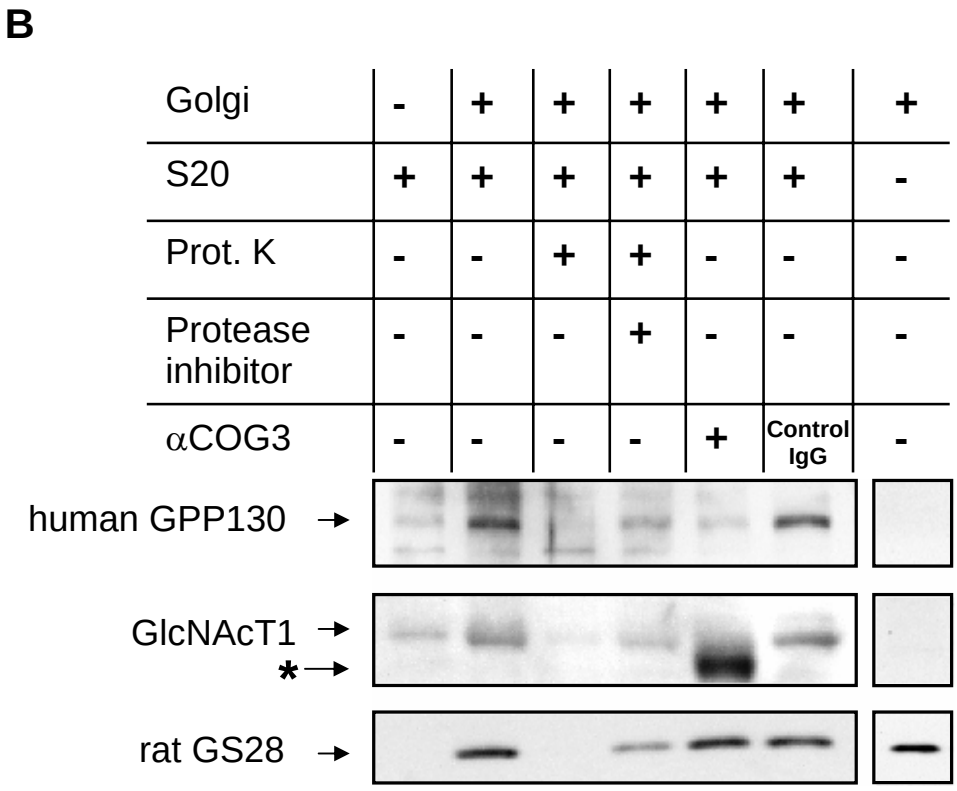


**Figure 11. Reconstitution of CCD vesicles docking to Golgi *in vitro*.** (**B**) Vesicle docking requires Cog3p and peripheral Golgi proteins. Golgi (detected with rat GS28 IgGs) were pretreated with α-Cog3p IgGs, or with Protease K +/- protease inhibitor and afterwards incubated with vesicles (detected with antibodies to human GPP130 and anti-myc-GlcNAcT1) as in A.

Incubation at $37^0$C does not discriminate between vesicle docking and fusion. Therefore, I performed docking reaction for 1 h at $4^0$C (Figure 11C). Again, more than 40% of vesicular marker GlcNAcT1-myc was co-sedimented with RLG in a time-dependent manner (Figure 11C, left “Pellet” panel), and a proportional depletion was observed in the supernatant. As a specificity control, we used mostly ER-resident protein PDI that was present in small amounts in both the S20 and RLG fractions. Importantly, our anti-PDI antibodies recognized both the rat and human protein species, which run differently on SDS-PAGE (Figure 10 and 11C, compare human and rat PDI bands). I found that human PDI was not co-sedimented with RLG, indicating that docking of CCD vesicles was specific.

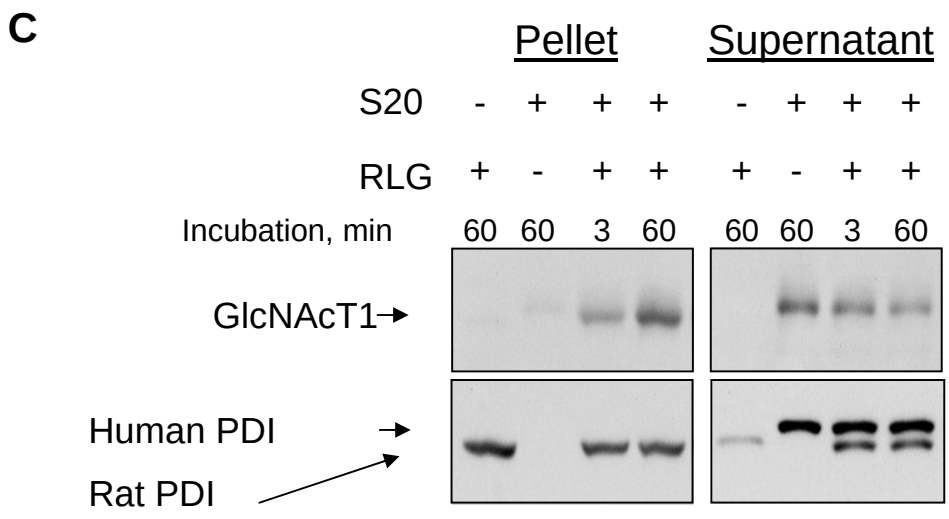


**Figure 11. Reconstitution of CCD vesicles docking to Golgi *in vitro*.** (**C**) Vesicle docking takes place at 4°C. Vesicle fraction was incubated with 10µg of RLG for time indicated at 4°C and then Golgi with docked vesicles were recovered and analyzed as in A. Note that human ER protein human PDI that is present in S20 fraction is not cosedimented with Golgi.

Finally, I tested if CCD vesicles purified on glycerol velocity gradient were active in a docking reaction (Figure 11D). I have found that more than 40% vesicles specifically docked to RLG. Importantly, this vesicle prep was cytosol-free, and RLG was the only source of Cog3 protein, indicating that docking of CCD vesicle is independent of soluble factors and that the COG complex is acting from the Golgi side to direct the vesicle docking process.

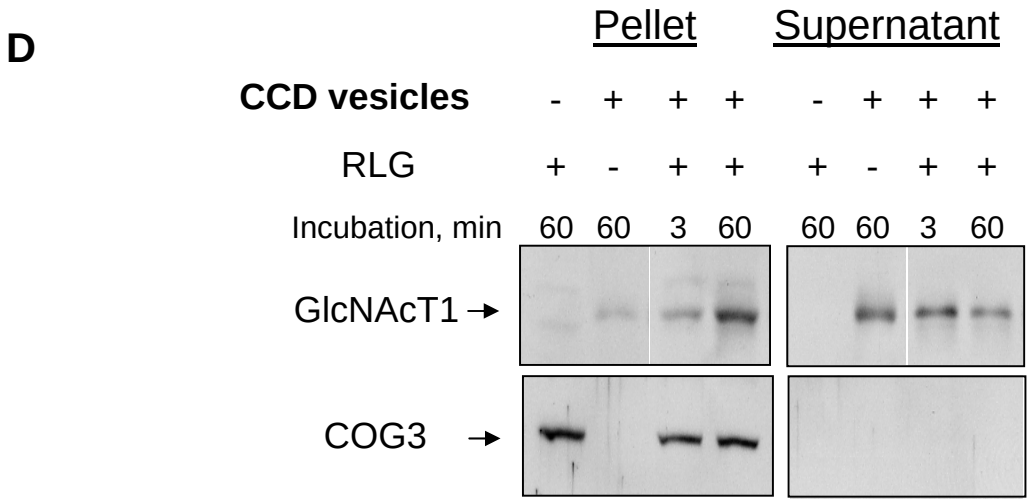


**Figure 11. Reconstitution of CCD vesicles docking to Golgi *in vitro*.** (**D**) CCD vesicles (GlcNAcT1) purified from glycerol velocity gradient bind to RLG (COG3) with ~40% efficiency.

*These findings have concluded that CCD vesicles are functional intra-Golgi intermediates, capable of docking to Golgi membranes in a COG complex-dependent reaction.*

## Key research accomplishments

1. Altered level of expression of COG3p (or COG complex) could be a common feature of cancer cells defective in protein trafficking and Golgi modifications.
2. The importance of the COG complex for both function and architecture of the Golgi apparatus does not depended on type of cells.
3 COG complex-dependent docking of isolated CCD vesicles was reconstituted *in vitro*, supporting their role as functional trafficking intermediates.

## Reportable outcomes

1. **Zolov, S.** siRNA-dependent Cog3 depletion causes rapid Golgi fragmentation. Participation in "Student Research Week" of the College of Medicine, University of Arkansas for Medical Sciences, Arkansas on April 19 – 22, **2004**
2. **Zolov, S.** and Lupashin, V. Cog3p depletion blocks vesicle-mediated Golgi retrograde trafficking in HeLa cells. Participation in ASCB (The American Society for Cell Biology) 44th Annual meeting, Washington Convention Center 801 Mount Vernon Place, NW Washington, DC 20001, December 4-8, **2004**.
3. **Zolov, S.** Cog3p depletion blocks vesicle-mediated Golgi retrograde trafficking in HeLa cells. Participation in "Student Research Week" of the College of Medicine, University of Arkansas for Medical Sciences, Little Rock, Arkansas, April 11-14, **2005**.
4. **Zolov S.N.** and Lupashin V.V. Cog3p depletion blocks vesicle-mediated Golgi retrograde trafficking in HeLa cells. ***J Cell Biol*** 168(5):747-59 (**2005**).
5. **Zolov, S.** and Lupashin, V. Mammalian COG complex serves as a "docking station" for retrograde Golgi vesicles. Participation in "Era of Hope" Department of Defense (DOD) Breast Cancer Research Meeting. Pennsylvania Convention Center, Philadelphia, Pennsylvania, June 8-11, p. 104, **2005**.
6. Lupashin, V., **Zolov, S.** and Shestakova, A. The COG complex regulates intra-Golgi cycling of vesicles that carry SNAREs and Glycosyltransferases. International Congress Center, Dresden, Germany, September 3-6, p. 156, **2005**.
7. **Zolov, S.** and Lupashin, V. CCD vesicles dock to Golgi *in vitro* in a Cog3p-dependent reaction. Participation in ASCB (The American Society for Cell Biology) 45th Annual meeting, Moscone Center, San Francisco, CA, December 10-14, **2005**.
8. Shestakova, A., **Zolov, S.** and Lupashin, V. COG complex-mediated recycling of Golgi glycosyltransferases is essential for normal protein glycosylation. ***Traffic*** 7:191-204 (**2006**).

## Conclusions

1. COG complex malfunction causes Golgi fragmentation into mini-stacks and vesicle accumulation.
2. Prolonged knockdown of COG3p affects glycosylation in secretory pathway.
3. Altered level of expression of COG3p (or COG complex) could be a common feature of cancer cells defective in protein trafficking and Golgi modifications. The importance of the COG complex for both function and architecture of the Golgi apparatus does not depend on type of cells.
4. Partial malfunction of the COG complex may play a role in establishing of cancer phenotype.
5. Constantly cycling medial-Golgi enzymes are transported from distal compartments in CCD vesicles. Dysfunction of COG complex leads to separation of glycosyltransferases from anterograde cargo molecules passing along secretory pathway, thus affecting normal protein glycosylation.

## Reference:


1. J. W. Dennis, M. Granovsky, C. E. Warren, *Biochim. Biophys. Acta*. **1473,** 21 (1999).
2. S. Keelokumpu, R. Sormunen, I. Kellokumpu, *FEBS Lett.* **516**, 217 (2002).
3. D. Ungar, T. Oka, E. E. Brittle, E. Vasile, V. V. Lupashin, J. E. Chatterton, J. E. Heuser, M. Krieger, M. G. Waters, *J. Cell Biol.* **157**, 405 (2002).
4. D. M. Kingsley, K. F. Kozarsky, M. Segal, M. Krieger, *J Cell Biol.*, **102**, 1576 (1986).
5. X. Wu, R. A. Steet, O. Bohorov, J. Bakker, J. Newell, M. Krieger, L. Spaapen, S. Kornfeld, H. H. Freeze, *Nat. Med.*, **10**, 518 (2004).
6. K. M. Ignatoskii, S. P. Ethier, *Breast Cancer Res Treat*., **54**, 173 (1999).
7. S. N. Zolov, V. V. Lupashin, *J. Cell Biol.* **168**, 747 (2005).
8. A. D. Linstedt, A. Mehta, J. Suhan, H. Reggio, H. P. Hauri, *Mol. Biol. Cell*, **8**, 1073 (1997).
9. G. Borland, J. A. Ross, K. Guy, *Immunology*, **93**, 139 (1998).
10. M. Fukuda, *J Biol Chem* **266**, 21327 (1991).
11. D. M. Kingsley, K. F. Kozarsky, M. Segal, M. Krieger, *J. Cell Biol.* **102**, 1576 (1986).
12. E. S. Suvorova, R. Duden, V. V. Lupashin, *J. Cell Biol*. **157**, 631 (2002).
13. Shestakova, A., Zolov, S. and Lupashin, V. COG complex-mediated recycling of Golgi glycosyltransferases is essential for normal protein glycosylation. *Traffic* **7**, 191 (2006).
14. F. G. Hanisch, *Biol. Chem.* **382**, 143 (2001).
15. M. Sameni, E. Elliott, G. Ziegler, P. H. Fortgens, C. Dennison, B. F. Sloane, *Pathol. Oncol. Res.*, **1**, 43 (1995).
16. A. Bensadoun, D. Weinstein, *Anal. Biochem.* **70**, 241 (1976).
17. Lin CC, Love HD, Gushue JN, Bergeron JJ, Ostermann J. ER/Golgi intermediates acquire Golgi enzymes by brefeldin A-sensitive retrograde transport in vitro. J Cell Biol. **147**, 1457 (1999).

# Appendices

1.

41

UNIVERSITY OF ARKANSAS FOR MEDICAL SCIENCES
COLLEGE OF MEDICINE
STUDENT RESEARCH WEEK
April 19 – 22, 2004
ABSTRACT FORM


PRINT NAME: Sergey N. Zolov

PRINT Faculty Sponsor: Vladimir V. Lupashin

ADDRESS: Department of Physiology and Biophysics 4301 W Markham slot 505, Little Rock, Arkansas 72205

TELEPHONE: HOME: 501-614-9747 UAMS: 501-603-1171 e-mail address: szolov@uams.edu


CATEGORY: GRADUATE STUDENT:___ MEDICAL STUDENT:___ HOUSESTAFF:___ POSTDOC FELLOWS: X

**On Wednesday, April 21st presenters must man their poster to be eligible for an award**
**Mark a time slot best for you** 9:00-11:00 AM X 1:00-3:00 PM___

siRNA dependent Cog3 depletion causes rapid Golgi fragmentation.


Sergey N. Zolov, Department of Physiology and Biophysics UAMS



The conserved oligomeric Golgi (COG) complex was identified as one of the evolutionary conserved protein complexes that regulate a cis-Golgi step in intracellular vesicular transport. This evolutionary conserved complex is composed of eight subunits. Mutations in the COG complex subunits result in defects in basic Golgi functions: glycosylation of secretory proteins, protein sorting and retention of Golgi resident proteins. We propose that the COG3 protein plays one of the main roles in these processes. We utilized RNA interference assay to knockdown of COG3p in HeLa cells to determine the effect of its depletion on Golgi proteins localization.

siRNA dependent Cog3 depletion cause rapid Golgi fragmentation and possibly accumulation of Golgi resident proteins in transport vesicles. Furthermore in COG3 depleted cells level of COG1, 2, 4 and 8 is also reduced while the level of COG5 and 6 subunits is not changed. We found that the COG complex physically interacts with components of intra-Golgi trafficking machinery including SNAREs and vesicle tether GM130. COG3 protein in normal conditions is localized on Golgi but in breast cancer cells in addition to the Golgi it is also found on peripheral structures where it colocalized with SNARE protein GS28. These results helps to further define the COG complex function in protein trafficking.


**The work presented is substantially that of the presenter and hence is eligible for award consideration:**

Zolov
Student Signature

Faculty Sponsor Signature

Department: Physiology # 505

Department: Physiology # 505

2.

*Abstracts*
*The American Society for Cell Biology*
*44th Annual Meeting*

*December 4-8, 2004*
*Washington, DC*

2551

**Cog3p depletion blocks vesicle-mediated Golgi retrograde trafficking in HeLa cells.**

S. Zolov, V. Lupashin; Physiology and Biophysics, University of Arkansas for Medical Sciences, Little Rock, AR

The Golgi apparatus organizes both the anterograde exocytic trafficking of newly synthesized proteins that travel from the endoplasmic reticulum to the plasma membrane and retrograde endocytic trafficking of cell surface molecules that travels back to the ER. The COG (Conserved Oligomeric Golgi) complex was identified as one of evolutionarily conserved multi-subunit protein complexes that regulate membrane trafficking in eukaryotic cells. We have previously proposed that yeast COG complex acts as a tether that connects cis-Golgi membranes and COPI-coated intra-Golgi vesicles. In this work we used siRNA strategy to efficiently knock-down Cog3p in Hela cells. Cog3p depletion is accompanied by reduction in Cog1, 2 and 4 protein levels and by rapid accumulation of COG complex dependent (CCD) vesicles carrying v-SNAREs gs15p and gs28p and cis-Golgi recycling glycoprotein gpp130. Some of these CCD vesicles appeared to be COPI coated. A prolonged block in CCD vesicle tethering induced extensive Golgi fragmentation. Similar Golgi fragmentation was observed when Hela cells were microinjected with anti-Cog3p antibodies. Fragmented Golgi membranes maintained their juxtanuclear localization, cisternal organization and were competent for anterograde trafficking of VSVG protein to the plasma membrane. In a contrast, Cog3p knock-down resulted in complete inhibition of retrograde trafficking of the Shiga toxin between the plasma membrane and the ER. We used native immunoprecipitations to show that the Golgi-located COG complex physically interacts with gs28p and COPI. In addition, the purified COG complex specifically tethers isolated CCD vesicles. For the first time we have demonstrated that the acute depletion of mammalian COG complex activity results in specific inhibition of tethering of retrograde intra-Golgi vesicles and that the efficient targeting of these CCD vesicles is essential for the maintenance of the Golgi structure. Supported by grants from the NSF (MCB-0234822) and DOD (DAMD17-03-1-0243).

2552

3.

**UNIVERSITY OF ARKANSAS FOR MEDICAL SCIENCES**
**COLLEGE OF MEDICINE**
**STUDENT RESEARCH WEEK**
**April 11 – 14, 2005**
**ABSTRACT FORM**

**PRINT**
**NAME:** Sergey N. Zolov

**PRINT**
**Faculty Sponsor:** Vladimir V. Lupashin

**ADDRESS:** Department of Physiology and Biophysics, room 238-2, Biomed 2, 4301 W Markham, Little Rock, Arkansas 72205

**TELEPHONE: HOME:** 501-614-9747 **UAMS:** 501-603-1171 **e-mail address:** szolov@uams.edu

**CATEGORY:** GRADUATE STUDENT:____MEDICAL STUDENT:____HOUSESTAFF:____POSTDOC FELLOWS: X

**On Wednesday, April 13th presenters must man their poster to be eligible for an award**
**Mark a time slot best for you 9:00-11:00 AM** X **1:00-3:00 PM**_____

## Cog3p depletion blocks vesicle-mediated Golgi retrograde trafficking in HeLa cells.

Sergey N. Zolov, Department of Physiology and Biophysics UAMS

The Golgi apparatus organizes both the anterograde exocytic trafficking of newly synthesized proteins that travel from the endoplasmic reticulum to the plasma membrane and retrograde endocytic trafficking of cell surface molecules that travels back to the ER. The Conserved Oligomeric Golgi (COG) complex is an evolutionarily conserved multi-subunit protein complex that regulates membrane trafficking in eukaryotic cells. Mutations in the COG complex subunits result in defects in basic Golgi functions: glycosylation of secretory proteins, protein sorting and retention of Golgi resident proteins. We propose that the COG3 protein plays one of the main roles in these processes.

In this work we used siRNA strategy to achieve an efficient knock-down of Cog3p in HeLa cells. Cog3p depletion is accompanied by reduction in Cog1, 2 and 4 protein levels and by accumulation of COG complex dependent (CCD) vesicles carrying v-SNAREs GS15 and GS28 and *cis*-Golgi glycoprotein GPP130. Some of these CCD vesicles appeared to be COPI coated. A prolonged block in CCD vesicles tethering is accompanied by extensive fragmentation of the Golgi ribbon. Fragmented Golgi membranes maintained their juxtanuclear localization, cisternal organization and are competent for the anterograde trafficking of VSVG protein to the plasma membrane. In a contrast, Cog3p knock-down resulted in inhibition of retrograde trafficking of the Shiga toxin. Further, the mammalian COG complex physically interacts with GS28 and COPI and specifically binds to isolated CCD vesicles.

We conclude that the mammalian COG complex serves as a “docking station” for retrograde Golgi vesicles. These results help to further define the COG complex function in protein trafficking.

This work was supported by grant from the Department of Defense (DAMD17-03-1-0243).

**The work presented is substantially that of the presenter and hence is eligible for award consideration:**

_____
Faculty Sponsor Signature

_____ Student Signature

Department: Physiology # 505 Department: Physiology # 505

for generating a standard curve. Concentrations of 18S gene were compared with those of the breast epithelium specific genes fat milk globule membrane antigen and whey acidic protein.

Our results led us to conclude that RT-PCR is sensitive for detecting RNA from small numbers of LCM selected cells, being able to detect few copies of RNA, whereas the amounts of RNA obtained by linear amplification did not suffice for its use in microarray analysis. These observations confirmed the usefulness of the application of LCM to cytospin preparations for obtaining pure cell populations for RNA extraction and of PCR RNA amplification for cDNA microarray analysis and of RT-PCR for gene expression level quantification. The possibilities of using a minimal number of cells and the utilization of RT-PCR instead of linear amplification for obtaining RNA in adequate amount and quality for performing cDNA microarray analysis represented a significant step to warrant that the breast epithelial cells from selected donors can be studied in the same fashion. These studies will lead to fruitful results through genomic hierarchical cluster analysis and bioinformatics for patient risk assessment. This meeting offers a great opportunity to scientists and health care providers of discussing with consumers and the general public affected by breast cancer the potential of this approach for assessing risk using molecular biomarkers.

*Original work supported by the U.S. Army Medical Research and Materiel Command under DAMD17-98-1-8083.*

## P13-21: A DECLINING PLASMA FIBRINOGEN ALPHA FRAGMENT IDENTIFIES HER2 POSITIVE BREAST CANCER PATIENTS AND REVERTS TO NORMAL LEVELS POST-SURGERY

**Qian Shi,[1] Lyndsay N. Harris,[1] Xin Lu,[2,3] Ana Petkovska,[1] Xiaochun Xu,[2] Justin Hwang,[1] Nora P. McElroy,[1] Robert Gentleman,[2] J. Dirk Iglehart,[1,4] and Alexander Miron[1,4]**
[1]Department of Cancer Biology, Dana-Farber Cancer Institute, Boston, MA; [2]Department of Biostatistics, Dana-Farber Cancer Institute, Boston, MA; [3]Department of Statistics, Harvard University, Boston, MA; [4]Department of Surgery, Brigham and Women's Hospital, Boston, MA
E-mail: qian_shi@dfci.harvard.edu

Breast cancer is the most common non-skin malignancy affecting women in the United States. Currently there is not a simple blood based diagnostic used to complement radiological screening and increase sensitivity of detection. We identify altered protein markers in plasma that revert to normal levels following surgical treatment. Since breast cancer is a heterogeneous disease, a homogenous HER2 positive subset of patients is compared to unaffected controls. A mass-spectrometric approach was used and supported by several statistical algorithms (Recursive Support Vector Machine, Random Forest Analysis and T-test) to define a set of biomarkers that segregated cancers from controls with an error rate of 17.6%. One of the markers is responsible for most of the resolving power in separating tumor from control samples as well as being one of the top significant markers that segregate pre and post surgical samples. This marker was identified as a fragment of fibrinogen Alpha (FGA) encompassing residues 586-610. It is present at higher levels in controls versus cancer and reverts to normal levels post surgery. Previously fibrinogen degradation products have been shown to increase in abundance in plasma from cancer patients in contrast to FGA586-610. The protease that cleaves FGA at amino acid 586 may be involved in cancer genesis or may also serve as a useful diagnostic. In conclusion we show that a reduction in plasma levels of a novel Fibrinogen Alpha c-terminal degradation product is indicative of cancer and reverts to normal levels following surgery in patients with HER2 positive disease.

*The U.S. Army Medical Research and Materiel Command under DAMD17-03-1-0330 supported this work.*

## P13-22: STROMAL HYPOXIA IN BREAST CANCER PROGRESSION

**Ladislav Tomes, M.D., Linda J. Curtis, and Peter H. Watson, M.D.**
Department of Pathology, University of Manitoba, Winnipeg, MB, Canada
E-mail: latomes@yahoo.com

Introduction: We hypothesized that stromal hypoxia is an important prognostic factor in breast cancer progression. In this fellowship project I set out to master techniques to identify novel genes responsible for differences in response to hypoxic stress between stroma and epithelium of invasive breast carcinoma.

Methods and Results: Using conventional PCR and Western blotting, I have shown that known epithelial hypoxic marker carbonic anhydrase IX (CAIX) is induced by hypoxia in fibroblasts in vitro on mRNA and protein level. Immunohistochemical examination of a series of invasive breast carcinomas showed that the frequency of stromal hypoxia, as identified by CAIX expression, was not directly related to necrosis or to epithelial hypoxia. Prognostic significance of stromal versus epithelial CAIX expression was also different (Tomes et al. 2003). The DNA microarray comparison of CAIX immunostained, laser microdissected frozen sections of invasive breast carcinoma identified novel hypoxia associated candidate genes. Differential expression of selected candidates was confirmed on mRNA level using real time PCR and Northern blotting. Immunostaining of tissue array, constructed from 120 invasive breast tumors, and statistical analysis of follow-up survival data, showed unexpected negative prognostic significance of candidate gene 92. Candidate 92 was previously asserted as a tumor suppressor gene. Relevance of candidate gene 92 in mammary gland was confirmed in mouse – observed gene expression levels varied during mammary gland development, lactation, and involution.

Summary: I mastered a chain of experimental methods used to identify novel differentially expressed genes. The candidate 92, identified in course of the project, can be used as a prognostic marker in clinical management of breast cancer, and it provides topic for further research elucidating it's mechanism of action.

*The U.S. Army Medical Research and Materiel Command under DAMD17-02-1-0465 supported this work.*

## P13-23: MAMMALIAN COG COMPLEX SERVES AS A "DOCKING STATION" FOR RETROGRADE GOLGI VESICLES

**Sergey Zolov, Ph.D., and Vladimir Lupashin, Ph.D.**
Department of Physiology and Biophysics, University of Arkansas for Medical Sciences, Little Rock, AR
E-mail: zolovsergey@uams.edu

In breast and some other cancers, the unusual production and secretion of aberrantly glycosylated proteins and lipids on the surface are associated with disease progression, metastasis and poor clinical outcome. Glycosylation abnormalities concern both N-linked and O-linked carbohydrate chains on glycoproteins and glycolipids. They likely impair many basic cellular functions, since terminal oligosaccharide units serve as highly specific biological recognition molecules implicated in major regulatory processes of the cell. These phenotypic changes in malignant cells highly correlate with marked structural and functional disorganization of the Golgi apparatus. The Conserved Oligomeric Golgi (COG) complex is a peripheral membrane protein complex localized on cis/medial Golgi cistern. This evolutionary conserved complex is composed of eight subunits. Cog1 and Cog2 deficient Chinese hamster ovary cells are viable, but exhibit defects in multiple Golgi glycosylation pathways establishing a role for the COG complex in mammalian Golgi function. Recently, two siblings were described with a fatal form of congenital disorders of glycosylation (CDG) caused by a mutation in the gene encoding COG7. All these data indicate that COG complex may participate in Golgi protein trafficking.

We utilized siRNA interference assay to knock-down COG3p in HeLa cells to determine how its acute knock-down would influence membrane trafficking and who are the protein partners of the COG complex on the mammalian Golgi? The results showed that Cog3p depletion is accompanied by reduction in Cog1, 2 and 4 protein levels and by rapid accumulation of COG complex dependent (CCD) vesicles carrying v-SNAREs gs15 and gs28 and cis-Golgi recycling glycoprotein GPP130. Some of these CCD vesicles appeared to be COPI coated. A prolonged block in CCD vesicle tethering is accompanied by extensive fragmentation of Golgi ribbon. Fragmented Golgi membranes maintained their juxtanuclear localization, cisternal organization and are competent for the anterograde trafficking of VSVG protein to the plasma membrane. In contrast, Cog3p knock-down resulted in inhibition of retrograde trafficking of the Shiga toxin. We found that the COG complex physically interacts with components of intra-Golgi trafficking machinery including v-SNARE GS28. In breast cancer cells the COG complex is localized not only on the Golgi but is also found on peripheral structures where it colocalizes with SNARE protein GS28.

We conclude that the mammalian COG complex serves as a "docking station" for retrograde Golgi vesicles. These results help to further define the COG complex function in protein trafficking.

*The U.S. Army Medical Research and Materiel Command under DAMD17-03-1-0243 supported this work.*

5.

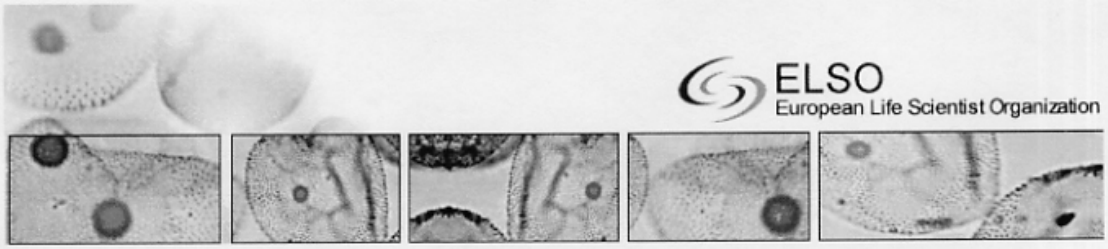

ELSO
European Life Scientist Organization



*Tuesday, 6th September 2005*

MINISYMPOSIUM FIFTEEN:
Membrane traffic

**The COG complex regulates intra-Golgi cycling of vesicles that carry SNAREs and Glycosyltransferases.**


**Vladimir Lupashin**, Sergei Zolov, Anna Shestakova
University of Arkansas for Medical Sciences, Little Rock



The COG complex is an evolutionarily conserved multi-subunit protein complex that regulates membrane trafficking in eukaryotic cells. In this work we used siRNA strategy to achieve an efficient knock-down of Cog3p in HeLa cells. For the first time we have demonstrated that Cog3p depletion is accompanied by reduction in Cog1, 2 and 4 protein levels and by accumulation of COG complex dependent (CCD) vesicles carrying v-SNAREs GS15 and GS28, putative cargo receptor GPP130 and cis-Golgi enzymes NAGT1 and Mann2. Some of these CCD vesicles appeared to be COPI coated. A prolonged accumulation of CCD vesicles is accompanied by extensive fragmentation of the Golgi ribbon and ultimately resulted in Golgi glycosylation defects. Fragmented Golgi membranes maintained their juxtanuclear localization, cisternal organization and are competent for the anterograde trafficking of underglycosylated CD44 and VSVG proteins to the plasma membrane and for correct sorting of LAMP2 to lysosomes. In a contrast, Cog3p knock-down resulted in inhibition of retrograde trafficking of the Shiga toxin. Further, the mammalian COG complex physically interacts with GS28 and COPI and specifically binds to isolated CCD vesicles. We propose that the COG complex is essential for correct tethering of retrograde intra-Golgi CCD vesicles that recycle SNAREs, cargo receptors and glycosylation machinery from distal compartments back to cis-Golgi.



[back]

6.



# *Late Abstracts The American Society for Cell Biology 45th Annual Meeting*

**December 10-14, 2005**
**The Moscone Center**
**San Francisco**

showed, after treatment with vanadium compounds, ultrastructural changes of Golgi complexes in comparison with the control group. We observed mild changes in the vanadyl sulfate group, slight changes in the ortovanadate-treated group, and considerable changes in the metavanadate group. In STS-diabetics cylindrical forms of Golgi body predominated. As compared with control in all vanadium treated groups reduction of body weight and fluid and food intake were observed. In comparison with untreated diabetes physiological improvement i.e. reduction of polyphagia and polyuria and polydypsia were caused by treatment with all investigated vanadium salts. Reduction of free blood sugar level was caused by vanadyl sulphate (c. 38%), sodium orthovanadate (c 23%) in all rats. In the sodium metavanadate - treated animals only 60% showed decreased blood sugar level (c.10%). None of investigated vanadium salts in experimental condition did normalize the activity of galactosyltransferase, the liver Golgi complexes marker enzyme.

L419

**Periodic Accumulation-Dispersion Cycle around the Golgi Apparatus Characterized by KIAA0290 Protein and Clathrin Light Chain in MDA-MB-435 Cells**

S. Sakaushi,[1] K. Senda-Murata,[1] K. Inoue,[1] H. Zushi,[1] T. Fukada,[1] S. Oka,[2,1] K. Sugimoto[1]; [1]Graduate School of Life and Environmental Sciences, Osaka Prefecture University, Sakai, Japan, [2]Research & Development Center, Nagase & Co., Ltd., Kobe, Japan

We have studied intracellular expression profiles of KIAA0290 protein by live imaging to approach its function. KIAA0290 protein (also called FCH domain only 1) has an FCH domain in the amino terminus but functions of the protein remain unknown. Live imaging microscopy revealed that EGFP-tagged KIAA0290 protein localized to the plasma membrane as well as the centrosome and scattered circularly as minute particles around the centrosome. Time-lapse analysis revealed that those particles periodically accumulated and dispersed around the centrosome approximately every 100 seconds. Simultaneous staining with Golgi apparatus-specific fluorescent ceramide revealed that the fine particles of KIAA0290 protein colocalized with the Golgi apparatus, while this Golgi-marker molecule did not show any accumulation-dispersion cycles. Treatment of the cells with brefeldin A inhibited the periodic fluctuations coincident with the disappearance of Golgi staining. The same intracellular localization and periodic movement were observed with stably expressed EGFP-clathrin light chain, which is known to be involved in intracellular vesicular transport. Our data suggest the presence of a periodic rhythm of the intracellular vesicular transport mechanism around the Golgi apparatus which is characterized by an accumulation-dispersion cycle of clathrin light chain and KIAA0290 protein. Our data also suggest that KIAA0290 protein is involved in the vesicular transport system around the Golgi complex.

L420

**Depletion of Vesicle-tethering Factor p115 Causes Mini-stacked Golgi Fragments with Delayed Protein Transport**

Y. Misumi,[1] M. Sohda,[1] T. Fusano,[1] S. Sakisaka,[2] Y. Ikehara[1]; [1]Cell Biology, Fukuoka University School of Medicine, Fukuoka, Japan, [2]Internal Medicine, Fukuoka University School of Medicine, Fukuoka, Japan

To maintain Golgi integrity and an ordered flow through the secretory pathway, a pair of membranes must specifically recognize and subsequently fuse with each other. Golgi must possess docking and fusion machinery that allows specific recognition of incoming membranes. One of the well-characterized tethering protein is p115, which is a peripheral membrane protein mainly localized to vesicular tubular intermediate clusters and the *cis*-Golgi. To examine the role of p115 in Golgi maintenance, we used small interfering RNA to deplete cellular p115 in HeLa cells. Depletion of p115 caused fragmentation of the Golgi apparatus, resulting in dispersed distribution of stacked short cisternae and a vesicular structure (mini-stacked Golgi). The mini-stacked Golgi with *cis*- and *trans*-organization is functional in protein transport and glycosylation, although secretion is considerably retarded in p115 knockdown cells. The fragmented Golgi was further disrupted by treatment with breferdin A and reassembled into the mini-stacked Golgi by removal of the drug, as observed in control cells. In addition, p115 knockdown cells maintained retrograde transport from the Golgi to the endoplasmic reticulum, although the rate was not so efficient as in control cells. While no alternation of microtubule networks was found in p115 knockdown cells, the fragmented Golgi resembled those of cells treated with anti-microtubule drugs. The results suggest that p115 is involved in vesicular transport between endoplasmic reticulum and the Golgi, along with microtubule networks.

L421

**CCD Vesicles Dock to Golgi In Vitro in a Cog3p-dependent Reaction**

S. Zolov, V. Lupashin; Physiology and Biophysics, University of Arkansas for Medical Sciences, Little Rock, AR

COG complex (for conserved oligomeric Golgi complex) is localized to the cis/medial cisternae of the Golgi apparatus and it is one of the key regulator of intracellular membrane trafficking. COG complex proposed function is to tether retrograde intra-Golgi vesicles. Our previous studies demonstrated that acute depletion of Cog3p caused accumulation of non-tethered COG complex-dependent (CCD) vesicles. These vesicles are COPI coated and packed with both recycling Golgi SNAREs (GS15, GS28) and putative retrograde cargo receptors, GPP130. CCD vesicles are likely to originate from *trans*-Golgi since they carry β-1,2-N-acetylglucosaminyltransferase-1 (GlcNacT1), and Mannosidase II, *medial*-Golgi enzymes that are known to cycle through *trans*-Golgi. To test if CCD vesicles indeed represent functional intra-Golgi transport intermediates we designed a novel *in vitro* system that reconstitute vesicle docking/fusion with isolated rat liver Golgi. The system based on sedimentation properties of Golgi (pelletable at 10,000xg) and CCD vesicles (not pelletable at 20,00xg). Both GlcNacT1-myc and GPP130 were used as vesicle markers. Our results indicated that CCD vesicles efficiently dock to isolated Golgi. Amount of sedimentable vesicle marker is proportional to the amount of added Golgi membranes. Vesicle-Golgi association is resistant to 250mM salt wash that normally strips loosely associated vesicles, indicating tight association and/or complete fusion. Acceptor Golgi membranes are sensitive to proteinase K treatment, indicating requirement for peripheral and/or transmembrane proteins. Indeed, both Golgi SNARE GS28 and Cog3p were completely digested by Proteinase K treatment. Most importantly, docking of CCD vesicles is sensitive to addition of anti-COG3 IgG. These results allow us to conclude that CCD vesicles are functional intra-Golgi intermediates that dock to Golgi membranes in a COG complex-dependent reaction. Supported by grants from the DOD (DAMD17-03-1-0243).

L422

**Multiple Regions of PITPβ Contribute to Golgi Localization**

K. E. Ile, S. E. Phillips, M. Boukhelifa, V. A. Bankaitis; Cell and Developmental Biology, University of North Carolina at Chapel Hill, Chapel Hill, NC

# Cog3p depletion blocks vesicle-mediated Golgi retrograde trafficking in HeLa cells

Sergey N. Zolov and Vladimir V. Lupashin

Department of Physiology and Biophysics, University of Arkansas for Medical Sciences, Little Rock, AR 72205

The conserved oligomeric Golgi (COG) complex is an evolutionarily conserved multi-subunit protein complex that regulates membrane trafficking in eukaryotic cells. In this work we used short interfering RNA strategy to achieve an efficient knockdown (KD) of Cog3p in HeLa cells. For the first time, we have demonstrated that Cog3p depletion is accompanied by reduction in Cog1, 2, and 4 protein levels and by accumulation of COG complex-dependent (CCD) vesicles carrying v-SNAREs GS15 and GS28 and cis-Golgi glycoprotein GPP130. Some of these CCD vesicles appeared to be vesicular coat complex I (COPI) coated. A prolonged block in CCD vesicles tethering is accompanied by extensive fragmentation of the Golgi ribbon. Fragmented Golgi membranes maintained their juxtanuclear localization, cisternal organization and are competent for the anterograde trafficking of vesicular stomatitis virus G protein to the plasma membrane. In a contrast, Cog3p KD resulted in inhibition of retrograde trafficking of the Shiga toxin. Furthermore, the mammalian COG complex physically interacts with GS28 and COPI and specifically binds to isolated CCD vesicles.

## Introduction

The Golgi apparatus is a hub for membrane trafficking pathways, organizing both the anterograde exocytic trafficking of newly synthesized proteins that travel from the ER to the plasma membrane and retrograde endocytic trafficking of cell surface molecules that travel back to the ER (for review see Shorter and Warren, 2002). COP I coat proteins function in intra-Golgi trafficking and in maintaining the normal structure of the Golgi complex (Duden, 2003). We and others have previously shown that the Golgi vesicular coat complex I (COPI)-modulated membrane trafficking used conserved oligomeric Golgi (COG) vesicle tethering complex (Ram et al., 2002; Suvorova et al., 2002; Oka et al., 2004).

COG complex consists of eight subunits (COG1-8; Kingsley et al., 1986; Whyte and Munro, 2001; Suvorova et al., 2001, 2002; Ram et al., 2002; Ungar et al., 2002). A COG role in Golgi membrane trafficking was suggested by biochemical and genetic studies in yeast (VanRheenen et al., 1998, 1999; Suvorova et al., 2002). Yeast COG complex interacts genetically and physically with Rab protein Ypt1p, intra-Golgi SNARE molecules, as well as with COPI (Suvorova et al., 2002).

Correspondence to Vladimir Lupashin: vvlupashin@uams.edu

Abbreviations used in this paper: CCD, COG complex-dependent; COG, conserved oligomeric Golgi; COPI, vesicular coat complex I; GalNAc-T2, *N*-acetylgalactosaminyltransferase-2; GalT-GFP, GFP-tagged β 1,4-galactosyltransferase; IF, immunofluorescence; IP, immunoprecipitation; KD, knockdown; PDI, protein disulphide isomerase; PNS, post-nuclear supernatant; siRNA, short interfering RNA; VSVG, vesicular stomatitis virus G protein; WB, Western blot.

Mutations in COG subunits disturb both structure and function of the Golgi in eukaryotic cells (Podos et al., 1994; Ram et al., 2002; Suvorova et al., 2002; Ungar et al., 2002; Farkas et al., 2003), but the exact cellular function of the COG complex remained elusive. It was recently shown that mammalian cells that carried either deletion of COG1 and 2 or truncated version of Cog7p are defective in Golgi glycosylation (Wu et al., 2004) and maintain slightly dilated Golgi cisternae with reduced levels of resident proteins GS15 and GS28 and GPP130 (Oka et al., 2004). These mutant phenotypes may reflect either the primary COG malfunction or secondary manifestations that occur in cells after a prolonged adaptation period. Deletion of either COG1 or COG2 in yeast cells is virtually incompatible with membrane trafficking and normal cell growth (VanRheenen et al., 1998; Ram et al., 2002), whereas Δ*COG1* and Δ*COG2* CHO cells are not compromised in growth or protein secretion. One possibility is that the primary COG deletion phenotype in these cells is masked and/or suppressed by secondary mutations in cell genome. To better understand the initial defects associated with the COG complex malfunction it is important to acutely interfere with its activity. Transfection with small interfering RNAs (siRNAs) and microinjection with inhibitory antibodies are two efficient methods for acute protein knockdown (KD) in mammalian cells.

We rationalized that the most evolutionary conserved COG subunit would be the best candidate for the KD. Yeast and mammalian Cog1 and Cog2 proteins do not share significant


The Journal of Cell Biology, Vol. 168, No. 5, February 28, 2005 747–759
http://www.jcb.org/cgi/doi/10.1083/jcb.200412003

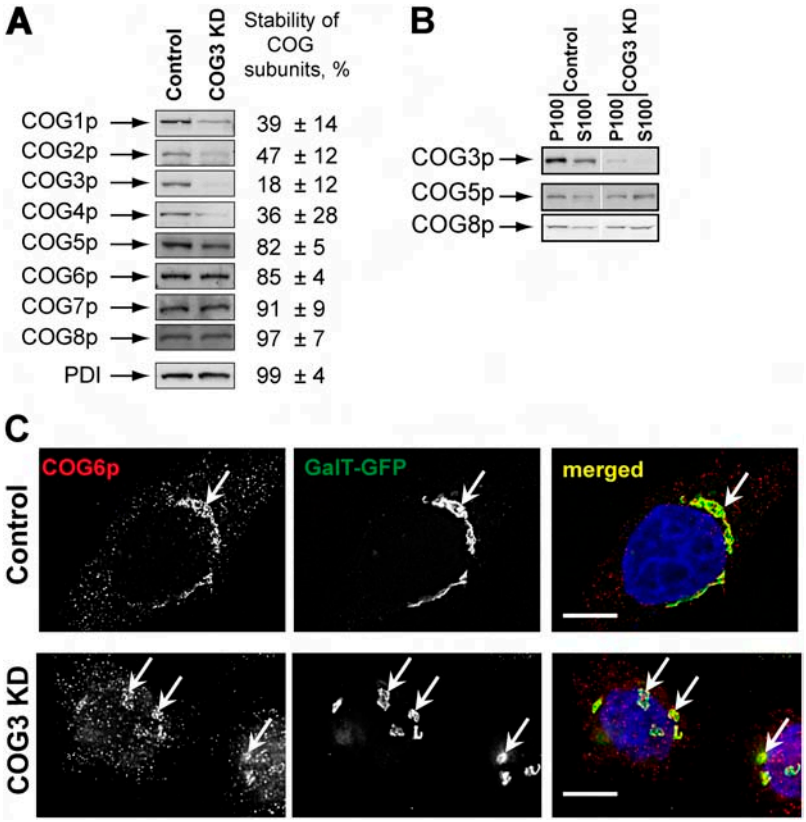


Figure 1. **SiRNA-induced COG3 KD is destabilizing Lobe A COG complex subunits.** (A) Expression of COG subunits after COG3 KD. WB of cell lysates from control and COG3 KD cells. Average levels of the COG subunits (±SD, $n = 4$) after 72 h of COG3 KD were determined by quantitative WB, and normalized to mock-transfected cells. (B) Membrane localization of COG complex subunits. WB of membrane (P100) and cytosol (S100) fractions. (C) Cog6p localization. Control and COG3 KD cells that stably express GalT-GFP were fixed and analyzed by three-color IF microscopy after immunostaining with anti-Cog6p. DNA was stained with DAPI. Arrows indicate Golgi or Golgi fragments. Bars, 10 μm.

similarities, whereas the protein sequence of yeast Cog3p is 41% similar to mammalian Cog3p (Suvorova et al., 2001). In this work, we used siRNA strategy for the efficient KD Cog3p in HeLa cells. Cog3p depletion is accompanied by reduction in Cog1, 2, and 4 protein levels and rapid accumulation of intracellular vesicles carrying v-SNAREs GS15 and GS28 and cis-Golgi glycoprotein GPP130. A prolonged COG3 KD induced extensive Golgi fragmentation. Fragmented Golgi membranes were deficient in retrograde trafficking of the Shiga toxin. Native immunoprecipitations (IPs) revealed that the COG complex physically interacts with Golgi SNARE molecules and COPI and specifically binds to isolated GPP130-containing vesicles in vitro. For the first time, we have demonstrated that the acute depletion of the mammalian COG complex results in specific inhibition of tethering of retrograde vesicles and that the efficient targeting of these vesicles is essential for the maintenance of the Golgi structure.

## Results

### Cog3p KD induces Golgi fragmentation

To interfere with the COG complex function in HeLa cells we depleted Cog3p by using RNA interference technique (Elbashir et al., 2001). Three different COG3-specific RNA duplexes were tested initially and one of them (sense, AGACUUGUGCAGUUUAACA) efficiently induced reduction of the Cog3 protein level (Fig. 1 A). The expression of other lobe A COG subunits Cog1p, Cog2p, and Cog4p was also reduced 72 h after COG3 KD, whereas protein level of the lobe B Cog5-8p subunits remained unchanged. Similarly, cellular levels were unchanged for other tested cell proteins: protein disulphide isomerase (PDI), actin, GS28, syntaxin 5, GPP130, and p115 (Fig. 1 and unpublished data). Cell transfection with a nonspecific siRNA did not change the levels of COG subunits expression (unpublished data).

Because the level of the lobe B COG subunits was not affected by the Cog3p depletion we have determined their intracellular localization by both immunofluorescence (IF) and Western blot (WB) assays. We have found that significant amounts of both Cog5p and Cog8p were still associated with the membrane fraction (Fig. 1 B). IF analysis of COG3 KD cells revealed that Cog6p (Fig. 1 C) and other lobe B subunits (unpublished data) were localized on large structures in juxtanuclear region that were colocalized with resident Golgi enzyme GFP-tagged β 1,4-galactosyltransferase (GalT-GFP; Fig. 1 C). Detailed analysis of COG3 KD cells revealed that both GalT-GFP and a Golgi tethering factor GM130 were found on fragmented Golgi membranes (Fig. 2).

To test the specificity of COG3 siRNA KD, we took advantage of the fact that human and mouse Cog3 proteins show 95% identity and, therefore, most likely would functionally substitute each other. In the same time, human and mouse COG3 siRNA target region share only 74% of homology with five miss-matched nucleotides (Fig. 3 A) and this difference can be used in gene-replacement siRNA experiments (Puthenveedu and Linstedt, 2004). In good agreement with our prediction, in HeLa cells, that were cotransfected with both hCOG3 siRNA and the plasmid that expressed mouse Cog3p,

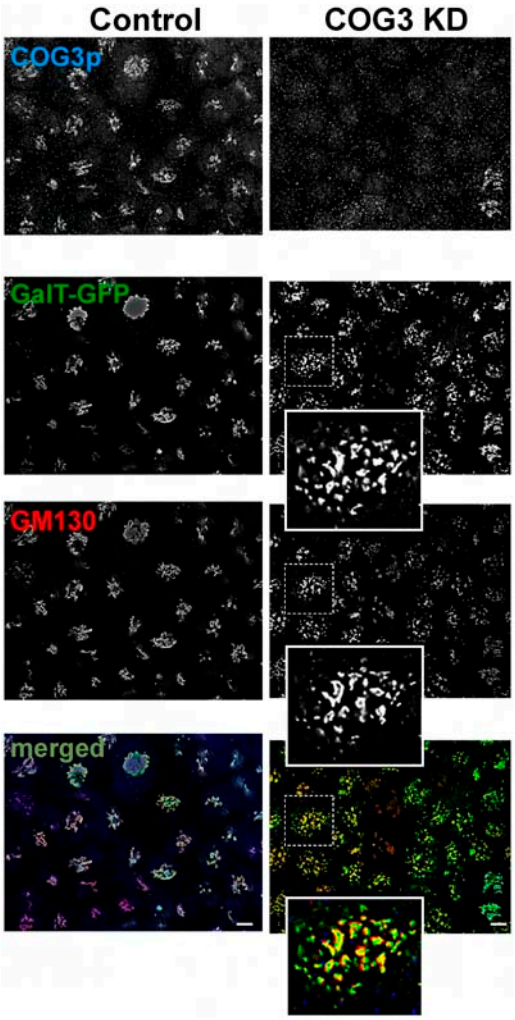


Figure 2. **Cog3p depletion induces Golgi fragmentation.** GalT-GFP HeLa cells were transfected with COG3 siRNA (right column) or mock transfected (left column). 72 h after transfection, cells were fixed and processed for IF with anti-Cog3p (COG3p row), and anti-GM130 (GM130 row) antibodies. The bottom row represent merged three-color images. Bars, 10 μm.

the Golgi fragmentation was completely or partially prevented (Fig. 3 B). Similar results were obtained when cells were transfected with mCOG3-containing vector 24 h after hCOG3 siRNA transfection (unpublished data). We concluded that the COG3 KD is specific and that the Cog3p depletion directly induces a reversible Golgi fragmentation.

To independently confirm an essential role for the COG complex in Golgi structure maintenance, we used affinity-purified antibodies against Cog3p (Suvorova et al., 2001). These antibodies were previously used for both IF and IP of the endogenous COG complex in mammalian cells (Suvorova et al., 2001; Ungar et al., 2002). We rationalized that upon microinjection into cells anti-Cog3p IgGs would specifically bind to the Cog3p and interfere with the COG complex function. Indeed, we have observed that 4 h after the antibodies microinjection the Golgi ribbon structure was converted into multiple mostly juxtanuclear localized small fragments (Fig. 4). This Golgi phenotype was persistent for up to 20 h after antibody microinjection without any visible signs of cell death. Microinjection with control antibodies did not change the morphology of the Golgi (unpublished data). We have concluded that anti-Cog3p antibodies like the COG3 siRNA act by blocking Cog3p function, which is necessary for the Golgi structure maintenance.

### Loss of Cog3p expression results in accumulation of Golgi v-SNAREs and cis-Golgi resident protein GPP130 in nontethered vesicles

Detailed IF analysis of different Golgi resident proteins in COG3 KD cells revealed that the majority of integral and peripheral membrane Golgi proteins, including cis-Golgi tethering factors p115 (Nelson et al., 1998) and GM130 (Nakamura et al., 1995), cis-Golgi t-SNARE syntaxin 5 (Hay et al., 1998), *cis/medial* Golgi tethering protein giantin (Linstedt and Hauri, 1993), and trans-Golgi tether p230 (Brown et al., 2001), were present almost exclusively on relatively large (1–3 μm in size) fragmented Golgi membranes (Fig. 5 A; unpublished data).



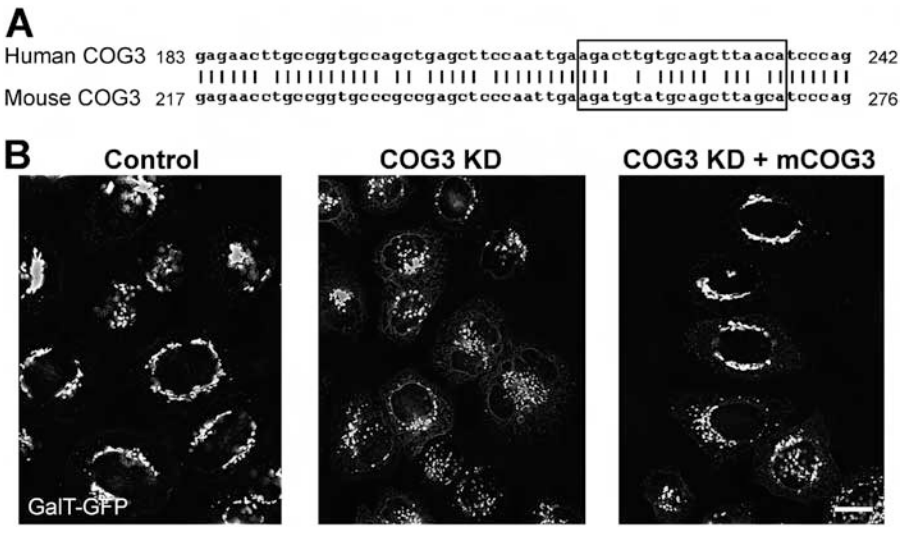


Figure 3. **Mouse COG3p expression partially suppresses hCOG3 KD-induced Golgi fragmentation.** (A) DNA alignment of a portion of the *hCOG3* and *mCOG3* sequences. siRNA target region is highlighted in the box. (B) GalT-GFP HeLa cells were either mock transfected (control), transfected with COG3 siRNA (COG3 KD), or simultaneously transfected with COG3p siRNA and mCOG3-encoding plasmid (COG3 KD +mCOG3) and imaged 72 h after transfection. Bar, 10 μm.

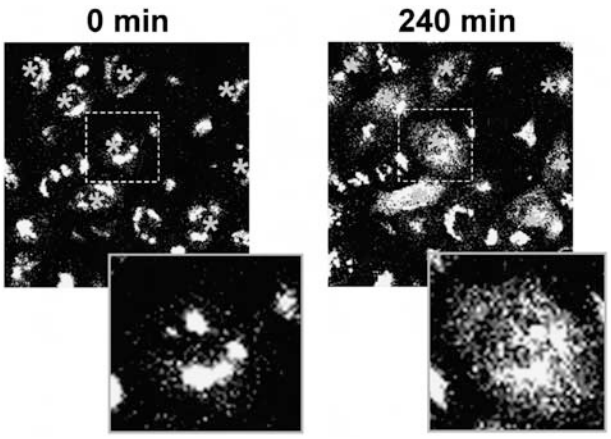


Figure 4. **Microinjection of anti-Cog3 antibodies disrupts Golgi structure.** GalT-GFP HeLa cells were microinjected with anti-Cog3p IgGs and imaged immediately (0 min) or 4 h (240 min) after the injection. Texas red was used as an injection marker. Note that in cells injected with anti-Cog3 IgGs Golgi (labeled with asterisks) become fragmented. Microinjections with the preimmune IgGs did not result in Golgi fragmentation (date not depicted).

Surprisingly, we have found that a subset of Golgi proteins, intra-Golgi v-SNAREs GS15 (Xu et al., 2002) and GS28 (Hay et al., 1998), and cis-Golgi phosphoprotein GPP130 (Linstedt et al., 1997) were localized preferentially to multiple small vesicle-like structures distributed throughout the cytoplasm of Cog3p KD cells (Fig. 5 B). In control cells all these three proteins were primarily localized to a juxtanuclear Golgi.

Small GPP130-positive structures in COG3 KD cells presumably represent nontethered vesicles, because, in cells permeabilized with the mild detergent digitonin, these structures were efficiently washed away from cells, whereas large Golgi cisternae remained inside the cells (Fig. 6 A). Similar digitonin sensitivity was previously observed for Golgi-derived vesicles that are transiently accumulated during mitosis (Jesch and Linstedt, 1998).

To verify our IF findings we performed a subcellular fractionation of both COG3 KD and mock-treated HeLa cells (Fig. 6 B). We have found that in COG3 KD cells >50% of both GPP130 and GS28 proteins are present in a 10K supernatant, whereas in lysates obtained from control cells these proteins are almost exclusively cofractionated with large membranes. Noticeably, the long syntaxin 5 isoform and the ER resident protein PDI did not significantly change their subcellular distribution in a COG3 KD cells.

To characterize membranes in 10K supernatant we have first used gel-filtration analysis on a Sephacryl S-1000 column (Fig. 6 C). This analysis revealed that in COG3 KD cells the peak of GPP130 was eluted in fractions 11 and 12, whereas in control cells GPP130 was mostly found in fractions 9 and 10. We have concluded that in COG3 KD cells the GPP130 was mostly associated with small vesicles.

To test GPP130 localization by another separation technique we used a glycerol velocity gradient. Post-nuclear supernatant (PNS) from COG3 KD cells was loaded on 10–30% glycerol gradient and membranes were separated by size (Fig. 6 D). WB analysis of collected fractions revealed that majority of GPP130 signal was peaked in a vesicular fraction 3, whereas large ER membranes (PDI lane) were concentrated at the bottom of the gradient. A small fraction (~25%) of GPP130 was also found at the bottom of the gradient and may represent a fraction of the protein that was associated with large Golgi fragments or vesicle aggregates. Because these vesicles were accumulated as a result of Cog3p depletion, we have named them a COG complex-dependent (CCD) vesicles. GPP130-containing Golgi membranes from identically fractionated control cells were rapidly pelleted to the bottom of the glycerol gradient (Jesch and Linstedt, 1998; unpublished data).

GPP130 is a heavily glycosylated cis-Golgi protein (Linstedt et al., 1997) that cycles through trans-Golgi and endosomal compartments (Puri et al., 2002) and rapidly degrades in

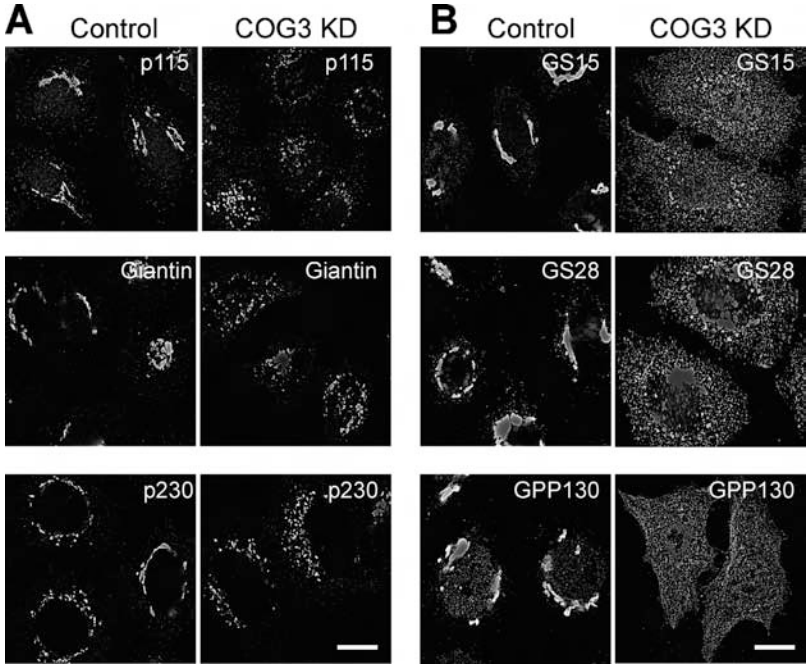


Figure 5. **COG3 KD results in accumulation of multiple vesicles that carry v-SNAREs GS15, GS28, and cis-Golgi recycling protein GPP130.** Control and COG3 KD cells were fixed 72 h after transfection and analyzed by IF using primary antibodies to indicated proteins and appropriate Alexa 488– and Alexa 595–conjugated secondary antibodies. (A) cis-Golgi tether p115, cis/medial Golgi marker giantin, and trans-Golgi tether p230 are present almost exclusively on Golgi ribbon in control cells and on fragmented juxtanuclear Golgi membranes in COG3 KD cells. (B) v-SNAREs GS15, GS28, and cis-Golgi marker GPP130 are Golgi located in control cells and predominantly localized on multiple small structures distributed throughout the COG3 KD cells. Bars, 10 μm.

both Δ*COG1* and Δ*COG2* CHO cell lines (Oka et al., 2004). We have found that both the protein level and the electrophoretic mobility of GPP130 were identical in both control and COG3-KD cells. Therefore, it can be concluded that in HeLa cells acute Cog3p depletion did not, at least initially, result in GPP130 down-regulation and did not alter its glycosylation.

To further analyze the content of CCD vesicles we prepared lysates from COG3 KD and control cells that stably express GFP-tagged *N*-acetylgalactosaminyltransferase-2 (GalNAc-T2). Both lysates were subjected to glycerol velocity gradient centrifugation, membranes from vesicle peak fractions 3 and 4 were concentrated and relative concentrations of Golgi and ER proteins were assessed by WB (Fig. 6 E). In an agreement with our IF data, we have found that in COG3 KD cells the amount of GPP130 in the CCD vesicle pool was increased by approximately fourfold. The concentrations of two other Golgi proteins, GS28 and GalNAc-T2-GFP were also increased by approximately twofold, whereas the amount of ER marker PDI remained unchanged. Small but detectable amounts of GPP130, GS28, and GalNAc-T2 in vesicular fractions prepared from control cells may represent a constitutive pool of recycling vesicles.

We also tested whether accumulated CCD vesicles could be recognized by the COG complex in vitro. The COG complex was purified from HeLa cells that transiently express YFP-Cog3p (Suvorova et al., 2001). Protein G–Agarose beads loaded with the COG complex were incubated with PNS fraction obtained from the COG3 KD cells. As a positive control for vesicle binding we used beads loaded with anti-GS15 antibodies and as a negative control for nonspecific binding we used protein G–Agarose beads. As expected, anti-GS15 beads efficiently pulled down GPP130-containing (Fig. 6 F, GS15 lane) and GS28-containing (unpublished data) vesicles. Importantly, the COG beads were also capable to precipitate GPP130-containing CCD vesicles (Fig. 6 F, compare lanes COG and control). We have concluded that CCD vesicles may directly bind to the COG complex and this interaction may be a fist step in vesicle tethering to the cis-Golgi.

Results of the subcellular fractionation experiments confirmed the IF data that showed accumulation of CCD vesicles in COG3 KD cells. It also raised an intriguing possibility that not only recycling SNARE proteins and GPP130, but also Golgi resident proteins like GalNAc-T2 may recycle in the COG complex-dependent manner. To test this hypothesis, we used HeLa cells that stably express VSV-tagged GalNAc-T2. It was shown previously that unlike the GFP-tag the small VSV-tag does not interfere with the GalNAc-T2 folding, function and localization (Storrie et al., 1998). Double IF labeling experiments revealed that the vesicular pool of GalNAc-T2-VSV increased significantly in COG3 KD cells (Fig. 6 G). In the same time, vesicularization of GalNAc-T2–containing Golgi region was not as dramatic as for GPP130-containing membranes and only a few vesicular profiles were double labeled with both Golgi markers. This may reflect different kinetics of GPP130 and GalNAc-T2 recycling as well as a possibility that different Golgi proteins may cycle in different membrane carries.

Does accumulation of CCD vesicles occur before or after COG3 KD-induced Golgi fragmentation? To answer this question we analyzed COG3 KD cells every 12 h after the initial COG3 siRNA transfection. We have found that 48 h after transfection both GS15 (Fig. 7) and GPP130 (unpublished data) were mostly found in CCD vesicles, whereas overall Golgi structure labeled with GalT-GFP has not yet been disturbed in a subpopulation of the COG3 KD cells. These data support the idea that accumulation of CCD vesicles may occur independently and before the Golgi fragmentation.

### Fragmented Golgi membranes are capable in supporting anterograde but not retrograde protein trafficking

Although siRNA-induced COG3 KD induced both accumulation of CCD vesicles and Golgi fragmentation, cells were able to multiply and their growth rate was not severely affected (unpublished data). Moreover, fragmented Golgi membranes maintained their juxtanuclear localization (Fig. 5 A). Detailed IF analysis revealed that cis-Golgi p115 (Nelson et al., 1998), and the medial Golgi GalNAc-T2 (Storrie et al., 1998), maintained their overlapping but distinct distribution on both control Golgi ribbon-like structure and Golgi fragments in COG3 KD cells (Fig. 8 A, GalNacT2/p115 frames). Similarly, localization of two *medial* Golgi proteins GalNAcT2 and giantin (Linstedt and Hauri, 1993) almost completely overlapped in both control and COG3 KD-treated cells (Fig. 8 A, GalNacT2/Giantin frames). And finally trans-Golgi localized p230 (Brown et al., 2001) maintained its relative localization in COG3 KD cells (Fig. 8 A, GalNacT2/p230 frames). We concluded that Cog3p KD resulted in Golgi fragmentation into multiple mini-Golgi stacks.

To confirm this conclusion the EM analysis of control and COG3 KD cells (Fig. 8) was performed. We found that in COG3 KD cells Golgi ribbon was disrupted onto multiple fragments, comprising three to four stacked cisternae (Fig. 8 B, ii). In addition to the Golgi fragments, a large number of ~60-nm vesicles were observed in COG3 KD cells (Fig. 8 B, iii). Thus, Cog3p depletion leads to both vesiculation of Golgi and break up of the ribbon to multiple mini-stacks.

To test whether these Golgi mini-stacks can support two basic Golgi functions, anterograde and retrograde proteins flow, we used GFP-tagged vesicular stomatitis virus G protein (VSVG) as a cargo marker for anterograde protein trafficking (Suvorova et al., 2001) and Cy3-labeled subunit B of the Shiga toxin (STB-Cy3) as a marker for the retrograde trafficking (Johannes et al., 1997).

2 d after siRNA treatment both control and COG3 KD cells were transfected with the vector that directs synthesis of the temperature-sensitive VSVG-GFP protein (Beckers et al., 1987). VSVG was accumulated in the ER for 16 h at the restrictive temperature (39.5°C). After that cells were transferred to the permissive temperature (32°C) to allow VSVG to travel toward plasma membrane and fixed 2 h later. This time frame is sufficient for VSVG delivery from the ER to PM in HeLa cells (Suvorova et al., 2001). Indeed, we have observed that the majority of both control and COG3 KD cells accumulated sig-

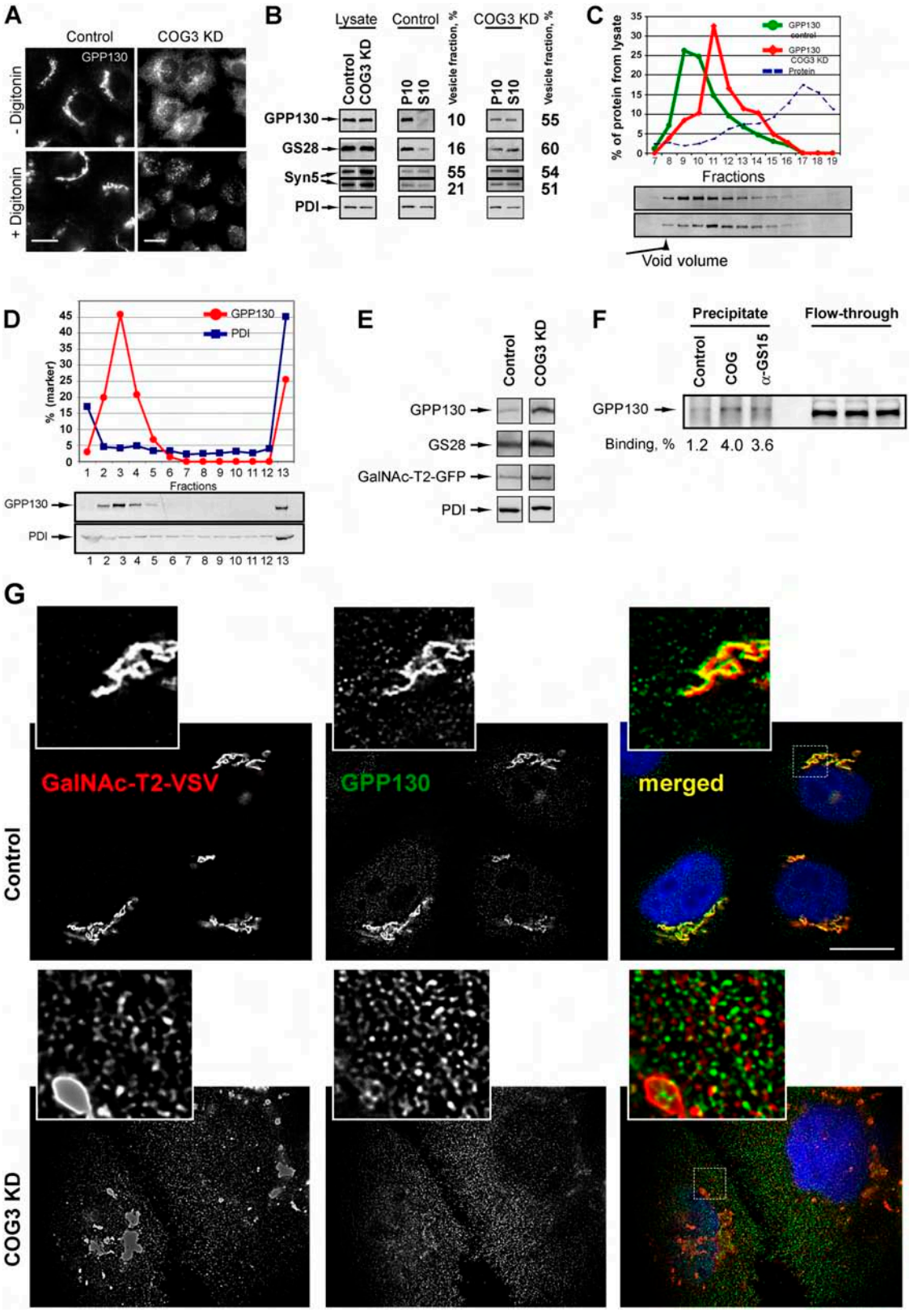


Figure 6. **Characterization of CCD vesicles.** (A) Apparent release of GPP130-containing vesicles upon digitonin permeabilization. Control or COG3 KD cells were either treated with buffer (−digitonin) or treated with 0.04 mg/ml digitonin, fixed, and analyzed by IF. Note that disperse vesicle-like staining of GPP130 in COG3 KD cells was eliminated after digitonin treatment. Bars, 10 μl. (B) WB analysis of total cell lysates and subcellular fractions prepared from COG3 KD and mock-treated HeLa cells. Cell lysates were fractionated on heavy membranes (P10) and light vesicle-containing fraction (S10). Equal amount of protein (10 μg) was loaded per lane and analyzed by WB with antibodies to GPP130, GS28, syntaxin 5, and PDI. A portion of marker proteins that was found in a vesicular fraction ($n = 2$) was determined by semi-quantitative WB. (C) Separation of GPP130-containing membranes by gel filtration. PNS from both control and COG3 KD cells was loaded on a Sephacryl S-1,000 column; 0.5-ml fractions were collected and analyzed by

nificant amounts of VSVG on the cell surface (Fig. 8 C, merged images, arrowheads). Some VSVG was also found on GS28-positive Golgi membranes in control cells and on Golgi fragments in COG3 KD cells. In COG3 KD cells the major pool of GS28 was localized on VSVG-negative CCD vesicles (Fig. 8 C, inset).

Detailed analysis of >200 VSVG-GFP-positive cells revealed some minor trafficking defects and/or kinetic delays in the ER-PM delivery of VSVG in COG3 KD cells (Fig. 8 D). Significantly, more cells in a control group demonstrated complete delivery of VSVG to the plasma membrane (22% vs. 6% in COG3 KD cells) and twice as many cells in the COG3 KD group accumulated VSVG in the ER (16% vs. 7% in COG3 KD cells). Nevertheless, because the absolute majority (84%) of the COG3 KD cells were able to deliver at least some VSVG molecules to the cell surface, we concluded that fragmented Golgi is, at least partially, competent to support anterograde protein trafficking. This result is in agreement with previous findings (Ram et al., 2002; Suvorova et al., 2002; Bruinsma et al., 2004) that demonstrate the COG complex defects in yeast cells do not interfere directly with the anterograde protein trafficking.

To investigate if Cog3p-depleted Golgi mini-stacks can function in retrograde plasma membrane to ER protein trafficking we have analyzed STB-Cy3 trafficking by using fluorescent live cell microscopy. In agreement with the data obtained in many different labs (Sandvig et al., 1994; Johannes et al., 1997) STB was rapidly internalized. In the majority of control cells STB signal was detected in juxtanuclear region 2 h after beginning of initial internalization (Fig. 8 E). In control cells 12 h later STB was entirely distributed between the ER and the Golgi cisternae, marked by GalNAc-T2-GFP, (Fig. 8 F, control row). In the COG3 KD cells, even at the 12 h time point, the majority of internalized STB was localized in punctuate structures on cell periphery (Fig. 8 F, COG3 KD row). Some STB was detected in a perinuclear region of transfected cells but these STB-labeled membrane structures were clearly distinct from the GalNAc-T2-GFP–containing Golgi fragments. None of the STB was detected in the ER of COG3 KD cells (Fig. 8, E and F, ER frames) indicating that retrograde trafficking through the Cog3-depleted Golgi was blocked.

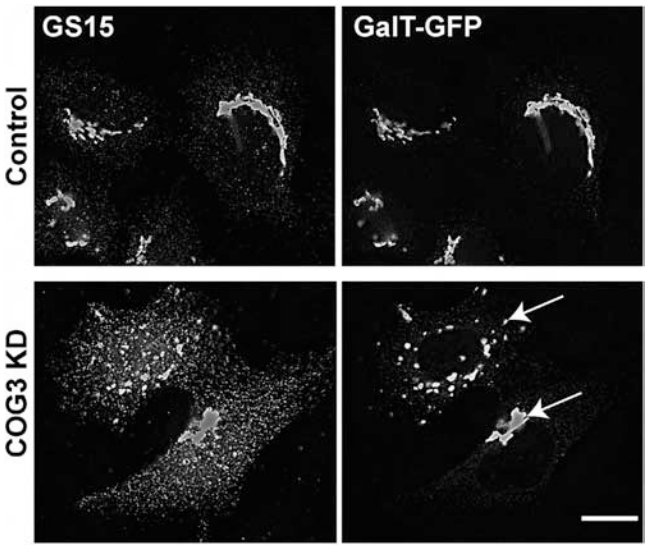


Figure 7. **Accumulation of CCD vesicles precedes COG3 KD-induced Golgi fragmentation.** Control or COG3 KD cells that stably express GalT-GFP were fixed 48 h after siRNA transfection and stained with anti-GS15 and secondary antibodies conjugated with Alexa 594. Images were acquired with 63× objective and deconvolved. Note that the Golgi (arrows) has not yet been fragmented in a subpopulation of the COG3 KD cells, whereas the majority of GS15 was associated with multiple CCD vesicles. Bar, 10 μm.

## COG complex physically interacts with the Golgi SNARE molecules and the COP I vesicular coat

We have previously demonstrated that the yeast COG complex regulates intra-Golgi retrograde trafficking and interacts with the essential components of core machinery of vesicular Golgi traffic, i.e., intra-Golgi SNARE proteins and COPI vesicular coat (Suvorova et al., 2002). To test if the mammalian COG complex may also interact with both SNARE and COPI components, we isolated Golgi from the rat liver and performed an IP of the COG complex, v-SNARE GS28, and PDI from detergent-solubilized membranes. WB analysis of coIP proteins revealed that both GS28 (~5% from total) and small amounts of t-SNARE Syntaxin5 were coprecipitated with the Cog3p (Fig. 9 A, lane 1; unpublished data). It was previously shown that Syntaxin5 and GS28 form a Golgi-localized SNARE complex (Hay et al., 1997) and our findings suggest that the COG complex can interact with either individual SNARE proteins or with the entire SNARE core complex. In the reciprocal precipitation, Cog3p was coIP by anti-GS28 antibodies (Fig. 9 A, lane 4). Neither Cog3p nor the Golgi SNARE molecules were precipitated with control beads (Fig. 9 A, lane 3). We have also determined that the β subunit of the COPI coat was specifically precipitated with anti-Cog3p antibodies (Fig. 9 B, lane 2). These results indicated that the mammalian COG complex like its yeast homologue

semi-quantitative WB. (D) Distribution of GPP130 and PDI on a velocity gradient. PNS from the COG3 KD cells was loaded on a 10–30% glycerol gradient. GPP130 and PDI were analyzed in fractions by semi-quantitative WB. Fraction 1 corresponds to the top of the gradient. (E) Analysis of CCD vesicle fraction. Fractions 3 and 4 from the glycerol gradient were concentrated by ultracentrifugation. Relative concentrations of Golgi and ER proteins were analyzed by WB as described in Materials and methods. (F) CCD vesicles specifically bind to the COG complex in vitro. PNS from COG3 KD cells was incubated with control beads, with beads loaded with the COG complex (COG), or with anti-GS15 IgGs (α-GS15). Precipitates were analyzed by WB with anti-GPP130 IgGs. (G) Accumulation of GalNAcT2 in CCD vesicles. Control or COG3 KD cells that stably express GalNAcT2-VSV were fixed and stained with mAbs to GPP130 or polyclonal anti–VSV-tag and secondary antibodies conjugated with Alexa 594 (GalNAc-T2-VSV) or Alexa 488 (GPP130) as described in Materials and methods. DNA was stained with DAPI. Images were acquired with 63× objective and deconvolved. Double IF labeling revealed that the vesicular pool of GalNAc-T2-VSV increased significantly in COG3 KD cells. Note that some vesicular profiles were double-labeled with both Golgi markers (insets). Bar, 10 μm.

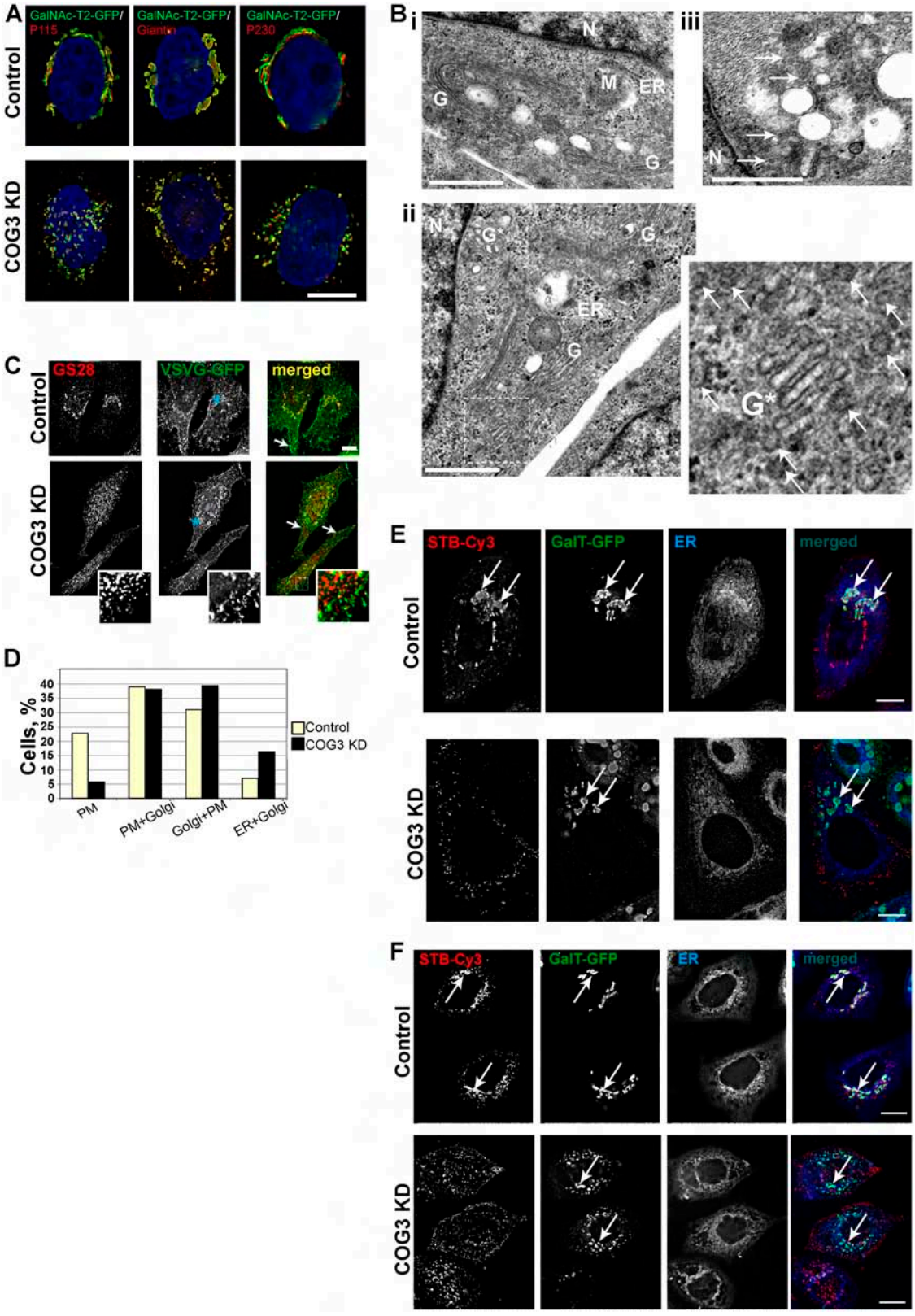


Figure 8. **Golgi in COG3 KD cells is disrupted to mini-stacks, which are proficient in anterograde VSVG delivery to plasma membrane and defective in retrograde trafficking of Shiga toxin B subunit.** (A) Control and COG3 KD cells that stably express GalNAcT2-GFP were fixed and stained with anti-p115, anti-giantin, or anti-p230 antibodies and secondary antibodies conjugated with Alexa 594. DNA was stained with DAPI. Images were acquired with 100× objective and deconvolved. Bar, 10 μm. (B) Ultrastructural analysis of Golgi in COG3 KD cells. Electron micrographs of the juxtanuclear region in control (i) and COG3 KD (ii and iii) cells. Note the Golgi mini-stack in ii and multiple 60-nm vesicles in COG3 KD cells (ii and iii, arrows). G, Golgi; M, mitochondria; N, nucleus; ER, endoplasmic reticulum. Bars, 1 μm. (C) Control and COG3 KD cells were transfected with the VSVG-GFP-ts045 vector. VSVG was accumulated in the ER for 16 h at 39.5°C. After that cells were transferred to 32°C, incubated for 2 h, fixed, and processed for IF with anti-GS28 antibodies.

could physically interact with both vesicular and Golgi-localized components of membrane transport machinery.

IF experiments indicated that CCD vesicles are distinct from both ER (Fig. 9 D) and early endosomes (Fig. 9 E). To test whether CCD vesicles are COPI-coated we performed double-IF in COG3 KD VSVG-GFP expressing cells (Fig. 9 C). A number of vesicle profiles were labeled with CCD vesicle marker GS15 and some were colabeled with antibodies against the epsilon subunit of COPI coat (Fig. 9 C, inset, arrowheads). In contrast, VSVG was colocalized with the GS15 only on a fragmented Golgi membrane (Fig. 9 C, inset, membranes marked with an asterisk). These data indicated that CCD vesicles do not carry anterograde cargo molecules and most likely represent COPI-coated retrograde intra-Golgi vesicles that bud from distal Golgi compartments and subsequently tether to the cis-Golgi in a COG complex-dependent manner.

## Discussion

Although both genetic and biochemical analysis indicated that the COG complex primarily regulates retrograde intra-Golgi membrane trafficking in budding yeast (Ram et al., 2002; Suvorova et al., 2002), the cellular role of the mammalian COG complex is less clear. COG has been implicated in the anterograde intra-Golgi trafficking (Walter et al., 1998), ER to Golgi protein delivery (Loh and Hong, 2002), glycoconjugate synthesis, intracellular protein sorting, and protein secretion (Kingsley et al., 1986; Chatterton et al., 1999; Wu et al., 2004). The most evolutionary conserved COG subunits bear 21–23% identity between yeasts and humans (Whyte and Munro, 2002). Therefore, it is hard to make any functional predictions that are simply based on protein similarities.

In this study, we report that the acute depletion of the Cog3p subunit of the human COG complex results in accumulation of nontethered transport vesicles, dramatic changes in overall Golgi structure and block of Shiga toxin retrograde trafficking. We have also obtained microscopic evidences that in COG3 KD cells the fragmented Golgi maintains its cisternal organization and that these Golgi mini-stacks are capable, at least partially, to support anterograde protein delivery from the ER to the plasma membrane. Finally, our data suggest that the COG complex can directly interact with the CCD retrograde vesicles via binding to both vesicular COPI coat and integral components of vesicular SNARE machinery.

The COG3 KD differentially influences the protein level of other COG subunits. Although the level of Cog1p, Cog2p, and Cog4p is reduced more than twofold, the expression of the other four subunits is not affected. Moreover Cog5-8p continue to localize properly to membranes in a juxtanuclear region. These data support our original model proposing two-lobed COG complex structure (Ungar et al., 2002; Loh and Hong, 2004) and suggests that Lobe B (COGs 5–8) may be attached to the Golgi membrane by its own receptor.

COG3 KD-induced Golgi fragmentation is specific and reversible because either simultaneous or subsequent introduction of the mouse siRNA-insensitive version of the Cog3p is able to restore a wild-type Golgi appearance. We have also demonstrated that the disruption of the Golgi structure is observed in cells microinjected with anti-Cog3p IgGs. The most likely explanation of this phenomenon is that the antibody microinjection induces the proteolytic degradation of the Cog3p similarly to the recently described antibody-induced degradation of the Golgi tethering factor p115 (Puthenveedu and Linstedt, 2001).

Observed Golgi fragmentation phenotype induced by the COG3 KD is distinct from the Golgi appearance in Δ*COG1* and Δ*COG2* CHO cells (Ungar et al., 2002) and indicate that the acute COG3 KD, at least transiently, disrupts normal structural organization of the Golgi complex. In the majority of COG3 KD cells fragmented Golgi membranes retain their juxtanuclear localization and their cisternal organization appear to be normal both at the light microscopy and the EM levels. The Golgi mini-stacks are capable to carry out a plasma membrane delivery of VSVG, though with reduced efficiency compared with a normal Golgi apparatus. This observation sharply differs from the effect of p115 KD on VSVG trafficking (Puthenveedu and Linstedt, 2004); it may reflect different roles of two cis-Golgi localized tethering factors in membrane trafficking. Moreover, in COG3 KD cells p115 is properly expressed (unpublished data) and its localization on the Golgi membranes is virtually undisturbed. Only a small fraction of the COG3 KD cells accumulates VSVG in the ER. These results agree with our previous data that yeast COG mutants do not show any primary anterograde trafficking defects (Suvorova et al., 2002) and that protein secretion in both Δ*COG1* and Δ*COG2* CHO cells is not compromised (Kingsley et al., 1986).

Specific vesicle accumulation is a most striking phenotype observed after the COG3 KD. These CCD vesicles seem to carry at least two different Golgi SNARE molecules, GS15 and GS28, and GPP130, a 130-kD, cis-Golgi protein that continuously cycle between the early Golgi and distal compartments (Linstedt et al., 1997). Significantly, it has been shown that these proteins are rapidly degraded in both ΔCOG1 and ΔCOG2 CHO cells (Oka et al., 2004). The most likely explanation is that after the acute COG3 KD, all three markers are

Both control and COG3 KD cells accumulated VSVG-GFP on the cell surface (merged images, arrows). Some VSVG was also found on GS28-positive Golgi membranes in control cells and on juxtanuclear Golgi fragments in COG3 KD cells. The major pool of GS28 was localized on a VSVG-GFP-negative CCD vesicles in COG3 KD cells (inset). Bar, 10 μm. (D) ~100 cells in both control and COG3 KD samples were analyzed and each cell was assigned in specific group bases on VSVG localization profile. PM, VSVG localized only on the plasma membrane; PM+Golgi, VSVG localized mostly on the plasma membrane, but partially (<30%) on the Golgi; Golgi+PM, VSVG localized on the plasma membrane, but mostly on the Golgi; and ER+Golgi, accumulation of the VSVG in the ER. All images were acquired with 63× objective and deconvolved. (E) Retrograde trafficking of STB-Cy3. Control and COG3 KD cells that stably express GalT-GFP were pulse incubated with the STB-Cy3 as described in Materials and methods and STB was allowed to internalize for 2 h. Cells were fixed and ER was visualized with ER-Tracker. Note that majority of STB in control cells reached the Golgi (arrows), whereas in COG3 KD cells the STB-Cy3 signal was detected only on cell periphery. Bars, 10 μm. (F) Same as in E, except GalNAc-T2-GFP HeLa cells were used and STB-Cy3 was internalized for 12 h. Bars, 10 μm.

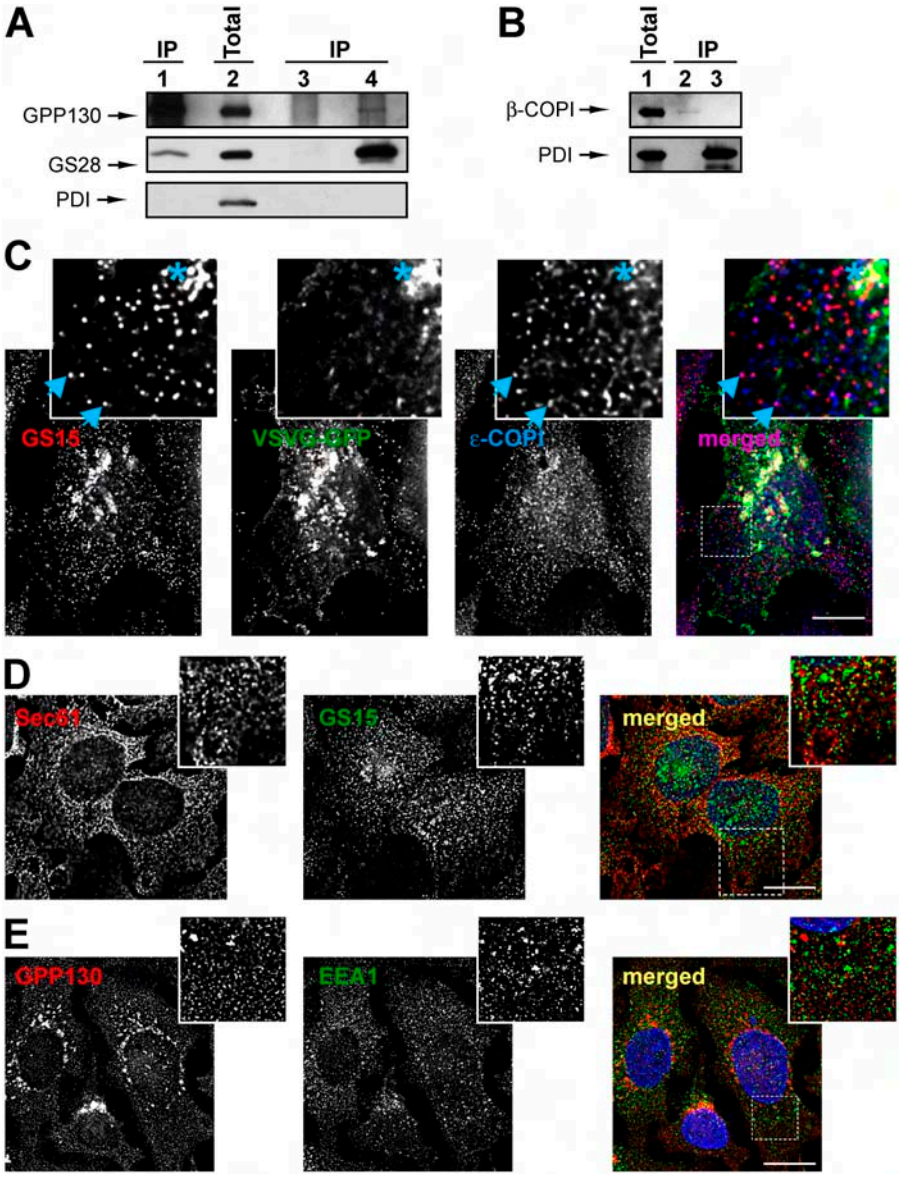


Figure 9. **The COG complex interacts with retrograde Golgi SNARE GS28 and β-COPI.** (A and B) Protein complexes from detergent-solubilized rat liver Golgi were IP using anti-Cog3p (A, lane 1; B, lane 2), anti-GS28 (A, lane 4), preimmune IgGs (A, lane 3), or anti-PDI (B, lane 3). 10% of the Golgi lysates were loaded as a control (A, lane 2; B, lane 1). Note that Cog3p, GS28, and β-COPI were not recovered with control beads or beads loaded with anti-PDI antibodies (A, lane 3; B, lane 3). (C) CCD vesicles are partially COPI coated and do not carry VSVG. COG3 KD cells that express VSVG-GFP were fixed and processed for IF with mouse anti-GS15 antibodies and rabbit anti–ε-COPI antibodies as described in Materials and methods. All images were acquired with 63× objective and deconvolved. Note that a number of GS15-labeled CCD vesicles were colabeled with antibodies to ε-COPI coat (inset, arrowheads). VSVG was partially colocalized with the GS15 only on a fragmented Golgi membrane (inset, membranes labeled with asterisk), but not on CCD vesicles. Bar, 10 μm. (D) CCD vesicles do not significantly colocalize with the ER. COG3 KD cells were fixed and stained with rabbit anti-Sec61p (red) and mouse anti-GS15 IgGs (green). Bar, 10 μm. (E) CCD vesicles are distinct from early endosomes. COG3 KD cells were fixed and stained with rabbit IgGs to GPP130 (red) and mouse anti-EEA1 IgGs (green). Bar, 10 μm.

transiently accumulated in nontethered recycling vesicles that are rapidly degraded. We have found that 90 h after COG3 KD the protein level of both GPP130 and GS28 was decreased (unpublished data). A number of Golgi resident proteins, including MG160 (Johnston et al., 1994), GP73 (Puri et al., 2002), GlcNAc T-1, and α-1,2 mannosidase II (Opat et al., 2001a,b) are shown to cycle through the trans-Golgi region. The prediction is that in COG3 KD cells all these proteins will, at least transiently, be accumulated in CCD vesicles.

What is the origin of CCD vesicles? IF data indicated that the major pool of CCD vesicle is clearly distinct from both ER and early endosomes. Some of CCD vesicles are likely to originate from the trans-Golgi because both GS28 and GS15 are SNARE molecules that function in the intra-Golgi trafficking (Xu et al., 2002; Volchuk et al., 2004). Alternatively, some CCD vesicles could originate from TGN/sorting endosomal/recycling compartments. GPP130 was shown to cycle through the trans-Golgi/early endosomal membranes (Linstedt et al., 1997) and both GS28 and GS15 could participate in the early endosomal SNARE complex (Tai et al., 2004). Current models of Golgi trafficking involving cisternal maturation (Pelham, 2001) predict that all Golgi residents move down the stack to the late Golgi. Indeed, a number of cis-Golgi residents in both yeast (Harris and Waters, 1996) and mammalian cells (Johnston et al., 1994; Bachert et al., 2001; Opat et al., 2001a) have been shown to rapidly acquire specific modifications of the late Golgi. The rapid rate of trans-Golgi modifications (Opat et al., 2001a) and relatively slow rate of the recycling through the ER (Miles et al., 2001) suggest that cis- and *medial*-Golgi resident proteins are recycled directly from the trans-Golgi and/or TGN to the corresponding early Golgi compartment. The COG complex localizes on *cis/medial* Golgi membranes (Suvorova et al., 2001; Ungar et al., 2002) and most likely regulates recycling of different resident Golgi proteins. We and others have shown that mutations in y*COG3* resulted in abnormal Golgi recycling of yeast Golgi proteins Sec22p and Och1p (Suvorova et al., 2002; Bruinsma et al., 2004).

CCD carriers are most likely to be formed in a COPI-dependent reaction. COPI vesicles bud from all Golgi cisternae and COPI is required for intra-Golgi transport in vitro (Orci et al., 1997). In the in vitro assay, Golgi resident proteins mannosidase II and GS28, were found to be concentrated in COPI vesicles (Lanoix et al., 1999, 2001), and these transport intermediates were able to fuse with cis-Golgi compartment (Love et al., 1998). The COG complex is a good candidate to orchestrate COPI vesicle tethering. Indeed, genetic and biochemical connections between yeast COG and COPI complexes (Ram et al., 2002; Suvorova et al., 2002) have been shown. Oka et al. (2004) reported recently that synthetic phenotypes arose in mutants deficient in both epsilon-COPI and either COG1 or COG2. During the investigation, we have found significant accumulation of COPI-positive vesicular profiles in COG3 KD cells (unpublished data) and demonstrated that some of these vesicles are double-labeled with the CCD vesicle cargo GS15. Finally we have shown that the COG complex binds to CCD vesicles in vitro and could be coIP with the β-COPI.

In conclusion we propose a model (Fig. 10) in which the cis-Golgi localized COG complex acts as a tether for retrograde COPI coated CCD vesicles that originate from distal trans-Golgi/endosomal compartments. The acute COG3 KD and corresponding defects in the Lobe A of the COG complex discontinue normal vesicle recycling. Non-tethered vesicles are transiently accumulated in cell cytoplasm as membrane-depleted Golgi ribbon is fragmented in multiple Golgi mini-stacks. Detailed biochemical analysis of CCD vesicles and the elucidation of exact roles of both lobes of the COG complex should help in our understanding of mechanisms of Golgi maintenance and function.

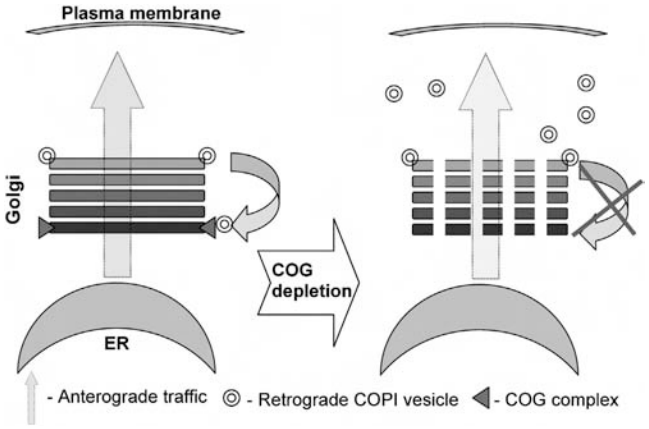


Figure 10. **Model for the COG complex function in membrane trafficking.** *Cis-Golgi* localized COG complex acts a tether for retrograde COPI-coated CCD vesicles that originate from the trans-Golgi/endosomal compartment(s). The COG3 KD abolishes vesicle tethering to the cis-Golgi. As a result multiple nontethered vesicles are transiently accumulated in cell cytoplasm and the membrane-depleted Golgi ribbon is fragmented into multiple Golgi mini-stacks.

## Materials and methods

**Reagents and antibodies**

Most laboratory reagents were purchased from Sigma-Aldrich. Antibodies used for WB and IF studies were obtained from standard commercial sources and as gifts from generous individual investigators or generated by us (see below). Antibodies (and their dilutions) were as follows: rabbit pAbs: anti-Cog1 (Ungar et al., 2002), anti-Cog2p (Podos et al., 1994; Ungar et al., 2002), anti-Cog3p (Suvorova et al., 2001), anti-Cog4p (Ungar et al., 2002), anti-Cog5p (Walter et al., 1998), anti-Cog6p, anti-Cog7p, anti-Cog8p (Ungar et al., 2002), anti-GPP130 (Covance), anti-giantin (a gift from A.D. Linstedt, Carnegie Mellon University, Pittsburgh, PA), anti-p115 (a gift from M.G. Waters, Merck Research Laboratories, Rahway, NJ), anti–ε-COPI (a gift from R. Duden, Royal Holloway University of London, Egham, Surrey), rabbit pAb and monoclonal (18C8) anti-syntaxin 5 (a gift from J. Hay, University of Michigan, Ann Arbor, MI), anti–β-COPI (Sigma-Aldrich), anti-VSVG tag (E11; Delta Biolabs); murine mAbs: anti-GPP130 (A1-118; a gift from A. Linstedt), anti-GM130 (BD Biosciences), anti–GS-28 (BD Biosciences), anti-GS15 (BD Biosciences), anti-p230 (BD Biosciences), and anti-PDI (Affinity BioReagents).

**Mammalian cell culture, plasmids, and transfection**

Monolayer HeLa cells were cultured in DME/F-12 media supplemented with 15 mM Hepes, 2.5 mM L-glutamine, 5% FBS, 100 U/ml penicillin G, 100 μg/ml streptomycin, and 0.25 μg/ml amphotericin B. Cells were grown at 37°C and 5% $CO_2$ in a humidified chamber. HeLa cells that stably expressed GalNAc-T2 fused to GFP or to a VSV-tag and GalT fused to GFP were provided by B. Storrie (University of Arkansas for Medical Sciences, Little Rock, AR; Storrie et al., 1998). The plasmid encoding VSVGtsO45-GFP was obtained from M.A. McNiven (Mayo Clinic, Rochester, MN). The plasmid pYFP-hCOG3 was described previously (Suvorova et al., 2001). pCMV-SPORT6 with cDNA of *mCOG3* (clone ID 4020725; NCBI Accession BC038030) was obtained from Invitrogen and mCOG3 sequence was verified by sequencing. Transfections were performed using TransIT-HeLaMONSTER Kit (Mirus Corporation).

**RNA interference experiment**

Human COG3 was targeted with a siRNA duplex (target sense, AGACTTGTGCAGTTTAACA). siRNAs were obtained as purified duplexes obtained from Dharmacon Research. Transfection was performed using Oligofectamine (Invitrogen) following the protocol recommended by Invitrogen. For WB, cells were plated in 24-well dishes, grown to a confluency of ~70%, transfected with siRNA for 24–72 h, and lysed in the SDS-PAGE sample buffer.

**IF microscopy**

IF microscopy was performed using an epifluorescence microscope (Axiovert 200; Carl Zeiss Microimaging, Inc.) with a Plan-Apochromat 63× oil immersion lens (NA 1.4) at RT. The secondary antibodies conjugated to Alexa Fluor 488 or 594 were obtained from Molecular Probes, Inc. The images were obtained using a QImaging Retiga Fast-EXi camera that was controlled via IP Lab software. During the processing stage, individual image channels were pseudocolored with RGB values corresponding to each of the fluorophore emission spectral profiles. Images were cropped using Adobe Photoshop software. Where indicated, images were digitally deconvolved (Huygens Professional, Scientific Volume Imaging).

**Live cell fluorescence microscopy**

For live cell fluorescence microscopy, cells were cultured in Lab-TekII Chambered Coverglass System (Nalge Nunc). Cells were maintained on the microscope stage in a chamber at RT in DME/F12 without phenol red and sodium pyruvate (Invitrogen).

For analysis of anterograde transports both COG3 KD and mock-treated HeLa cells 60 h after siRNA treatment were transfected with a vector that encoded VSVGts045-GFP protein and were kept at the 39.5°C for 16 h (Suvorova et al., 2001). After that the temperature was reduced to permissive one (32°C) to allow the VSVG to travel toward the plasma membrane. After 2 h of chase, cells were fixed and stained for GS28.

For analysis of retrograde transport Cy3-Shiga toxin B subunit (STB-Cy3; Mallard et al., 1998) was used. STB-Cy3 was a gift from B. Storrie. 60 h after the start of COG3 KD HeLa cells that stably express the Golgi markers GalT-GFP or GalNacT2-GFP were incubated with STB-Cy3 for 30 min at 4°C, washed, refueled with fresh DME medium without phenol red, and incubated for 2 or 12 h at 37°C and 5% $CO_2$ in a humidified chamber. ER was visualized with the ER-Tracker blue-white PDX (Molecular Probes). Images were obtained as described above.

**EM**

Cells were fixed with 3% glutaraldehyde in PBS for 2 h at 4°C. Cells were washed three times with PBS, fixed with 2% $OsO_4$ in PBS, washed again,

dehydrated in a graded ethanol series, and embedded in Epon 812. Ultrathin sections were obtained using RMC MT-7000 microtome, double stained with uranyl acetate and lead citrate. Specimens were examined using JEOL JEM-1010 electron microscope at 80 kV with magnification ranging from 15,000 to 75,000×.

**Microinjection of anti-COG3 antibodies**

HeLa cells that stably expressed GalT-GFP were microinjected with anti-Cog3p IgGs with the Narishigee Micromanipulator and imaged immediately and 4 h after the injection using a 40×, 1.3 NA Fluor objective fitted to a confocal microscope (model LSM410; Carl Zeiss MicroImaging, Inc.). The antibody concentration was 2 mg/ml, Texas red was used as an injection marker. Microinjection of the preimmune IgGs was used as the control.

**Cell fractionation and preparation of CCD vesicles**

HeLa cells were cultured to ~80% confluence in 60-mm dishes and transfected with COG3 siRNA. 78 h after transfection (KD efficiency of Cog3p ~80%), cells were washed three times with PBS and then scraped in 0.3 ml of 20 mM Hepes-KOH buffer, pH 7.4, supplemented with a proteinase inhibitor cocktail (Roche Diagnostics Corporation) on ice. The cells were disrupted using a Potter homogenizer. Subcellular fractions were obtained by standard differential centrifugation. The PNS was obtained at 500 *g* (5 min, 3°C). Heavy membranes, including ER and the Golgi were pelleted at 10,000 *g* (10 min, 3°C). Light membranes, including transport vesicle were obtained by centrifugation conducted in a rotor (model TLA-100; Beckman Coulter) at 100,000 *g* (1 h, 3°C). All membrane pellets were resuspended in 2% SDS in volumes equal to volume of original lysate. Membrane and cytoplasmic proteins were denatured by heating at 95°C for 5 min. To normalize the sample loading for WB analysis, protein content was measured using the BCA reagent (Pierce Chemical Co.).

**Glycerol velocity centrifugation and gel filtration**

Gradient fractionation was prepared as described previously (Jesch and Linstedt, 1998) with some modification. To prepare the lysate, 72 h COG3 KD HeLa cells from one 10-cm plate were collected by trypsinization, pelleted (500 *g* for 5 min), then washed once in PBS, and once in STE buffer (250 mM sucrose, 10 mM triethylamine, pH 7.4, 1 mM EDTA, with protease inhibitors), homogenized by 20 passages through a 25-gauge needle in 0.5-ml buffer STE without sucrose, and then centrifuged at 1,000 *g* for 2 min to obtain PNS. This supernatant was used for both gradient fractionation and gel filtration. PNS (1 ml) was layered on linear 10–30% (wt/vol) glycerol gradients (12 ml in 10 mM triethylamine, pH 7.4, and 1 mM EDTA on a 0.5 ml 80% sucrose cushion) and centrifuged at 280,000 *g* for 60 min in a SW40 Ti rotor (Beckman Coulter).

1 ml fractions were collected from the top. All steps were performed at 4°C. 50 μl of each fraction was combined with sample buffer, then loaded on SDS-PAGE and analyzed by WB.

For gel filtration analysis, PNS was loaded onto 29 × 0.7 cm Sephacryl S-1000 gel filtration column. Material was eluted in STE buffer at flow rate of 0.3 ml/h. 0.5-ml fractions were collected and analyzed by WB.

**Interaction of the COG complex with CCD vesicles**

The COG complex was isolated from HeLa cells that express YFP-Cog3p (Suvorova et al., 2001). Cells from two 10-cm plates were homogenized in equal volumes of cold CTN buffer (2% CHAPS, 40 mM Tris-HCl, pH 7.4, 300 mM NaCl, protease inhibitor cocktail) on ice. Cell lysates were clarified by centrifugation at 20,000 *g* for 10 min. The supernatant was transferred into a new presiliconized tube, diluted twice with TBST (TBS with 0.05% Tween 20), and incubated with 50 μl of protein A Sepharose CL-4B (Amersham Biosciences) on a tube rotator for 30 min, then beads were sedimented at 500 *g* (1 min, 3°C). The supernatant was transferred in a new tube, 2 μg of anti-GFP antibodies were added, and the tube was incubated on the tube rotator for 4 h in a cold room. After that 30 μl of protein G–Agarose beads were added to the samples and incubated for 1 h. Beads were sedimented by centrifugation at 110 *g* for 1 min and washed four times with TBST. The COG complex-loaded beads were transferred to a new tube, washed again and finally resuspended in 60 μl of TBST. 20 μl of beads were tested for the presence of YFP-Cog3p and other COG subunits by WB.

40 μl of COG complex beads were incubated for 4 h with the CCD vesicles enriched supernatant from the COG3 KD cells. Beads were washed three times and eluted with the sample buffer. Similar Incubation with untreated protein G–agarose beads or protein G–agarose beads preloaded with anti-GS15 antibodies was used as a control.

**IP experiments using rat liver Golgi membranes**

Rat liver Golgi membranes were purified as described by Hamilton et al. (1991) and frozen in aliquots in liquid nitrogen. All of the following operations were performed in a cold room. Membranes were thawed on ice in an equal volume of cold CTN buffer and incubated for 30 min. 50 μl of protein A Sepharose in TBS was added and incubated on a tube rotator for 30 min. Insoluble material and beads were pelleted at 20,000 *g* for 10 min at 3°C. The supernatant was transferred to a new tube and diluted twice with TBST. 2 μg of anti-Cog3p, anti-GS28 or anti-PDI antibodies were added to the diluted samples and incubated on tube rotator for 4 h. 20 μl of protein G agarose were added to the samples and incubated for another hour. After incubation the beads were sedimented by low speed centrifugation at 110 *g* for 1 min and washed four times with TBST. After that beads were transferred to a new tube, resuspended in 30 μl of 2× sample buffer, heated for 5 min at 95°C, loaded on SDS-PAGE, and analyzed by WB.

**SDS-PAGE and Western blotting**

SDS-PAGE and WB were performed as described by Suvorova et al. (2002). A signal was detected using a chemiluminescence reagent kit (PerkinElmer Life Sciences) and quantitated using ImageJ software (http://rsb.info.nih.gov/ij/).

We thank B. Storrie and R. Kurten for help with IF and microinjections and M. Crocker for great help with EM. We are very grateful to O. Pavliv for excellent technical assistance and to A. Shestakova for valuable comments on this manuscript. We also thank R. Duden, J. Hay, F. Hughson (Princeton University, Princeton, NJ), M. Krieger (Massachusetts Institute of Technology, Cambridge, MA), A. Linstedt, D. Ungar (Princeton University), and others who provided antibodies and other valuable reagents.

This work was supported by grants from the National Science Foundation (MCB-0234822) and the Department of Defense (DAMD17-03-1-0243).

Submitted: 1 December 2004
Accepted: 11 January 2005

## References

Bachert, C., T.H. Lee, and A.D. Linstedt. 2001. Lumenal endosomal and Golgi-retrieval determinants involved in pH-sensitive targeting of an early Golgi protein. *Mol. Biol. Cell.* 12:3152–3160.

Beckers, C.J., D.S. Keller, and W.E. Balch. 1987. Semi-intact cells permeable to macromolecules: use in reconstitution of protein transport from the endoplasmic reticulum to the Golgi complex. *Cell.* 50:523–534.

Brown, D.L., K. Heimann, J. Lock, L. Kjer-Nielsen, C. van Vliet, J.L. Stow, and P.A. Gleeson. 2001. The GRIP domain is a specific targeting sequence for a population of trans-Golgi network derived tubulo-vesicular carriers. *Traffic.* 2:336–344.

Bruinsma, P., R.G. Spelbrink, and S.F. Nothwehr. 2004. Retrograde transport of the mannosyltransferase Och1p to the early Golgi requires a component of the COG transport complex. *J. Biol. Chem.* 279:39814–39823.

Chatterton, J.E., D. Hirsch, J.J. Schwartz, P.E. Bickel, R.D. Rosenberg, H.F. Lodish, and M. Krieger. 1999. Expression cloning of LDLB, a gene essential for normal Golgi function and assembly of the ldlCp complex. *Proc. Natl. Acad. Sci. USA.* 96:915–920.

Duden, R. 2003. ER-to-Golgi transport: COP I and COP II function (Review). *Mol. Membr. Biol.* 20:197–207.

Elbashir, S.M., J. Harborth, W. Lendeckel, A. Yalcin, K. Weber, and T. Tuschl. 2001. Duplexes of 21-nucleotide RNAs mediate RNA interference in cultured mammalian cells. *Nature.* 411:494–498.

Farkas, R.M., M.G. Giansanti, M. Gatti, and M.T. Fuller. 2003. The *Drosophila* Cog5 homologue is required for cytokinesis, cell elongation, and assembly of specialized Golgi architecture during spermatogenesis. *Mol. Biol. Cell.* 14:190–200.

Hamilton, R.L., A. Moorehouse, and R.J. Havel. 1991. Isolation and properties of nascent lipoproteins from highly purified rat hepatocytic Golgi fractions. *J. Lipid Res.* 32:529–543.

Harris, S.L., and M.G. Waters. 1996. Localization of a yeast early Golgi mannosyltransferase, Och1p, involves retrograde transport. *J. Cell Biol.* 132:985–998.

Hay, J.C., D.S. Chao, C.S. Kuo, and R.H. Scheller. 1997. Protein interactions regulating vesicle transport between the endoplasmic reticulum and Golgi apparatus in mammalian cells. *Cell.* 89:149–158.

Hay, J.C., J. Klumperman, V. Oorschot, M. Steegmaier, C.S. Kuo, and R.H. Scheller. 1998. Localization, dynamics, and protein interactions reveal distinct roles for ER and Golgi SNAREs. *J. Cell Biol.* 141:1489–1502.

(published erratum appears in *J. Cell Biol*. 1998. 42:following 881).

Jesch, S.A., and A.D. Linstedt. 1998. The Golgi and endoplasmic reticulum remain independent during mitosis in HeLa cells. *Mol. Biol. Cell.* 9:623–635.

Johannes, L., D. Tenza, C. Antony, and B. Goud. 1997. Retrograde transport of KDEL-bearing B-fragment of Shiga toxin. *J. Biol. Chem.* 272: 19554–19561.

Johnston, P.A., A. Stieber, and N.K. Gonatas. 1994. A hypothesis on the traffic of MG160, a medial Golgi sialoglycoprotein, from the trans-Golgi network to the Golgi cisternae. *J. Cell Sci.* 107:529–537.

Kingsley, D.M., K.F. Kozarsky, M. Segal, and M. Krieger. 1986. Three types of low density lipoprotein receptor-deficient mutant have pleiotropic defects in the synthesis of N-linked, O-linked, and lipid-linked carbohydrate chains. *J. Cell Biol.* 102:1576–1585.

Lanoix, J., J. Ouwendijk, C.C. Lin, A. Stark, H.D. Love, J. Ostermann, and T. Nilsson. 1999. GTP hydrolysis by arf-1 mediates sorting and concentration of Golgi resident enzymes into functional COP I vesicles. *EMBO J.* 18:4935–4948.

Lanoix, J., J. Ouwendijk, A. Stark, E. Szafer, D. Cassel, K. Dejgaard, M. Weiss, and T. Nilsson. 2001. Sorting of Golgi resident proteins into different subpopulations of COPI vesicles: a role for ArfGAP1. *J. Cell Biol.* 155:1199–1212.

Linstedt, A.D., and H.P. Hauri. 1993. Giantin, a novel conserved Golgi membrane protein containing a cytoplasmic domain of at least 350 kDa. *Mol. Biol. Cell.* 4:679–693.

Linstedt, A.D., A. Mehta, J. Suhan, H. Reggio, and H.P. Hauri. 1997. Sequence and overexpression of GPP130/GIMPc: evidence for saturable pH-sensitive targeting of a type II early Golgi membrane protein. *Mol. Biol. Cell.* 8:1073–1087.

Loh, E., and W. Hong. 2002. Sec34 is implicated in traffic from the endoplasmic reticulum to the Golgi and exists in a complex with GTC-90 and ldlBp. *J. Biol. Chem.* 277:21955–21961.

Loh, E., and W. Hong. 2004. The binary interacting network of the conserved oligomeric Golgi (COG) tethering complex. *J. Biol. Chem.* 279:24640–24648.

Love, H.D., C.C. Lin, C.S. Short, and J. Ostermann. 1998. Isolation of functional Golgi-derived vesicles with a possible role in retrograde transport. *J. Cell Biol.* 140:541–551.

Mallard, F., C. Antony, D. Tenza, J. Salamero, B. Goud, and L. Johannes. 1998. Direct pathway from early/recycling endosomes to the Golgi apparatus revealed through the study of shiga toxin B-fragment transport. *J. Cell Biol.* 143:973–990.

Miles, S., H. McManus, K.E. Forsten, and B. Storrie. 2001. Evidence that the entire Golgi apparatus cycles in interphase HeLa cells: sensitivity of Golgi matrix proteins to an ER exit block. *J. Cell Biol.* 155:543–555.

Nakamura, N., C. Rabouille, R. Watson, T. Nilsson, N. Hui, P. Slusarewicz, T.E. Kreis, and G. Warren. 1995. Characterization of a cis-Golgi matrix protein, GM130. *J. Cell Biol.* 131:1715–1726.

Nelson, D.S., C. Alvarez, Y.S. Gao, R. Garcia-Mata, E. Fialkowski, and E. Sztul. 1998. The membrane transport factor TAP/p115 cycles between the Golgi and earlier secretory compartments and contains distinct domains required for its localization and function. *J. Cell Biol.* 143:319–331.

Oka, T., D. Ungar, F.M. Hughson, and M. Krieger. 2004. The COG and COPI complexes interact to control the abundance of GEARs, a subset of Golgi integral membrane proteins. *Mol. Biol. Cell.* 15:2423–2435.

Opat, A.S., F. Houghton, and P.A. Gleeson. 2001a. Steady-state localization of a medial-Golgi glycosyltransferase involves transit through the trans-Golgi network. *Biochem. J.* 358:33–40.

Opat, A.S., C. van Vliet, and P.A. Gleeson. 2001b. Trafficking and localisation of resident Golgi glycosylation enzymes. *Biochimie.* 83:763–773.

Orci, L., M. Stamnes, M. Ravazzola, M. Amherdt, A. Perrelet, T.H. Sollner, and J.E. Rothman. 1997. Bidirectional transport by distinct populations of COPI-coated vesicles. *Cell.* 90:335–349.

Pelham, H.R. 2001. Traffic through the Golgi apparatus. *J. Cell Biol.* 155: 1099–1101.

Podos, S.D., P. Reddy, J. Ashkenas, and M. Krieger. 1994. LDLC encodes a brefeldin A-sensitive, peripheral Golgi protein required for normal Golgi function. *J. Cell Biol.* 127:679–691.

Puri, S., C. Bachert, C.J. Fimmel, and A.D. Linstedt. 2002. Cycling of early Golgi proteins via the cell surface and endosomes upon lumenal pH disruption. *Traffic.* 3:641–653.

Puthenveedu, M.A., and A.D. Linstedt. 2001. Evidence that Golgi structure depends on a p115 activity that is independent of the vesicle tether components giantin and GM130. *J. Cell Biol.* 155:227–238.

Puthenveedu, M.A., and A.D. Linstedt. 2004. Gene replacement reveals that p115/SNARE interactions are essential for Golgi biogenesis. *Proc. Natl. Acad. Sci. USA*. 101:1253–1256.

Ram, R.J., B. Li, and C.A. Kaiser. 2002. Identification of sec36p, sec37p, and sec38p: components of yeast complex that contains sec34p and sec35p. *Mol. Biol. Cell.* 13:1484–1500.

Sandvig, K., M. Ryd, O. Garred, E. Schweda, P.K. Holm, and B. van Deurs. 1994. Retrograde transport from the Golgi complex to the ER of both shiga toxin and the nontoxic shiga B-fragment is regulated by butyric acid and cAMP. *J. Cell Biol.* 126:53–64.

Shorter, J., and G. Warren. 2002. Golgi architecture and inheritance. *Annu. Rev. Cell Dev. Biol.* 18:379–420.

Storrie, B., J. White, S. Rottger, E.H. Stelzer, T. Suganuma, and T. Nilsson. 1998. Recycling of Golgi-resident glycosyltransferases through the ER reveals a novel pathway and provides an explanation for nocodazole-induced Golgi scattering. *J. Cell Biol.* 143:1505–1521.

Suvorova, E.S., R.C. Kurten, and V.V. Lupashin. 2001. Identification of a human orthologue of Sec34p as a component of the cis-Golgi vesicle tethering machinery. *J. Biol. Chem.* 276:22810–22818.

Suvorova, E.S., R. Duden, and V.V. Lupashin. 2002. The Sec34/Sec35p complex, a Ypt1p effector required for retrograde intra-Golgi trafficking, interacts with Golgi SNAREs and COPI vesicle coat proteins. *J. Cell Biol.* 157:631–643.

Tai, G., L. Lu, T.L. Wang, B.L. Tang, B. Goud, L. Johannes, and W. Hong. 2004. Participation of the syntaxin 5/Ykt6/GS28/GS15 SNARE complex in transport from the early/recycling endosome to the TGN. *Mol. Biol. Cell.* 15:4011–4022.

Ungar, D., T. Oka, E.E. Brittle, E. Vasile, V.V. Lupashin, J.E. Chatterton, J.E. Heuser, M. Krieger, and M.G. Waters. 2002. Characterization of a mammalian Golgi-localized protein complex, COG, that is required for normal Golgi morphology and function. *J. Cell Biol.* 157:405–415.

VanRheenen, S.M., X. Cao, V.V. Lupashin, C. Barlowe, and M.G. Waters. 1998. Sec35p, a novel peripheral membrane protein, is required for ER to Golgi vesicle docking. *J. Cell Biol.* 141:1107–1119.

VanRheenen, S.M., X. Cao, S.K. Sapperstein, E.C. Chiang, V.V. Lupashin, C. Barlowe, and M.G. Waters. 1999. Sec34p, a protein required for vesicle tethering to the yeast Golgi apparatus, is in a complex with Sec35p. *J. Cell Biol.* 147:729–742.

Volchuk, A., M. Ravazzola, A. Perrelet, W.S. Eng, M. Di Liberto, O. Varlamov, M. Fukasawa, T. Engel, T.H. Sollner, J.E. Rothman, and L. Orci. 2004. Countercurrent distribution of two distinct SNARE complexes mediating transport within the Golgi stack. *Mol. Biol. Cell.* 15:1506–1518.

Walter, D.M., K.S. Paul, and M.G. Waters. 1998. Purification and characterization of a novel 13 S hetero-oligomeric protein complex that stimulates in vitro Golgi transport. *J. Biol. Chem.* 273:29565–29576.

Whyte, J.R., and S. Munro. 2001. The Sec34/35 Golgi transport complex is related to the Exocyst, defining a family of complexes involved in multiple steps of membrane traffic. *Dev. Cell.* 1:527–537.

Whyte, J.R., and S. Munro. 2002. Vesicle tethering complexes in membrane traffic. *J. Cell Sci.* 115:2627–2637.

Wu, X., R.A. Steet, O. Bohorov, J. Bakker, J. Newell, M. Krieger, L. Spaapen, S. Kornfeld, and H.H. Freeze. 2004. Mutation of the COG complex subunit gene COG7 causes a lethal congenital disorder. *Nat. Med.* 10:518–523.

Xu, Y., S. Martin, D.E. James, and W. Hong. 2002. GS15 forms a SNARE complex with syntaxin 5, GS28, and Ykt6 and is implicated in traffic in the early cisternae of the Golgi apparatus. *Mol. Biol. Cell.* 13:3493–3507.

Traffic 2006; **7:** 191–204
Blackwell Munksgaard


doi: 10.1111/j.1600-0854.2005.00376.x

# COG Complex-Mediated Recycling of Golgi Glycosyltransferases is Essential for Normal Protein Glycosylation

**Anna Shestakova, Sergey Zolov and Vladimir Lupashin***

*Department of Physiology and Biophysics, University of Arkansas for Medical Sciences, Little Rock, AR 72205, USA*
**Corresponding author: Vladimir Lupashin, vvlupashin@uams.edu*

**Defects in conserved oligomeric Golgi (COG) complex result in multiple deficiencies in protein glycosylation. On the other hand, acute knock-down (KD) of Cog3p (COG3 KD) causes accumulation of intra-Golgi COG complex-dependent (CCD) vesicles. Here, we analyzed cellular phenotypes at different stages of COG3 KD to uncover the molecular link between COG function and glycosylation disorders. For the first time, we demonstrated that *medial*-Golgi enzymes are transiently relocated into CCD vesicles in COG3 KD cells. As a result, Golgi modifications of both plasma membrane (CD44) and lysosomal (Lamp2) glycoproteins are distorted. Localization of these proteins is not altered, indicating that the COG complex is not required for anterograde trafficking and accurate sorting. COG7 KD and double COG3/COG7 KD caused similar defects with respect to both Golgi traffic and glycosylation, suggesting that the entire COG complex orchestrates recycling of *medial*-Golgi-resident proteins. COG complex-dependent docking of isolated CCD vesicles was reconstituted *in vitro*, supporting their role as functional trafficking intermediates. Altogether, the data suggest that constantly cycling *medial*-Golgi enzymes are transported from distal compartments in CCD vesicles. Dysfunction of COG complex leads to separation of glycosyltransferases from anterograde cargo molecules passing along secretory pathway, thus affecting normal protein glycosylation.**

**Key words: COG, glycosylation, Golgi, retrograde traffic, tethering**

**Received 22 September 2005, revised and accepted for publication 1 November 2005, published on-line 8 December 2005**

The Golgi apparatus is a hub for membrane-trafficking pathways, organizing both anterograde and retrograde trafficking of molecules (1). It plays a key role in the intracellular trafficking, processing and secretion of glycoproteins, glycolipids and proteoglycans (2). Sequential modifications of glycoproteins by Golgi enzymes depend on the non-uniform distribution of different glycosylation enzymes within Golgi stack (3–5).

Anterograde vesicular transport and cisternal maturation are two alternative models of intra-Golgi transport (6). A fundamental difference between these two models is the differential movement of resident and cargo proteins. The anterograde vesicular transport model predicts that cargo molecules will move forward in transport vesicles, while resident proteins are specifically retained. The cisternal maturation model predicts that cargo molecules will move through the stack passively as the cisternae move forward, while resident proteins will be recycled by retrograde transport to establish differential concentrations across the stack. These two models are not mutually exclusive and may occur simultaneously (7). Inherent in the cisternal maturation model is the importance of recycling in localization of glycosyltransferases, SNAREs and other resident Golgi proteins.

Studies in yeast and mammalian cells have led to the identification of several multisubunit protein complexes that are thought to be involved in Golgi vesicle tethering and/or compartment function, including the conserved oligomeric Golgi (COG) (8,9), the TRAPP, (10) and the GARP (Vps51–54) (11) complexes (12). COG complex is preferentially localized to the *cis*/*medial* cisternae of the Golgi apparatus (13–15) and is involved in Golgi membrane traffic (16–20). Conserved oligomeric Golgi complex is a peripheral membrane hetero-oligomer which consists of eight subunits named COG1–8 (15–18,21–23). On the basis of yeast and mammalian genetic and biochemical studies (22–25) and on the results of the electron microscopy (15), COG subunits have been grouped into two lobes consisting of COG1–4 (essential Lobe A) and COG5–8 (non-essential Lobe B). Mutations in the subunits of the COG complex severely distress Golgi glycosylation machinery (17,20–22,26). In Δ*COG1* and Δ*COG2* CHO mutant cells processing of glycoproteins and glycolipids is defective and heterogeneous, resulting in substantial global alterations in cell surface glycoconjugates (27). A recently found mutation in human COG7 gene leads to the type II congenital disorder of glycosylation (CDG) (26). The heterogeneity of protein glycosylation defects suggests that mutations in COG complex affect the activity or compartmentalization of multiple Golgi enzymes without sizeable disruption of secretion and endocytosis. The activity of glycosylation enzymes depends on their proper intra-Golgi localization (28,29). Thus, COG may play a direct role in transport, retention and/or retrieval of components of Golgi-glycosylation machinery. Studies in yeast have identified a large number of COG-interacting genes

encoding proteins implicated in Golgi trafficking (8,9,17). We have shown that COG complex directly interacts with Rab GTPase Ypt1p, intra-Golgi SNAREs, as well as with the COPI coat complex. In addition, electron microscopy revealed that *cog2* and *cog3* temperature-sensitive yeast mutants accumulate vesicles (30).

It has been recently demonstrated that the acute knock-down (KD) of the COG3 was accompanied by reduction in Cog1, Cog 2 and Cog 4 protein levels and resulted in the accumulation of COG complex-dependent (CCD) vesicles carrying Golgi v-SNARE molecules (19). Prolonged block in CCD vesicle tethering is accompanied by substantial fragmentation of the Golgi ribbon. Fragmented Golgi membranes maintain their juxtanuclear localization, cisternal organization and competence for anterograde protein trafficking to the plasma membrane. These findings let us hypothesize that COG complex acts as a tether which connects COPI vesicles with *cis*-Golgi membranes during retrograde intra-Golgi traffic. Additional evidence that COG plays a role in the retrograde vesicular transport of Golgi proteins, including glycosylation enzymes, came from surveying the steady-state levels of Golgi proteins in wild-type and COG-deficient mammalian cells (31). Seven Golgi membrane proteins, including processing enzyme α-1,3-1,6-mannosidase II (Mann II), were found to exhibit reduced steady state levels in both Δ*COG1* and Δ*COG2* CHO cells.

How can the COG complex determine localization of enzymes within the Golgi? One way to achieve this is to interact directly with cytoplasmic tails of resident Golgi proteins and retain them in an appropriate compartment. Another way is to control the basic structure of the Golgi or its lumenal environment (pH, ion concentrations) (21). The most likely hypothesis is that the COG complex is directly involved in tethering of intra-Golgi COPI vesicles which transport recycling enzymes to appropriate compartments. To test this hypothesis and determine molecular mechanism by which malfunctioning of the COG complex may generate defects in Golgi-glycosylation machinery, we investigated cellular phenotypes after both acute and prolonged COG3 and COG7 KD. We found that progression of COG3 KD was positively correlated with Golgi-glycosylation defects, and glycosylation of both lysosomal and plasma membrane proteins was severely altered after prolonged COG3 KD. Underglycosylated proteins were correctly delivered to their cellular locations, indicating that even a prolonged block in Cog3p function does not affect anterograde trafficking and protein sorting. We also discovered that as early as 3 days after COG3 KD *medial*-Golgi enzyme, β-1,2-*N*-acetylglucosaminyltransferase-1 (GlcNAcT1) becomes mislocalized into vesicular fraction. GlcNAcT1 containing vesicles were distinct from ER, endosomes and lysosomes and most likely identical to previously described CCD vesicles enriched with Golgi v-SNARE proteins (19). Similar relocation into CCD vesicles was found for another *medial*-Golgi enzyme, Mann II and to a lesser extent *medial/trans*-Golgi enzyme N-acetylgalactosaminyltransferase 2 (GalNAcT2) and *trans*-Golgi enzyme β-1,4galactosyltransferase (GalT). Prolonged COG3 KD finally leads to degradation of both GlcNAcT1 and Mann II. Similar effects were observed in COG7 KD and COG3/COG7 double KD HeLa cells.

On the basis of our findings, we conclude that alterations in the function of COG complex caused specific mislocalization of *medial*-Golgi enzymes and Golgi v-SNAREs into recycling intra-Golgi CCD vesicles. Efficient and COG-dependent docking of CCD vesicles to purified Golgi membranes was reconstituted *in vitro*, supporting functional status of these transport intermediates. Conserved oligomeric Golgi complex most likely functions in tethering of retrograde enzyme-carrying CCD vesicles to the proper Golgi compartment.

## Results

### *Prolonged COG3 knock-down leads to defects in protein glycosylation*

Our previous studies demonstrated that acute depletion of Cog3p caused accumulation of non-tethered CCD vesicles and Golgi fragmentation but, at least initially, did not result in increased gel mobility of Golgi glycoprotein GPP130, arguing that protein glycosylation was not altered (19). This result was rather surprising, since severe Golgi-glycosylation defects were previously observed in both Δ*COG1* and Δ*COG2* CHO mutant cells (21), and similar glycosylation abnormalities were detected in yeast *cog3-ts* (*sec34–2*) mutant (17). We hypothesized that the observed phenotype of the acute COG3 KD might represent a primary Cog3p-dependent defect in membrane trafficking, leading to deficient Golgi glycosylation. To test out this hypothesis, we investigated whether the extended deficiency in Cog3p function would affect Golgi-glycosylation machinery (Figure 1A). First, we determined the steady-state glycosylation status of two endogenous membrane glycoproteins – plasma membrane-localized CD44 (32) and extensively glycosylated with 16 N-linked carbohydrate chains lysosomal resident protein Lamp2 (33). HeLa cells were treated with COG3 siRNA for 3, 6 and 9 days. Acute KD is referred to as 3 days after siRNA treatment; prolonged KD is 6 and 9 days after siRNA treatment. Cog3 protein has been efficiently depleted, and after 3 days of KD, its level comprised 10% of the initial one (Figure 1A, right panel, upper lane). We have previously shown that acute COG3 KD affects the stability of Lobe A but not Lobe B subunits of the COG complex (19). Similarly, there was destabilization of Cog4p and most probably whole Lobe A after prolonged COG3 KD. Cellular levels of Lobe B subunits were also slightly decreased (Figure S1, available online at http://www.blackwell-synergy.com). Prolonged COG3 KD or similar transfection with control (scrambled) siRNA did not affect viability of HeLa cells.

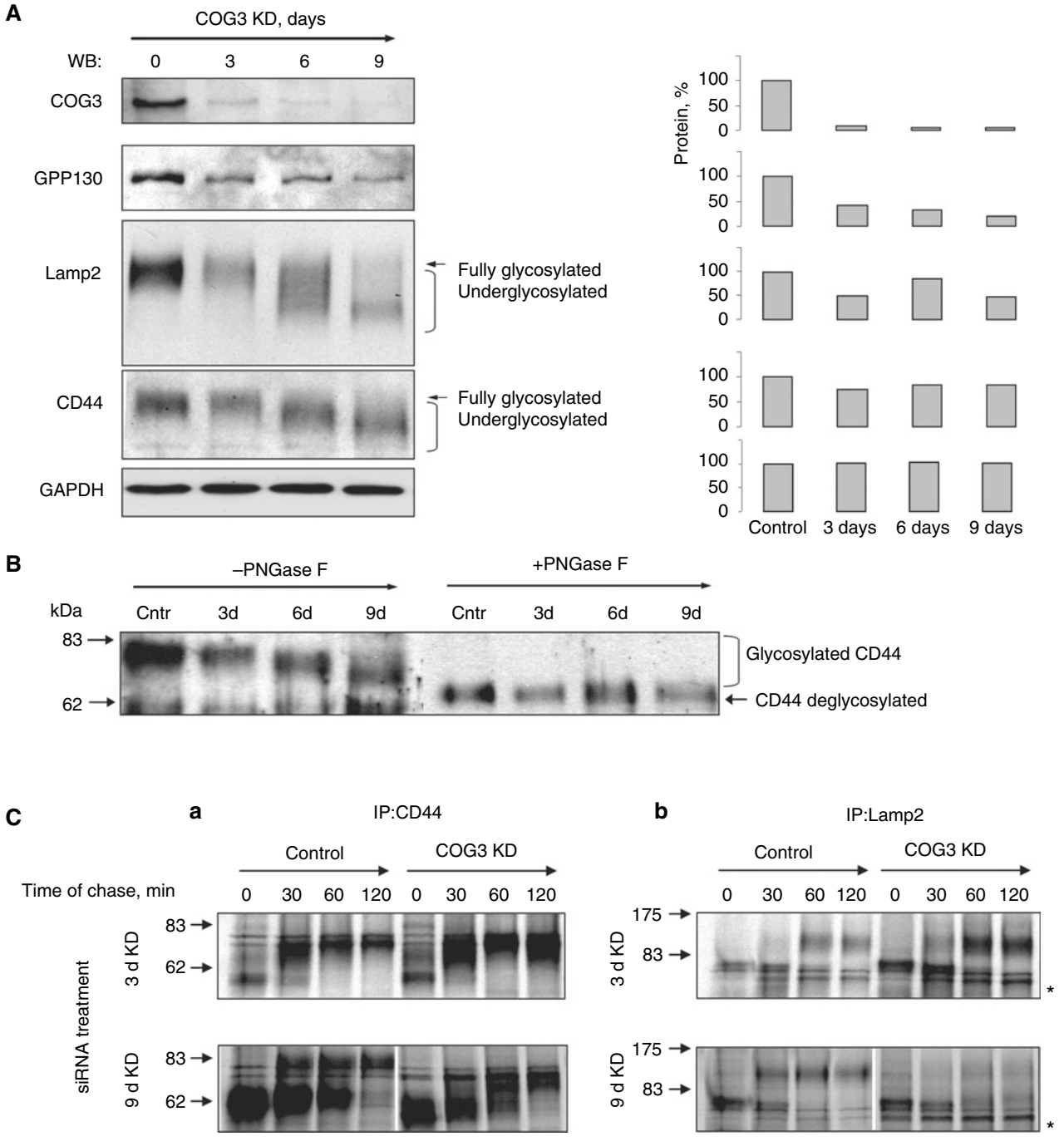


**Figure 1: Prolonged COG3 knock down (KD) affects glycosylation and stability of membrane glycoproteins of secretory pathway.** A) Steady-state cellular level and gel mobility of glycoproteins of secretory pathway. HeLa cells were mock (0) or COG3 siRNA treated for 3, 6 and 9 days. Total cell lysates were prepared at corresponding time points, subjected to SDS-PAGE and WB with the indicated antibodies. Right panel represents quantification of immunoblotted proteins. B) Increase in gel mobility of CD44 after COG3 KD is due to its defective glycoprotein modification. Cell lysates after 3, 6 and 9 days of COG3 KD were incubated with a PNGase F (500 U/reaction) as described in *Materials and Methods*. Samples were loaded on SDS-PAGE and WB with anti-CD44 antibody. C) Pulse-chase labeling of CD44 and Lamp2 glycoproteins. Cells were metabolically labeled with $^{35}$S-Methionine for 10 min and then chased for indicated time points. Cell lysates were subjected to IP with anti-CD44 and anti-Lamp2 antibodies. Precipitated proteins were loaded on SDS-PAGE and visualized by PhosphorImager. Star indicates a non-specific band.

In agreement with our previous observations, after 3 days of COG3 KD, all tested glycoproteins, i.e. GPP130, Lamp2 and CD44, did not show a visible change in their mobility on SDS-PAGE (Figure 1A, compare control (0) and 3 days lanes). In contrast, after 6 days of COG3 KD, the gel mobility of both Lamp2 and CD44 was altered, indicating the production of underglycosylated protein species. The glycosylation defects became more pronounced after 9 days of COG3 KD. Western blot analysis demonstrated that a decrease in molecular weight of both CD44 and Lamp2 positively correlated with the duration of COG3 KD (Figure 1A, left panel, compare molecular weights of CD44 and Lamp2 after 3 and 9 days of COG3 KD). Smearing of the bands corresponding to CD44 and Lamp2 may argue for heterogeneity in glycosylation, emerging after 6 and 9 days of COG3 KD. Interestingly, the bulk of the GPP130 did not change its gel mobility even after 9 days of COG3 KD. Instead, the level of GPP130 protein was dramatically decreased after prolonged COG3 KD (Figure 1A, right panel). A similar expression profile was observed for Lamp2. After 9 days of COG3 KD, the protein level of Lamp2 was reduced by more than 50% (Figure 1A, right panel). The latter result might be caused by the instability of underglycosylated Lamp2 protein (34).

To confirm our assumption that the increase in gel mobility is caused by defective glycosylation, both control and COG3 KD cell lysates were subjected to peptide:N-glycosidase F (PNGase F) treatment (Figure 1B). We found that deglycosylation of all forms of CD44 observed in COG3 KD cells produced a single 62 kDa polypeptide. A similar result was obtained for Lamp2, in which the molecular weight was reduced from approximately 110 to 82 kDa after PNGase F treatment (data not shown). This result confirmed our hypothesis that increased gel mobility of CD44 and Lamp2 after COG complex KD is entirely due to deficient glycosylation. After prolonged COG3 KD, underglycosylated glycoproteins were sensitive to Endo H treatment (Figure S2, available online at http://www.blackwell-synergy.com), indicating defects in early Golgi glycosylation.

To determine whether COG3 KD affects the kinetics of glycoprotein modifications in the Golgi, we performed a pulse-chase experiment (Figure 1C). Both the extent of glycosylation and its kinetics were almost indistinguishable for control and 3 days COG3 KD cells, with only minute smearing of CD44 band observed at the 120 min time point (Figure 1C, panel a). This smearing most likely represents the early onset of glycosylation defects. In contrast, a pronounced defect in glycosylation of CD44 and Lamp2 (Figure 1C, 9 KD lanes) was detected after 9 days of COG3 KD. Even after 2 h of chase, both CD44 and Lamp2 remained underglycosylated. Prolonged (9 days) growth on plates and/or continuous treatments with transfection reagent slowed down the kinetics of CD44 glycosylation in both COG3 siRNA and mock-transfected cells. Interestingly, in both plates, 120 min was a sufficient time to chase the bulk of CD44 to the Golgi glycosylated form, indicating that protein movement through the Golgi in COG3 KD cells was not sufficiently altered. We have previously observed a similar slight delay in plasma-membrane delivery of VSVG in COG3 KD cells (19).

The behavior of Lamp2 was more complex, with the accumulation of a whole array of partially glycosylated forms accumulated in COG3 KD cells after 120 min of chase. These findings allowed us to hypothesize that after prolonged COG3 KD, either glycoproteins are not targeted properly and thus can not encounter the Golgi glycosylation machinery or Golgi glycosylation machinery itself is mislocalized, thus not allowing Golgi enzymes to process proteins.

### *Underglycosylated glycoproteins are correctly localized in COG3 KD cells*

To address the first question of possible impairment of anterograde trafficking of glycoproteins of the secretory pathway under conditions of COG3 KD, we determined localization of CD44 and Lamp2 after prolonged COG3 KD. As shown in Figure 2(A), after 9 days of COG3 KD, CD44 was mostly localized on the plasma membrane. A small portion of CD44 signal was detected on intracellular membranes that were distinct from GPP130-positive membranes and most likely represented recycling pool of CD44. Strikingly, staining of non-permeabilized cells demonstrated that the intensity of CD44 signal was similar for both control (100%) and 9 days of COG3 KD (94%) cells, indicating that anterograde trafficking and plasma membrane expression of CD44 was not compromised (Figure 2B). There was no staining for the lumenal Golgi protein GlcNAcT1 in non-permeabilized cells (Figure S3 available online at http://www.blackwell-synergy.com).

Similarly, proper localization was found for the lysosomal protein Lamp2 (Figure 2C). Nine days after COG3 KD, Lamp2 was associated with scattered membrane compartments distinct from endosomes, ER and Golgi remnants (data not shown). To obtain additional evidence that the Lamp2-positive compartments are indeed lysosomal in nature, cells were treated with Cascade Blue Dextran, which is known to travel via the endocytic pathway finally accumulating in lysosomes (Figure 2D). Immunofluorescent assays demonstrated that in both control ($80 \pm 3\%$ of colocalization) and 9 days ($69 \pm 4\%$ of colocalization) of COG3 KD cells, endocytosed dextran was colocalized with Lamp2, indicating that underglycosylated Lamp2 was sorted properly to lysosomes in COG3-depleted cells.

### Medial-*Golgi enzymes are severely mislocalized in COG3 KD cells*

Results from the experiments described above allowed us to conclude that in Cog3p deprived cells, underglycosylated proteins are delivered properly to both the plasma membrane and lysosomes. Most likely, on their way to final destination, they are transported through the

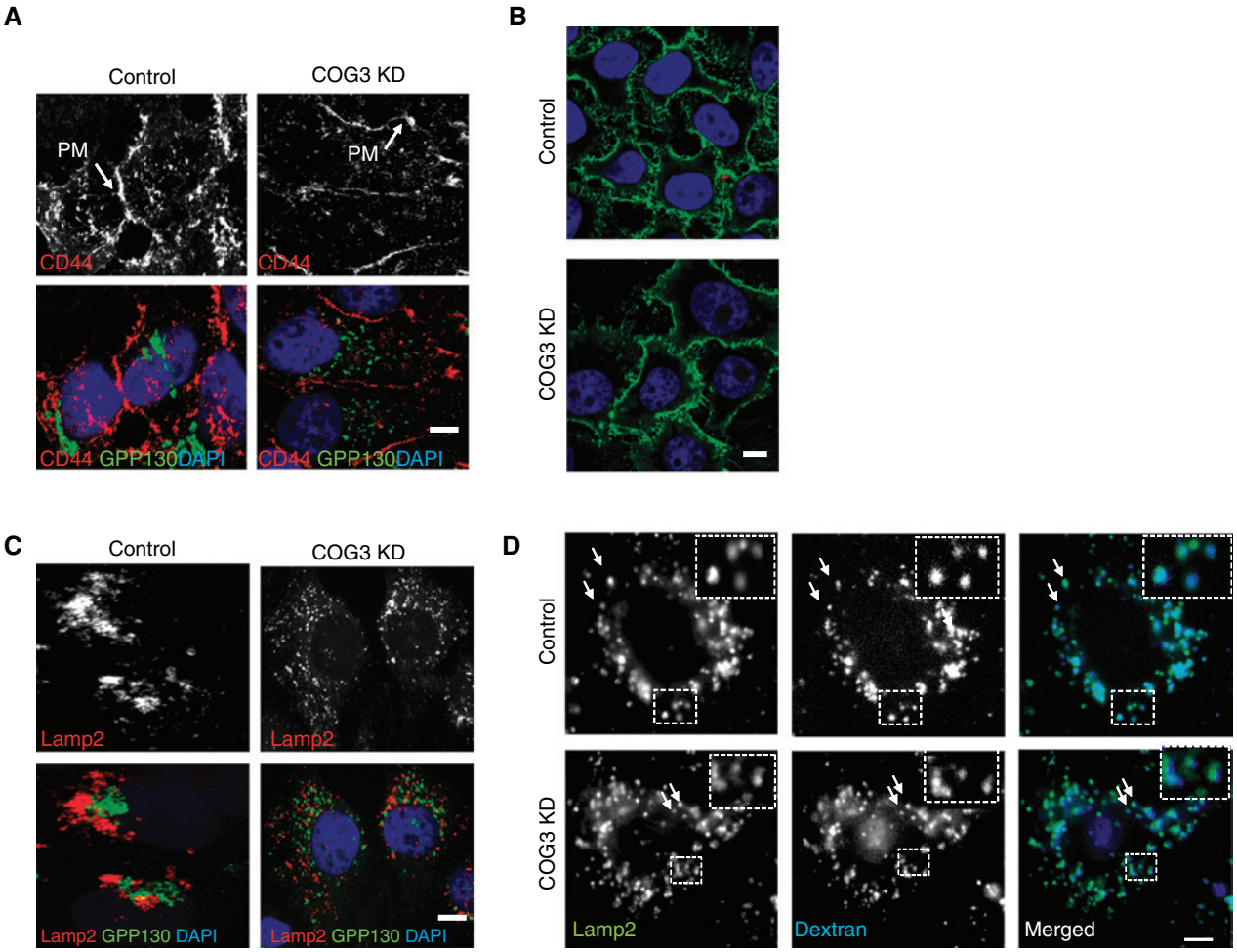


**Figure 2: Underglycosylated CD44 and Lamp2 are correctly localized in control and COG3 knock down (KD) cells.** A) Localization of CD44 is similar in control and COG3 KD cells. Control and 9 days COG3 KD cells were fixed, permeabilized and triple stained with anti-CD44 (red), GPP130 (green) and DAPI (blue). Arrows indicate plasma membrane. B) Plasma membrane delivery of CD44 is not compromised in COG3 KD cells. Control and 9 days COG3 KD cells were fixed and stained with anti-CD44 (green) without permeabilization. C) Localization of Lamp2 is similar in control and COG3 KD cells. Control and 9 days COG3 KD cells were fixed and triple stained with anti-Lamp2 (red), GPP130 (green) and DAPI (blue). D) Lamp2 is colocalized with lysosomes in control and COG3 KD cells. Control and 9 days of COG3 KD cells were treated with Cascade Blue Dextran as described in *Materials and Methods* and stained with anti-Lamp2 (green). Cascade Blue Dextran is visualized at 420 nm spectrum (blue). Arrows indicate lysosomes. All images were collected at equal signal gains using CARV microscopy. Bar, 10 μm.

fragmented Golgi. Thus, the anterograde protein flow is undistorted, and the trafficking itinerary is not modified in COG KD cells. Why do glycoproteins become underglycosylated? We hypothesized that Golgi-glycosylation machinery itself is mislocalized in COG3 KD cells. Both IF and subcellular fractionation were employed to determine localization of key components of the Golgi-glycosylation machinery. We have specifically focused our investigation on GlcNAcT1 localized at steady-state within the *medial*-Golgi cisternae (5). It has been shown that newly synthesized GlcNAcT1 is transported rapidly through the Golgi stack to the *trans*-Golgi network and then is recycled back to the *cis*-Golgi with a half-time of about 150 min, suggesting that this protein is continuously recycled from the late Golgi (29,35). Furthermore, GlcNAcT1 was detected in COPI-dependent transport intermediates which fused with the *cis*-cisternae in the *in vitro* assays (36,37). To account for any non-specific staining with primary or secondary antibodies in IF experiments, we used a mixed population (1:1) of HeLa cells stably expressing Golgi glycosyltransferases tagged either with myc or vsv epitope tag. It has been previously shown that in these cells, tagged enzymes were only slightly (two- to fourfold) overexpressed, and their localization and trafficking was indistinguishable from endogenous enzymes (5). We found that GlcNAcT1 is tightly associated with the Golgi ribbon in mock-transfected cells treated with scrambled siRNA and is rapidly redistributed into vesicular structures after COG3 KD (Figure 3A). A subpopulation of the enzyme colocalized with GM130

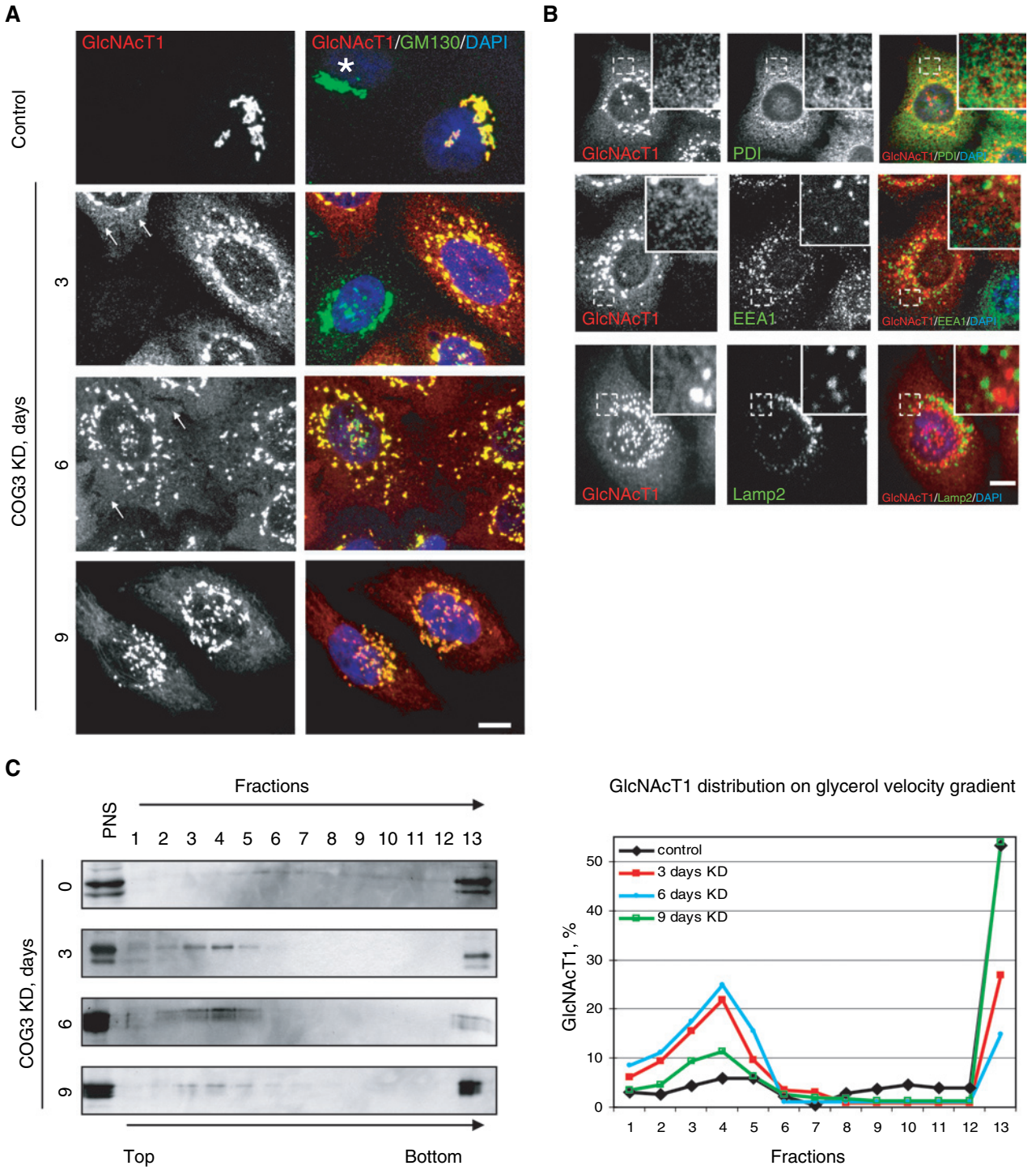


**Figure 3: COG3 knock down (KD) induces relocation of Golgi enzyme β-1,2-*N*-acetylglucosaminyltransferase-1 (GlcNAcT1).** A) Control (0), 3, 6 and 9 days after COG3 KD mixture of cells stably expressing GlcNAcT1-myc and Mann II-vsv were fixed and triple stained with anti-myc (red), Golgi marker anti-GM130 (green) and DAPI (blue). Arrows indicate conserved oligomeric Golgi complex-dependent (CCD) vesicles. Star indicates cell without GlcNAcT1-myc. B) 3 days COG3 KD cells as in (A) were fixed and triple stained with anti-myc (red), ER marker PDI (green), early endosomal marker EEA1 (green), lysosomal marker Lamp2 (green) and DAPI (blue). C) Glycerol velocity gradient fractions were immunoblotted with anti-myc (left panel) and quantified (right panel). Combined signal of fractions 1–13 was taken for 100%. Quantification of each lane represents an average of three independent experiments. Black, red, blue and green lines represent distribution of GlcNAcT1 in control, 3, 6 and 9 days of COG3 KD cells, respectively.

and most likely remained associated with fragmented Golgi mini-stacks. A similar vesicular distribution of GlcNAcT1 was observed in cells after 3 and 6 days of COG3 KD (Figure 3A, 3 and 6 days rows). More reticular GlcNAcT1-positive structures were found in cells after prolonged Cog3p depletion (Figure 3A, 9 days row). These reticular structures were similar to classical ER appearance, and indeed partial colocalization of Golgi enzyme with ER marker PDI was observed in cells after 9 days of COG3 KD (Figure S4, available online at http://www.blackwell-synergy.com). Localization of GlcNAcT1 in acutely depleted cells was distinct from that of ER, endosomal and lysosomal markers (Figure 3B), and most likely, indicated accumulation of the enzyme in CCD vesicles carrying v-SNAREs GS15 and GS28 and *cis*-Golgi glycoprotein GPP130 (19). On the glycerol velocity gradient, GPP130 was detected in the same fractions as GlcNAcT1. Indeed, separation of cell lysates on glycerol velocity gradient demonstrated that a significant fraction of GlcNAcT1 was associated with small vesicles (Figure 3C, fractions 3 and 4). CCD vesicles associated fraction of GlcNAcT1 was increased from 5% (control) to more than 50% (3 and 6 days COG3 KD). The vesicular fraction in 9 days COG3 KD cells decreased as compared to acutely depleted cells, arguing that the majority of GlcNAcT1 molecules were now associated with larger membrane structures like Golgi or ER (Figure 3C, lower panel, fraction 13). This biochemical result is in good agreement with the IF data. Both PDI and GM130 were exclusively found in soluble (fraction 1) and Golgi/ER (fraction 13) pools (19; data not shown).

To test whether the localization of other Golgi enzymes is affected by COG3 KD, we used cells stably expressing vsv-tagged *medial*-Golgi enzyme Mann II and *medial/trans*-Golgi enzyme GalNAcT2 (5). IF analysis revealed that upon COG3 KD, both Mann II and, to a lesser extent, GalNAcT2 were redistributed into vesicular structures, supporting our hypothesis of their accumulation in CCD vesicles (Figure 4A). Indeed, there was significant increase in Mann II protein in the vesicle fraction isolated on glycerol velocity gradient (Figure 4B). Relative enrichment of Mann II in the vesicle fraction (approximately four- to fivefold) was similar to one observed for GPP130 and GlcNAcT1

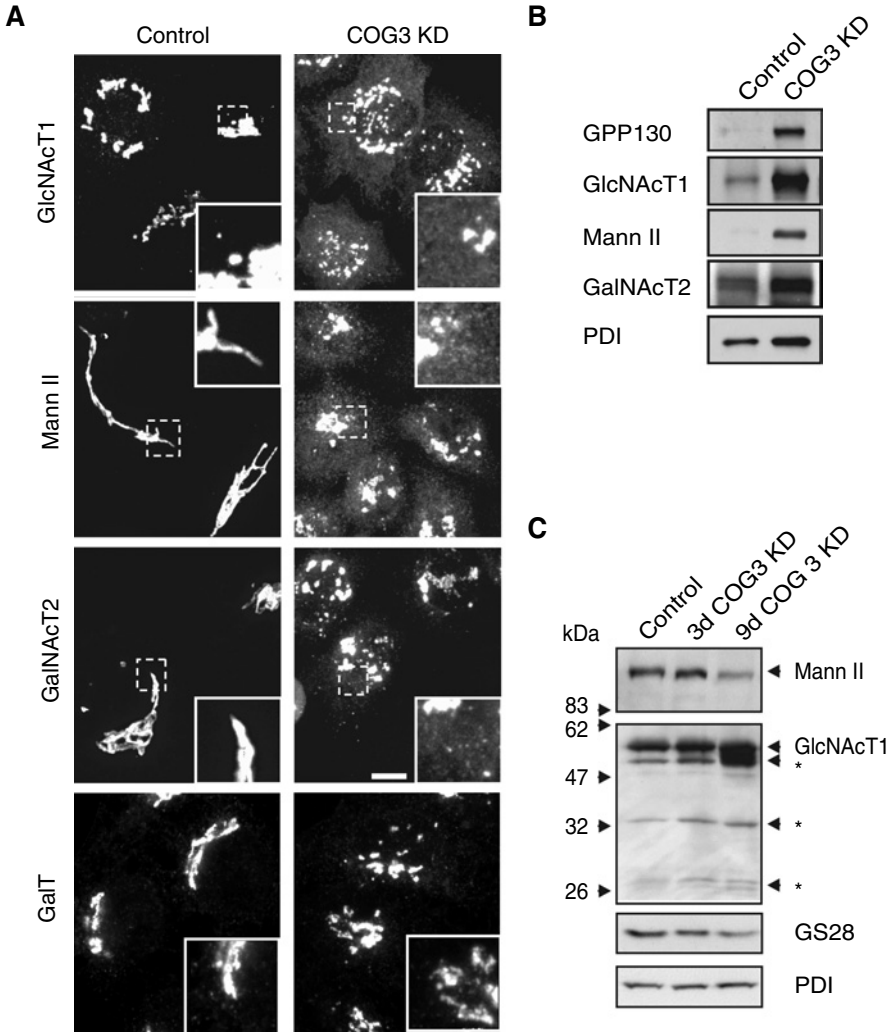


**Figure 4: COG3 knock down (KD) induces relocation and partial degradation of *medial*-Golgi enzymes.** A) Control and 3 days COG3 KD cells stably expressing GlcNAcT1-myc, Mann II-vsv and GalNAcT2-vsv were fixed and stained with anti-myc, anti-vsv, or anti-GalT antibodies. Images were collected using CARV microscopy. Bar, 10 μm. B) Control and COG3 KD vesicle fractions (combined glycerol gradient fractions 3 and 4) were immunoblotted with GPP130, anti-myc for GlcNAcT1, anti-vsv for Mann II, anti-vsv for GalNAcT2 and anti-PDI antibodies as indicated. C) Control, 3 and 9 days COG3 KD cell lysates (10 μg) were immunoblotted with anti-vsv (upper panel), anti-myc (lower panel), anti-human GS28 and anti-PDI antibodies. Star indicates putative degradation product of GlcNAcT1.

(Figure 4B, compare GPP130, GlcNAcT1 and Mann II rows). Vesicular accumulation of GalNAcT2-vsv (approximately twofold) was at the level previously observed for GalNAcT2-GFP and GS28 (19). We concluded that COG3 KD causes specific accumulation of *medial*-Golgi enzymes in recycling intra-Golgi CCD vesicles. Another *trans*-Golgi enzyme, GalT, was found mostly on fragmented Golgi (Figure 4A, GalT row). This result is in good agreement with GalT-GFP localization in COG3 KD cells observed previously (19).

Since the severe redistribution of Golgi enzymes was observed after both acute and prolonged COG3 KD, we questioned how it would affect enzyme stability. Western blot analysis of total cellular homogenates revealed that prolonged, but not acute, COG3 KD resulted in a twofold decrease of Mann II cellular level (Figure 4C, Mann II row) and in accumulation of GlcNAcT1-degradation products (Figure 4C, GlcNAcT1 panel). We also noticed a slight increase in total cellular level of GlcNAcT1. Intracellular levels of the control protein PDI was found unchanged, while the level of another CCD vesicle protein GS28 (19) was also reduced by approximately 50% after prolonged COG3 KD (Figure 4C, GS28 row). These data correlate well with previously observed degradation of GS28 (GOS-28) in Δ*COG1* CHO cells (31).

***COG7 KD leads to mislocalization of GlcNAcT1 and GS15***

To test whether the entire COG complex is required for proper localization of Golgi glycosyltransferases, we used an siRNA strategy to knock-down Cog7p (subunit of COG Lobe B). It has been found recently that mutation in human COG7 gene led to secretion of underglycosylated proteins (26), a mutant phenotype similar to the one observed after prolonged COG3 KD. After 3 days of COG7 KD, the Cog7p was efficiently depleted (Figure 5B), and both GlcNAcT1 and GS15 became severely mislocalized (Figure 5A). This effect was specific since both GM130 (Figure 5A, panel GM130) and GalNAcT2 (Figure 5, panel GalNAcT2) remained associated with large perinuclear Golgi fragments. Transfection with control (scrambled) siRNA did not have any effect on localization of Golgi proteins (Figure 5A, top row). Similarly, to the prolonged COG3 KD, the SDS-PAGE mobility of lysosomal glycoprotein Lamp2 in COG7 KD cells was altered, indicating defects in Golgi glycosylation. In addition to obvious similarities between COG3 KD and COG7 KD mutant phenotypes, we noticed some unique characteristics of COG7 KD cells – glycosylation defects were manifested slightly earlier and GM130/GalNAcT2-containing Golgi membranes were less fragmented and often misshapen into 'cotton ball-like' structures. We also detected that the cellular level of Golgi-resident proteins GM130 and Syntaxin 5 was reduced in COG7 KD cells to less than 50% as compared to mock-treated or COG3KD cells. A Golgi-located short 37 kDa form of Syntaxin 5 was affected to a greater extent with only approximately

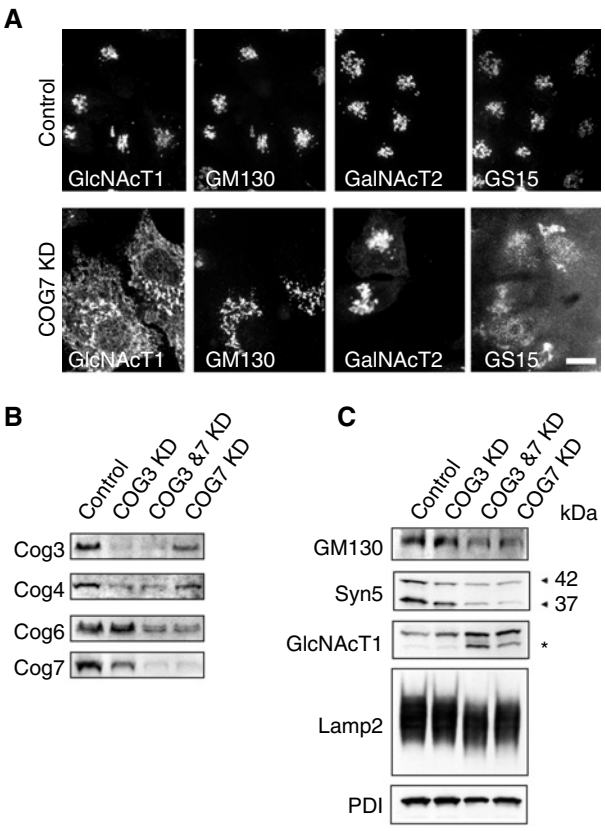


**Figure 5: COG7 knock down (KD) induces relocation of GlcNAcT1 and GS15.** A) Mixture of cells expressing GlcNAcT1-myc and GalNAcT2-vsv were mock (control) or COG7 siRNA treated for 3 days. Fixed cells were stained with anti-myc or anti-vsv antibodies. Images were collected at equal signal gains, using CARV microscopy. Bar, 10 μm. B) Control, COG3, COG3 & COG7 and COG7 KD whole-cell lysates (10 μg protein/lane) were immunoblotted with anti-Cog3, anti-Cog4, anti-Cog6 and anti-Cog7 antibodies. C) Lysates as in (B) were immunoblotted with indicated antibodies, anti-myc for GlcNAcT1; PDI was used as a loading control. Star indicates putative degradation product of GlcNAcT1.

20% protein remained in COG7 KD cells. We have shown previously that yeast Syntaxin 5 homologue, Sed5p, interacted with COG complex directly (17), and the cellular level of Sed5p was severely reduced in double Δ*COG1*/Δ*COG6* mutant cells (23). Reduced level of GM130 and Syntaxin 5 in COG7 KD cells may reflect direct interaction between Cog7p and/or Lobe B with Golgi membrane-associated components of vesicle docking/fusion machinery. Observed differences between COG3 KD and COG7 KD phenotypes are likely due to diverse specialization of two lobes of the COG complex and will be examined in future studies.

Simultaneous depletion of Cog3p and Cog7p affected glycosylation of Lamp2 and stability of GlcNAcT1 more severely as compared to individual COG subunit KD (Figure 5C) (COG3 & 7 lane), indicating faster progression of *medial*-Golgi enzyme-trafficking defects in a double

Lobe A/Lobe B mutant. This result correlates well with the previously observed severe glycosylation defect in double Δ*COG1*/Δ*COG6* yeast mutant cells (23).

On the basis of the results described above, we concluded that any alterations in COG complex function in human cells cause specific mislocalization of preferentially *medial*-Golgi enzymes and Golgi v-SNARE molecules and their accumulation in normally transient CCD vesicles. Conserved oligomeric Golgi complex most likely functions in tethering of these transport intermediates to proper Golgi compartment. The cellular biosynthetic machinery is able to 'ignore' the initial defects in Golgi protein recycling, but continuous separation of glycosylation machinery from the secretory pathway affects Golgi modifications of secretory, plasma membrane, and lysosomal glycoproteins and could ultimately lead to congenital disorders of glycosylation (26).

### *CCD vesicles dock to Golgi* in vitro *in a Cog3p-dependent reaction*

Results obtained from this and previous (19) works indicated that both *medial*-Golgi glycosyltransferases and intra-Golgi SNAREs transiently accumulated in CCD vesicles in COG3 KD cells. To test if these vesicles represent a functional intra-Golgi transport intermediate, we designed an *in vitro* system which measured vesicle docking/fusion with isolated rat liver Golgi (RLG). The system is similar to the yeast COPII vesicle tethering setup (38) and is based on sedimentation properties of isolated RLG (pelletable at 10 000 × *g*) and CCD vesicles obtained from COG3 KD HeLa cell lysate (not pelletable at 20 000 × *g*). Both GlcNAcT1-myc and GPP130 were used as vesicle markers. GS28 was used as Golgi marker. Monoclonal antibodies to ratGS28 and human GPP130 specifically recognized corresponding proteins in RLG and HeLa cell lysates (Figure S7, available online at http://www.blackwell-synergy.com). We have found that CCD vesicles are able to dock to isolated Golgi (Figure 6). The amount of sedimentable vesicle marker (up to 30% from total input) was proportional to the amount of added Golgi membranes and vesicle–Golgi association was resistant to 250 mM KCl wash, which normally strips vesicles from Golgi membranes (39), indicating tight association and/or complete fusion (Figure 6A). Acceptor Golgi membranes were sensitive to proteinase K pretreatment, indicating requirement for peripheral and/or transmembrane proteins. Indeed both COG3 and Golgi SNARE GS28 were completely destroyed by Proteinase K treatment (Figure 6B and data not shown). Most importantly, docking of CCD vesicles was sensitive (approximately 70% inhibition) to addition of anti-COG3 IgG but not to addition of pre-immune (control) IgG (Figure 6B, compare α-COG3 (+) and control IgG columns). We have concluded that CCD vesicles are functional intra-Golgi intermediates capable of docking to Golgi membranes in a COG complex-dependent reaction.

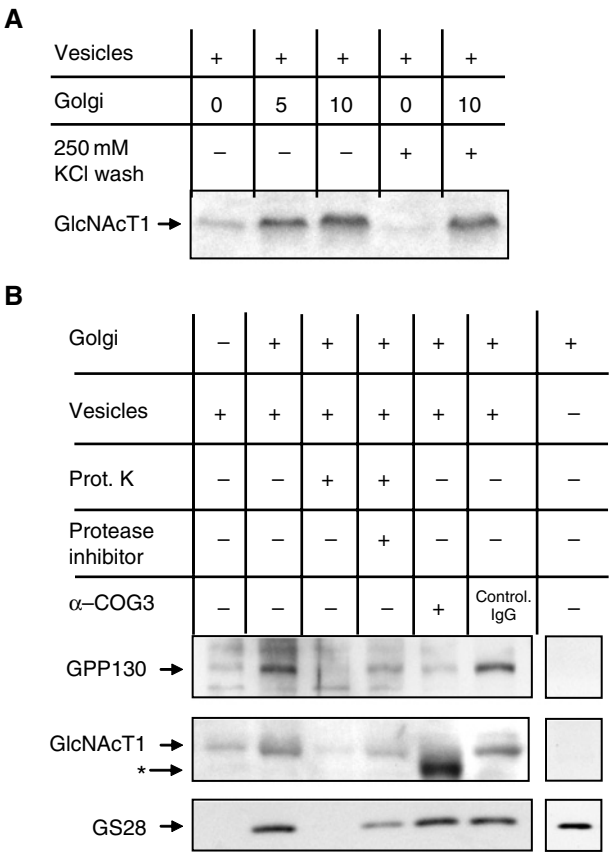


**Figure 6: Conserved oligomeric Golgi complex-dependent (CCD) vesicles dock to Golgi membranes *in vitro*.** A) Vesicle docking is proportional to amount of added Golgi and resistant to salt wash. Cells stably expressing GlcNacT1-myc were treated with COG3 siRNA. A vesicle fraction from COG3 KD cells (S20) was incubated with purified rat liver Golgi as described in *Materials and Methods*. After incubation with CCD vesicles, Golgi membranes were pelleted at 10 000 × *g* and washed with low or high-salt buffer. Golgi membranes were repelleted and analyzed for CCD vesicle marker GlcNAcT1 by WB with anti-myc antibodies. B) Vesicle docking is sensitive to protease treatment of acceptor Golgi membranes and is inhibited by anti-COG3 IgG. CCD vesicle marker GlcNAcT1 (anti-myc Ab), GPP130 (anti-human GPP130) and Golgi marker GS28 (anti-rat GS28 Ab) were detected by WB. Star indicates heavy chain of anti-Cog3p IgG bound to Golgi membrane.

## Discussion

The COG complex has been assigned a role of one of the key components in intracellular membrane trafficking (40). Majority of up-to-date data argue that the COG complex resides on *cis/medial*-Golgi and functions as a tether of retrograde intra-Golgi vesicles (15–17,31). Indeed, both yeast (30) and mammalian (19) cells deficient in a Cog3p subunit accumulate multiple CCD vesicles. These vesicles most likely are COPI coated and packed with recycling Golgi SNAREs (GS15, GS28) (41) and putative retrograde cargo receptors as GPP130 (42). Another well-studied feature of COG-deficient cells is significantly impaired

modification of glycoconjugates. In both mammalian (Δ*COG1*, Δ*COG2* and Δ*COG7*) (21,26) and yeast (Δ*COG1*, Δ*COG3*, Δ*COG4* and Δ*COG6*) (17,18,22,23) COG mutant cells, virtually all N- and O-linked Golgi-associated glycosylation reactions are impaired.

In this article, we examined the hypothesis that retrograde intra-Golgi trafficking of components of the glycosylation machinery is directed by the COG complex. We have shown that the duration of COG3 KD positively correlates with development of Golgi-glycosylation defects (Figure 1). Sorting and delivery of anterograde secretory cargo proteins (Figure 2) is not altered. For the first time, we demonstrated that depletion of both Lobe A (Cog3p) and Lobe B (Cog7p) of the COG complex severely affects localization of *medial*-Golgi enzymes GlcNAcT1 and Mann II, inducing their relocation into CCD vesicles. This finding agrees well with the observed mislocalization of yeast Golgi-glycosylation enzyme Och1p in a *cog3* mutant (20).

CCD vesicles are likely to originate from either the *trans*-Golgi or TGN, since both GlcNAcT1 and Mann II are known to cycle through the Golgi stack to the *trans*-Golgi network and then back to the *cis*-Golgi (29,35). It has been shown recently that formation of COPI vesicles is linked to the assembly of the actin complex (43,44). The actin cytoskeleton is affected in yeast *cog3* mutant cells, (13) and actin is shown to be coimmunoprecipitated with the mammalian COG complex (45). One attractive idea is that COG complex directs the movement of CCD vesicles along specialized intra-Golgi actin railways through communication with the actin cytoskeleton. In support to this notion, Cog3p (CG3248) was found to interact with the actin-binding protein Arp3 (CG7558) in a recent *Drosophila* two-hybrid screen (46). We also observed that CCD vesicles are positioned along the actin cables in COG3 KD cells (Figure S6).

Vesicles containing Golgi enzymes are likely to be retrograde in respect to direction of their trafficking since both endogenous (CD44 and Lamp2) (Figure 2) and model (GFP-VSVG) (19) anterograde secretory cargo molecules are not detected in CCD vesicles at the fluorescence microscopy level; after prolonged KD of COG complex, vesicles are partially consumed by the ER, depositing their content into the endoplasmic reticulum (Figure 3C and S4). Latter result is in agreement with previously observed partial relocation in ER of Mann II in Δ*COG1* and Δ*COG2* CHO mutant cells (31). We have previously demonstrated that both GS15 and GS28 are enriched in CCD vesicles (19). Most likely, these v-SNAREs form a functional fusion complex with t-SNARE Syntaxin 5, which itself is a COG-interacting protein (17). One plausible explanation for the eventual consumption of CCD vesicles by ER is based on the observation that the long form of Syntaxin 5 cycles between the Golgi and ER (47). We have found that the ER form of Syntaxin 5 is less sensitive to COG7 KD as compared to the Golgi form of t-SNARE (Figure 5C). Consequently, in COG7 KD cells, partial colocalization of GlcNAcT1 with ER markers was observed as early as 4 days after KD (Figure S5, available online at http://www.blackwell-synergy.com). Therefore, a relative increase in the ER localized form of Syntaxin 5 in COG KD cells could potentiate fusion of CCD vesicles with the ER membrane. Interestingly, in recently described mammalian cells depleted of Syntaxin 5, the COG-sensitive protein GS28 was found in dispersed vesicle structures (48).

The *in vitro* experiments (Figure 6) support the idea that CCD vesicles are functional intra-Golgi trafficking intermediates. Isolated CCD vesicles are capable of docking and, most probably, fusion with purified Golgi membranes, since as a result of vesicle–Golgi coincubation, vesicle cargo proteins GlcNAcT1 and GPP130 became associated with large membranes and this association is salt-resistant. Vesicle docking is dependent on Golgi peripheral and/or transmembrane proteins, since proteinase treatment of isolated Golgi virtually abolished vesicle docking. The efficient docking of vesicles requires a functional COG complex on the Golgi membrane, since both protease treatment and pretreatment with anti-Cog3p IgGs efficiently block vesicle–Golgi interaction. Latter result supports the model of Golgi-localized COG complex tethering intra-Golgi retrograde vesicles (Figure 7).

Both GPP130 and GlcNAcT1 containing vesicles behave similarly in the *in vitro* system, suggesting that the CCD vesicle population is homogeneous and that both proteins are being recycled using the same trafficking intermediates.

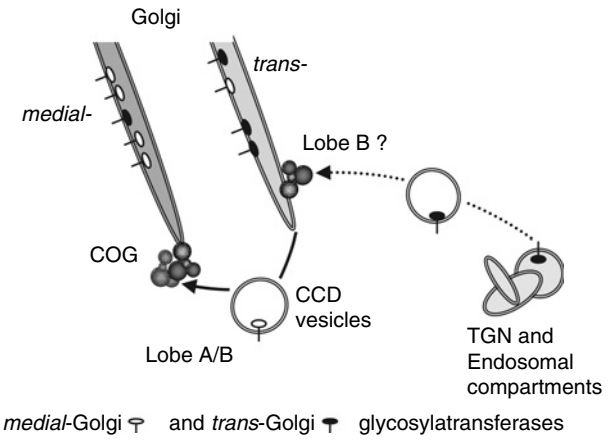


**Figure 7: Model of the function of conserved oligomeric Golgi (COG) complex in trafficking of Golgi enzymes.** The COG complex primarily resides on the *medial*-Golgi. It orchestrates tethering of constantly cycling retrograde COG complex-dependent (CCD) vesicles that bud from *trans*-Golgi (solid line). These Golgi intermediates carry resident Golgi proteins, including *medial*-Golgi glycosyltransferases. Lobe B of the COG complex might also associate with *trans*-Golgi and accept vesicles that retrieve *trans*-Golgi enzymes from *trans*-Golgi network and endosomal compartments (dashed line). During malfunction of COG complex, retrograde membrane intermediates accumulate in cytoplasm.

Conversely, known trafficking itineraries of GPP130 and GlcNAcT1 are different. *Medial*-Golgi localized GlcNAcT1 cycles via the *trans*-Golgi and ER (29), while *cis*-Golgi-resident GPP130 visits the endosomal system and plasma membrane (49). Prolonged COG3 and COG7 depletion ultimately leads to partial relocalization of the GlcNAcT1 signal to the ER, while GPP130 is not detected in the ER (unpublished data). There was a reduction of GPP130 (but not GlcNAcT1) protein levels after prolonged COG KD (compare Figure 1A and Figure 4C). Additional biochemical and immuno-EM studies will be required to characterize CCD vesicles in details.

Comparison of COG3 and COG7 KD phenotypes indicates that depletion of either Lobe A or Lobe B subcomplexes primarily affects localization of GlcNAcT1 and GS15, indicating that the whole COG complex is required for proper recycling of *cis/medium*-Golgi-resident proteins. On the other hand, acute COG7 KD phenotype differs from COG3 KD. Glycosylation defects are manifested slightly earlier in COG7 KD cells (Figure 5C and data not shown), and Golgi membranes in those cells are often misshapen into cotton ball or sponge-like structures. In addition, acute double COG3/COG7 KD affected glycosylation of both Lamp2 and GlcNAcT1 more severely as compared to single depletion, indicating that double KD is affecting activity or compartmentalization of multiple Golgi enzymes. There is evidence that loss-of-function mutation in Lobe A subunits causes defects in early Golgi-glycosylation reactions (17,20,21), whereas a loss-of-function mutation in Lobe B subunits causes *trans*-Golgi-glycosylation defects (26). Taking into account that in mammalian cells Lobe B exists both as a part of the large COG complex and as a separate small subcomplex (15), we propose the model (Figure 7). Our model suggests that the whole Lobe A/Lobe B COG complex regulates efficient vesicle tethering to the *cis/medial*-Golgi membranes. The lobe B subcomplex could also specifically tether vesicles to *trans*-Golgi cisternae. Similar separation of functions was discovered recently for *cis*- and *trans*-Golgi-operating anterograde tethers TRAPP I and II (10). Proposed compartment-specific functions for COG lobes may reflect a common principle in the evolution of oligomeric complexes operating in membrane trafficking.

## Materials and Methods

### *Reagents and antibodies*

Reagents were as follows: PNGase F, EndoH (New England Biolabs, Beverly, MA, USA); Cascade Blue Dextran (Molecular Probes, Eugene, OR, USA); Protein G-Sepharose (Calbiochem, La Jolla, CA, USA); Protein A-Sepharose (Amersham Biosciences, Piscataway, NJ, USA). Antibodies used for Western Blotting (WB), immunofluorescence (IF), immunoprecipitation (IP) studies were obtained from commercial sources and as gifts from generous individual investigators or generated by us as indicated below. Antibodies (and their dilutions) were as follows: rabbit – both anti-myc (WB 1:5000, IF 1:3000) and anti-vsv (WB 1:2500, IF 1:400) from Bethyl Laboratories (Montgomery, TX, USA); anti-Cog3p (WB 1:1000) (16); anti-GPP130 (WB 1:1000, IF 1:2000; Covance Laboratories, Madison, WI, USA); anti-CD44 (WB 1:400; Santa Cruz Biotechnology, Santa Cruz, CA, USA); murine: anti-GM130 (IF 1:250); anti-human GS28 (WB 1:1000, IF 1:100) and anti-EEA1 (IF 1:250) (all from BD Biosciences, San Jose, CA, USA); anti-GPP130 (WB 1:100, gift from Adam Linstedt, CMU); anti-PDI (WB 1:5000, IF 1:200, IP 1:2000; Affinity BioReagents, Golden, CO, USA); anti-rat GS28 (WB 1:500; Stressgene, Victoria, BC, Canada); anti-GAPDH (WB 1:1000; Ambion, Austin, TX, USA); anti-CD44 (clone H4C4) and Lamp2 (clone H4B4) (WB 1:200, IF 1:100; Developmental Studies Hybridoma Bank, University of Iowa); and anti-GalT (IF 1:20, gift from Brian Storrie, UAMS)

### *Mammalian cell culture*

Monolayer HeLa cells were cultured in DMEM/F-12 media supplemented with 15 mM HEPES, 2.5 mM L-glutamine, 5% FBS, 100 U/mL penicillin G, 100 μg/mL streptomycin, and 0.25 μg/mL amphotericin B. Cells were grown at 37 °C and 5% $CO_2$ in a humidified chamber. HeLa cells stably expressing tagged Golgi apparatus proteins were maintained in the presence of 0.4 mg/ml G418 sulfate. HeLa cells stably expressing GlcNAcT1-myc, Mann II-vsv and GalNAcT2-vsv were obtained from B. Storrie's laboratory (UAMS). All cell culture media and sera were obtained from Invitrogen (Carlsbad, CA, USA).

### *RNA interference*

Human COG3 was targeted with siRNA duplex as described previously (19) by Oligofectamine (Invitrogen, Carlsbad, CA, USA). To achieve 3, 6 and 9 days of COG3 KD, cells were transfected each 72-h period. Human COG7 was targeted with a mixture of two Stealth siRNA duplexes (target sense, 1-CCAAGCUCUC-CAGAACAUGCCCAAA; 2-CCUGAAAAUCCCUC-UUUGCC-AAGUAU) (Invitrogen). Stealth siRNA duplex (target sense, CCAACCGACUUAAUGGCGCGGUAUU) was used as a mock control (Invitrogen). Cells were transfected with Lipofectamine 2000 (Invitrogen, Carlsbad, CA, USA) twice each 24-h period according to protocol recommended by Invitrogen. For IF microscopy and WB, HeLa cells were grown in 35 mm dishes (on coverslips for IF) at 60% confluence and lyzed in 2% SDS after 3, 6 and 9 days of COG3 KD or 3 days of COG7 KD.

### *Radioactive labeling and immunoprecipitation*

Pulse-chase experiments were performed using the $^{35}$S-Methionine (ICN Biomedicals, Aurora, OH, USA). HeLa cells grown in four 60-mm dishes were mock or siRNA treated for 3 and 9 days, washed twice with DPBS and starved in DMEM without methionine for 30 min. Pulsed by addition of 200 μCi/mL $^{35}$S-Methionine for 10 min and chased with complete growth medium containing 2 mM of cold methionine/cysteine mix for 0, 30, 60 and 120 min (at 37 °C). All further steps were performed at room temperature. Cells were washed twice with DPBS and lyzed in 1 mL of TES buffer [50 mM Tris-HCl, pH 7.4, 150 mM NaCl, 1 mM EDTA, 1% Triton X-100, 0.1% SDS and 0.2% sodium azide, protease inhibitor cocktail]. Lysates were incubated with 30 μL of protein A Sepharose CL-4B beads on the tube rotator for 1 h and centrifuged at 20 000 × *g* for 10 min. Supernatants were transferred to new tubes and incubated overnight with 2 μg of anti-CD44 antibodies (1:50) in a cold room. Samples were clarified by centrifugation as above, and 20 μL of Protein G-Agarose beads were incubated for 1 h and centrifuged at 110 × *g* for 1 min, washed four times with TBST. Beads were then transferred to a new tube, resuspended in 30 μL of ×1 sample buffer; concentrated supernatants were loaded on SDS-PAGE. Proteins were quantified using a Phosphoimager analysis. After IP with anti-CD44, supernatants of the cell lysates were subjected to IP with anti-Lamp2 (2 mkg).

### *Immunofluorescence microscopy*

Cells grown on coverslips were processed at room temperature as described previously with some modifications (15). Cells were washed once with PBS and fixed by incubating for 10 min with 4% paraformaldehyde (Electron Microscopy Systems, Washington, PA, USA) in PBS, pH 7.4. The coverslips were then washed for 1 min with 0.1% TritonX-100 in PBS, incubated in 0.1% Na-borohydride in PBS for 5 min and washed with 50 mM $NH_4Cl$ in PBS for 5 min. Cells were then blocked in 0.1% saponin, 1% BSA in PBS for 15 min. Cells were then incubated for 30 min with primary antibodies and washed off extensively with 0.1% saponin in PBS. Secondary antibodies (Alexa®594 goat anti-rabbit IgG conjugate and Alexa®488 goat anti-mouse IgG conjugate (Molecular Probes)

diluted 1:400 in 1% gelatin and 0.1% saponin in PBS were applied for 30 min, and then coverslips were extensively washed with PBS and water. The coverslips were mounted in Prolong Gold Antifade Reagent (Molecular Probes). IF microscopy was performed using an epifluorescence microscope (Axiovert 200; Carl Zeiss International, Thornwood, NY, USA) equipped with the CARV I and CARV II Confocal Imager modules (BioVision Technologies, Exton, PA, USA) with a Plan-Apochromat ×63 oil immersion lens (NA 1.4) at RT. The images were obtained as confocal stacked images and processed on Macintosh computers using IPLab 3.9.3 software (Scanalytics, Fairfax, VA, USA). During the processing stage, individual image channels were pseudocolored with RGB values corresponding to each of the fluorophore emission spectral profiles. Images were cropped using Adobe Photoshop 6.0 software.

### *Endocytosis of fluorescent dextran*

HeLa cells stably expressing GlcNAcT1-myc were grown on coverslips in 6-well plates. Cells were mock or COG3 siRNA treated for 9 days. Cells were treated with Cascade Blue Dextran as previously described (50) with some modifications. Cell cultures were incubated with Cascade Blue Dextran at 0.6 mg/mL in culture medium for 12 h before performing IF assay. Cells were washed with PBS and incubated in fresh medium for 3 h; coverslips were fixed and stained with anti-Lamp2 and anti-myc antibodies.

### *Treatment with endoglycosydases*

HeLa cells were grown in 6-well plates and transfected with COG3 siRNA for 3, 6 and 9 days. Cells were lyzed in 2% SDS and denatured for 15 min at 95 °C. To decrease SDS concentration to 0.5%, 9 μL of each lysate was diluted in 27 μL of water. One half was incubated with supplied buffer and the other with PNGase F (51) (1 μL, 500 units) or Endo H (0.1 μL, 100 units). Samples were incubated at 37 °C for 1 h, dissolved in ×6 sample buffer, subjected to SDS-PAGE and immunoblotted with anti-CD44 and anti-Lamp2 antibodies.

### *Glycerol velocity gradient*

Gradient fractionation was prepared as described previously (19,52) with some modifications. Control and COG3 KD cells were analyzed in pairs simultaneously and under the same conditions. GlcNAcT1-myc were grown in one 6-cm plate, treated with COG3 siRNA, collected by trypsinization, pelleted (2000 × *g* for 2 min), washed once with PBS and STE buffer (250 mM sucrose, 10 mM triethylamine, pH 7.4, 1 mM EDTA) and homogenized by 20 passages through a 25-gauge needle in 0.6 mL of STE-S (STE buffer without sucrose) containing cocktail of protein inhibitors (Roche Molecular Biochemicals, Indianapolis, IN, USA). Efficiency of homogenization was determined by staining with Trypan Blue. Cell homogenates were centrifuged at 1000 × *g* for 2 min to obtain PNS. This PNS (0.6 mL) was layered on linear 10–30% (wt/vol) glycerol gradient (12 mL in 10 mM triethylamine, pH 7.4 and 1 mM EDTA on a 0.5 mL 80% sucrose cushion) and centrifuged at 280 000 × *g* for 60 min in a SW40 Ti rotor (Beckman Coulter, Miami, FL, USA). One milliliter fractions were collected from the top. All steps were performed at 4 °C. Fifty microliter of each fraction as well as an aliquot of PNS were combined with 6× sample buffer, loaded on SDS-PAGE and analyzed by WB. For the analysis of CCD vesicle pool, proteins from fractions 3–5 of glycerol velocity gradient were concentrated by TCA precipitation (53).

### *In vitro CCD vesicle docking assay*

Acceptor RLG membranes were isolated as described previously (19). 20 000 × *g* supernatant (S20) from COG3 KD HeLa cells stably expressing GlcNAcT1-myc was used as a source of both donor CCD vesicles and cytosol. To prepare cell homogenates of 3 days, COG3 KD cells were grown in 10-cm plate, washed twice with PBS and once with 20 mM HEPES pH 7.4 buffer containing 250 mM sucrose. Sucrose buffer was removed, and cells were scraped from the dish in 1 mL of cold 20 mM HEPES pH 7.4 containing cocktail of protein inhibitors (Roche) and 1 mM DTT. Cells were homogenized on ice by 20 passages through a 25-gauge needle. Unbroken cells were removed by centrifugation at 1000 × *g* for 2 min to obtain PNS. After that, membranes were stabilized by addition of an equal volume of buffer containing 25 mM KCl and 2.5 mM MgOAc (final concentrations). Large membranes were subsequently removed by centrifugation at 10 000 × *g* for 10 min and by repeated centrifugation at 20 000 × *g* for 10 min to obtain S20. Standard vesicle docking reaction (100 μL total volume) contained 50 μL of S20, 0–10 μL of acceptor Golgi membranes (1.5 mg/mL), 10 μL of ATP-regeneration mixture in a 20 mM HEPES, pH 7.4, 25 mM KCl and 2.5 mM $MgCl_2$, 1 mM DTT (buffer HKMD). Reaction was incubated for 30 min at 37 °C, cooled on ice, and then Golgi membranes were pelleted at 10 000 × *g* for 10 min and washed once with 100 μL of HKMD buffer or high salt buffer (HKMDS buffer with 250 mM KCl). Pellet was resuspended in 20 μL of SDS sample buffer; 10 μL of sample was loaded on SDS-PAGE and analyzed by WB. For Proteinase K treatment, Golgi membranes were incubated for 5 min at 37 °C with Proteinase K (0.25 μg/mL) (Sigma Chemical, St Louis, MO, USA). The reaction was stopped by addition of 1/10 of the volume of 10× cocktail of protein inhibitors, and the membranes were washed twice with HKMD buffer. For mock treatment, cocktail of protein inhibitors was added before Proteinase K treatment. For IgG interference experiment, 5 μL of affinity-purified anti-Cog3p IgGs (0.54 mg/mL) or preimmune IgGs in HKMD buffer were added to vesicle-docking reaction.

### *SDS-polyacrylamide gel electrophoresis and Western blotting*

SDS-PAGE and WB were performed as described previously (17). A signal was detected using a chemiluminescence reagent kit (PerkinElmer Life Sciences, Boston, MA, USA) and quantified using ImageJ software (http://rsb.info.nih.gov/ij/).

## Supplementary Material

The following figures are available as part of the online article from http://www.blackwell-synergy.com

**Figure S1:** Stability of COG subunits is altered after 9 days of COG3 KD. Control and 9 days of COG3 KD cell lysates (10 μg of total protein each) were immunoblotted with antibodies against COG complex subunits. GAPDH was used as a loading control.

**Figure S2:** Lamp2 becomes EndoH sensitive after 6 and 9 days of COG3 KD. Control (0), 3, 6 and 9 days of COG3 KD total cell lysates were treated with EndoH as described in *Materials and Methods*. Samples were immunoblotted with anti-Lamp2 antibodies. Compare lanes 6 and 9 in control and EndoH panels.

**Figure S3:** CD44 is primarily localized on the plasma membrane in permiabilized and non-permeabilized cells after 9 days of COG3 KD. Non-permiabilized (upper row) and permeabilized (lower row) cells after 9 days of COG3 KD were triple stained with anti-CD44 (green), anti-myc for GlcNAcT1 (red) and DAPI (blue). There is no GlcNAcT1 signal in non-permeabilized cells. Images were collected at equal signal gains using CARV II microscopy. Bar 10 μm.

**Figure S4:** GlcNAcT1 is partially colocalized with ER marker PDI after 9 days of COG3 KD. Cells after 9 days of COG3 KD were fixed and stained with anti GlcNAcT1-myc (red), ER marker PDI (green) and nuclei marker DAPI (blue). Partial colocalization of GlcNAcT1 and PDI signals is evident in perinuclear region (merged image). Images were collected at equal signal gains, using CARV II microscopy. Bar 10 μm.

**Figure S5:** GlcNAcT1 is partially colocalized with ER marker PDI after 3 days of COG7 KD. Cells after 3 days of COG7 KD were stained with anti-myc (red), anti-PDI (green) and DAPI (blue). Notice partial colocalization of GlcNAcT1 and PDI signals. Arrows indicate ER nuclear ring. Images were collected at equal signal gains using CARV microscopy. Bar 10 μm.

**Figure S6:** CCD vesicles are positioned along actin cables in COG3 KD cells. Cells after 3 days of COG3 KD were stained with anti GlcNAcT1-myc (green), phalloidin-Alexa 594 (red) and DAPI (blue). Notice that CCD

vesicles (arrowheads) are positioned along actin cables (arrows) in the merged image. Images were collected using CARV microscopy. Bar 10 μm.

**Figure S7:** Antibodies recognized specific antigens in RLG and HeLa S20 fractions. Aliquots of RLG and COG3 KD HeLa S20 (approximately 10 μg each) were separated on 10% SDS-PAGE and immunoblotted with antibodies as indicated.

## Acknowledgments

We are very grateful to O. Pavliv for excellent technical assistance. We also thank M. Jennings, F. Hughson, A. Linstedt, B. Storrie, E. Sztul, D. Ungar and others who provided reagents and critical reading of the manuscript. Supported by grants from the National Science Foundation (MCB-0234822) and the DOD (DAMD17-03-1-0243).

## References

1. Shorter J, Warren G. Golgi architecture and inheritance. Annu Rev Cell Dev Biol 2002;18:379–420.
2. Warren G, Malhotra V. The organisation of the Golgi apparatus. Curr Opin Cell Biol 1998;10:493–498.
3. Dunphy WG, Fries E, Urbani LJ, Rothman JE. Early and late functions associated with the Golgi apparatus reside in distinct compartments. Proc Natl Acad Sci USA 1981;78:7453–7457.
4. Kornfeld R, Kornfeld S. Assembly of asparagine-linked oligosaccharides. Annu Rev Biochem 1985;54:631–664.
5. Rabouille C, Hui N, Hunte F, Kieckbusch R, Berger EG, Warren G, Nilsson T. Mapping the distribution of Golgi enzymes involved in the construction of complex oligosaccharides. J Cell Sci 1995;108 (4):1617–1627.
6. Pelham HR, Rothman JE. The debate about transport in the Golgi – two sides of the same coin? Cell 2000;102:713–719.
7. Orci L, Stamnes M, Ravazzola M, Amherdt M, Perrelet A, Sollner TH, Rothman JE. Bidirectional transport by distinct populations of COPI-coated vesicles. Cell 1997;90:335–349.
8. VanRheenen SM, Cao X, Lupashin VV, Barlowe C, Waters MG. Sec35p, a novel peripheral membrane protein, is required for ER to Golgi vesicle docking. J Cell Biol 1998;141:1107–1119.
9. VanRheenen SM, Cao X, Sapperstein SK, Chiang EC, Lupashin VV, Barlowe C, Waters MG. Sec34p, a protein required for vesicle tethering to the yeast Golgi apparatus, is in a complex with Sec35p. J Cell Biol 1999;147:729–742.
10. Sacher M, Barrowman J, Wang W, Horecka J, Zhang Y, Pypaert M, Ferro-Novick S. TRAPP I implicated in the specificity of tethering in ER-to-Golgi transport. Mol Cell 2001;7:433–442.
11. Conibear E, Stevens TH. Vps52p, Vps53p, and Vps54p form a novel multisubunit complex required for protein sorting at the yeast late Golgi. Mol Biol Cell 2000;11:305–323.
12. Lupashin V, Sztul E. Golgi tethering factors. Biochim Biophys Acta 2005;1744:325–339.
13. Spelbrink RG, Nothwehr SF. The yeast GRD20 gene is required for protein sorting in the trans-Golgi network/endosomal system and for polarization of the actin cytoskeleton. Mol Biol Cell 1999;10: 4263–4281.
14. Kim DW, Sacher M, Scarpa A, Quinn AM, Ferro-Novick S. High-copy suppressor analysis reveals a physical interaction between Sec34p and Sec35p, a protein implicated in vesicle docking. Mol Biol Cell 1999;10:3317–3329.
15. Ungar D, Oka T, Brittle EE, Vasile E, Lupashin VV, Chatterton JE, Heuser JE, Krieger M, Waters MG. Characterization of a mammalian Golgi-localized protein complex, COG, that is required for normal Golgi morphology and function. J Cell Biol 2002;157:405–415.
16. Suvorova ES, Kurten RC, Lupashin VV. Identification of a human orthologue of Sec34p as a component of the cis-Golgi vesicle tethering machinery. J Biol Chem 2001;276:22810–22818.
17. Suvorova ES, Duden R, Lupashin VV. The Sec34/Sec35p complex, a Ypt1p effector required for retrograde intra-Golgi trafficking, interacts with Golgi SNAREs and COPI vesicle coat proteins. J Cell Biol 2002;157:631–643.
18. Ram RJ, Li B, Kaiser CA. Identification of sec36p, sec37p, and sec38p: components of yeast complex that contains sec34p and sec35p. Mol Biol Cell 2002;13:1484–1500.
19. Zolov SN, Lupashin VV. Cog3p depletion blocks vesicle-mediated Golgi retrograde trafficking in HeLa cells. J Cell Biol 2005;168:747–759.
20. Bruinsma P, Spelbrink RG, Nothwehr SF. Retrograde transport of the mannosyltransferase Och1p to the early Golgi requires a component of the COG transport complex. J Biol Chem 2004;279:39814–39823.
21. Kingsley DM, Kozarsky KF, Segal M, Krieger M. Three types of low density lipoprotein receptor-deficient mutant have pleiotropic defects in the synthesis of N-linked, O-linked, and lipid- linked carbohydrate chains. J Cell Biol 1986;102:1576–1585.
22. Whyte JR, Munro S. The Sec34/35 golgi transport complex is related to the exocyst, defining a family of complexes involved in multiple steps of membrane traffic. Dev Cell 2001;1:527–537.
23. Fotso P, Koryakina Y, Pavliv O, Tsiomenko A, Lupashin V. Cog1p plays a central role in the organization of the yeast conserved oligomeric golgi (COG) complex. J Biol Chem 2005;280:27613–27623.
24. Oka T, Vasile E, Penman M, Novina CD, Dykxhoorn DM, Ungar D, Hughson FM, Krieger M. Genetic analysis of the subunit organization and function of the conserved oligomeric golgi (COG) complex: studies of COG5- and COG7-deficient mammalian cells. J Biol Chem 2005;280:32736–32745.
25. Ungar D, Oka T, Vasile E, Krieger M, Hughson FM. Subunit architecture of the conserved oligomeric Golgi complex. J Biol Chem 2005;280:32729–32735.
26. Wu X, Steet RA, Bohorov O, Bakker J, Newell J, Krieger M, Spaapen L, Kornfeld S, Freeze HH. Mutation of the COG complex subunit gene COG7 causes a lethal congenital disorder. Nat Med 2004;10:518–523.
27. Reddy P, Krieger M. Isolation and characterization of an extragenic suppressor of the low-density lipoprotein receptor-deficient phenotype of a Chinese hamster ovary cell mutant. Mol Cell Biol 1989;9: 4799–4806.
28. Harris SL, Waters MG. Localization of a yeast early Golgi mannosyltransferase, Och1p, involves retrograde transport. J Cell Biol 1996;132:985–998.
29. Opat AS, Houghton F, Gleeson PA. Steady-state localization of a medial-Golgi glycosyltransferase involves transit through the trans-Golgi network. Biochem J 2001;358:33–40.
30. Wuestehube LJ, Duden R, Eun A, Hamamoto S, Korn P, Ram R, Schekman R. New mutants of *Saccharomyces cerevisiae* affected in the transport of proteins from the endoplasmic reticulum to the Golgi complex. Genetics 1996;142:393–406.
31. Oka T, Ungar D, Hughson FM, Krieger M. The COG and COPI complexes interact to control the abundance of GEARs, a subset of Golgi integral membrane proteins. Mol Biol Cell 2004;15:2423–2435.
32. Borland G, Ross JA, Guy K. Forms and functions of CD44. Immunology 1998;93:139–148.
33. Eskelinen EL, Illert AL, Tanaka Y, Schwarzmann G, Blanz J, Von Figura K, Saftig P. Role of LAMP-2 in lysosome biogenesis and autophagy. Mol Biol Cell 2002;13:3355–3368.
34. Kundra R, Kornfeld S. Asparagine-linked oligosaccharides protect Lamp-1 and Lamp-2 from intracellular proteolysis. J Biol Chem 1999;274:31039–31046.

35. Hoe MH, Slusarewicz P, Misteli T, Watson R, Warren G. Evidence for recycling of the resident *medial/trans* Golgi enzyme *N*-acetylglucosaminyltranserase I, in ldlD cells. J Biol Chem 1995;270: 25057–25063.
36. Love HD, Lin CC, Short CS, Ostermann J. Isolation of functional Golgi-derived vesicles with a possible role in retrograde transport. J Cell Biol 1998;140:541–551.
37. Martinez-Menarguez JA, Prekeris R, Oorschot VM, Scheller R, Slot JW, Geuze HJ, Klumperman J. Peri-Golgi vesicles contain retrograde but not anterograde proteins consistent with the cisternal progression model of intra-Golgi transport. J Cell Biol 2001;155:1213–1224.
38. Cao X, Ballew N, Barlowe C. Initial docking of ER-derived vesicles requires Uso1p and Ypt1p but is independent of SNARE proteins. EMBO J 1998;17:2156–2165.
39. Lin CC, Love HD, Gushue JN, Bergeron JJ, Ostermann J. ER/Golgi intermediates acquire Golgi enzymes by brefeldin A-sensitive retrograde transport in vitro. J Cell Biol 1999;147:1457–1472.
40. Oka T, Krieger M. Multi-component protein complexes and Golgi membrane trafficking. J Biochem (Tokyo) 2005;137:109–114.
41. Hay JC, Klumperman J, Oorschot V, Steegmaier M, Kuo CS, Scheller RH. Localization, dynamics, and protein interactions reveal distinct roles for ER and Golgi SNAREs [published erratum appears in J Cell Biol 1998 August 10;142 (3): following 881]. J Cell Biol 1998;141: 1489–1502.
42. Natarajan R, Linstedt AD. A cycling cis-Golgi protein mediates endosome-to-Golgi traffic. Mol Biol Cell 2004;15:4798–4806.
43. Fucini RV, Chen JL, Sharma C, Kessels MM, Stamnes M. Golgi vesicle proteins are linked to the assembly of an actin complex defined by mAbp1. Mol Biol Cell 2002;13:621–631.
44. Chen JL, Fucini RV, Lacomis L, Erdjument-Bromage H, Tempst P, Stamnes M. Coatomer-bound Cdc42 regulates dynein recruitment to COPI vesicles. J Cell Biol 2005;169:383–389.
45. Loh E, Hong W. Sec34 is implicated in traffic from the endoplasmic reticulum to the Golgi and exists in a complex with GTC-90 and ldlBp. J Biol Chem 2002;2:2.
46. Giot L, Bader JS, Brouwer C, Chaudhuri A, Kuang B, Li Y, Hao YL, Ooi CE, Godwin B, Vitols E, Vijayadamodar G, Pochart P, Machineni H, Welsh M, Kong Y *et al.* A protein interaction map of *Drosophila melanogaster.* Science 2003;302:1727–1736.
47. Hui N, Nakamura N, Sonnichsen B, Shima DT, Nilsson T, Warren G. An isoform of the Golgi t-SNARE, syntaxin 5, with an endoplasmic reticulum retrieval signal. Mol Biol Cell 1997;8:1777–1787.
48. Suga K, Hattori H, Saito A, Akagawa K. RNA interference-mediated silencing of the syntaxin 5 gene induces Golgi fragmentation but capable of transporting vesicles. FEBS Lett 2005;579:4226–4234.
49. Puri S, Bachert C, Fimmel CJ, Linstedt AD. Cycling of early Golgi proteins via the cell surface and endosomes upon lumenal pH disruption. Traffic 2002;3:641–653.
50. Nemoto T, Kojima T, Oshima A, Bito H, Kasai H. Stabilization of exocytosis by dynamic F-actin coating of zymogen granules in pancreatic acini. J Biol Chem 2004;279:37544–37550.
51. Plummer TH Jr, Tarentino AL. Purification of the oligosaccharide-cleaving enzymes of Flavobacterium meningosepticum. Glycobiology 1991;1:257–263.
52. Jesch SA, Linstedt AD. The Golgi and endoplasmic reticulum remain independent during mitosis in HeLa cells. Mol Biol Cell 1998;9:623–635.
53. Bensadoun A, Weinstein D. Assay of proteins in the presence of interfering materials. Anal Biochem 1976;70:241–250.